

Bilag no. 7
ADVOKATFIRMAET SVENDSEN



**Final report for the Swedish Energy Agency project 21597-3
(TRANS)**

**LONG-RANGE SOUND PROPAGATION OVER THE SEA
WITH APPLICATION TO WIND TURBINE NOISE**

TRITA-AVE 2007:22 ISSN 1651-7660

Mathieu Boué

Vindforsk

Table of contents

Abstract	4
1 Introduction	5
2 Basics about Long Range Outdoor Sound Propagation	6
2.1 Atmospheric Absorption.	6
2.2 ground Effect.....	7
2.3 Shoreline Effect.....	8
2.4 Wind and Temperature Gradients	9
2.5 Specificities of Sound propagation over sea at large distance	10
3 Measurements Methods.	12
3.1 Measurement site.	12
3.2 Sound Sources.....	14
3.3 Receivers	14
3.4 Meteorological Measurements	16
4 Post-processing techniques	17
4.1 Time Domain Averaging.....	17
4.2 Kalman filtering	19
4.3 Fast Fourier Transform	19
4.4 Conclusion.....	19
5 Results and Analysis	20
5.1 Meteorological Measurements Results	20
5.1.1 Wind speed and direction.....	20
5.1.2 Sound Data	22
6 Predictions models	25
6.1 F.F.P.	25
6.2 Ray Tracing	25
6.3 Parabolic Equation	26
7 Conclusion.....	28
APPENDIX 1: Wind speed, wind directions profiles at transmission loss at Öland in June 2005	29
APPENDIX 2: Wind speed and wind directions profiles at Öland in June 2005	33
APPENDIX 3: Measurements data.	63
References:	67

Table of figures

Figure 1: Ground effect	7
Figure 2: Propagation of sound rays with different conditions of wind and temperature gradients	9
Figure 3: Different cases of ground influence.....	10
Figure 4: Effect of the LLJ over sea on the sound waves	11
Figure 5: In situ Setup	12
Figure 6: Site for the measurements.....	13
Figure 7: Sound Sources at the Utgrunden Lighthouse	14
Figure 8: Microphone array at the receiver point.....	15
Figure 9: Directivity pattern of the microphone array for 3 frequencies	16
Figure 10: Setup for measurement of wind protection performances.....	16
Figure 11: Time averaging method: 4a, 4b, 4c for the studied frequency f_1 ; 4d, 4e, 4f for another frequency f_2	18
Figure 12: a Time signal; b Signal after Time Domain Averaging; c Signal after Kalman Filtering	18
Figure 13: Algorithm of the Post processing Techniques.....	20
Figure 14: Direction of propagation (plain line) and downwind conditions (between the dashed lines) according to Swedish recommendation.....	21
Figure 15: Wind direction measured at Utgrunden during sound measurements	21
Figure 16: Transmission loss distribution as a function of the percentage of occurrences.....	22
Figure 17: Transmission loss distribution as a function of the percentage of occurrences. All frequencies added	23
Figure 18: Cumulative Distribution of the Transmission Loss.	23
Figure 19: Cumulative Distribution for the Transmission Loss. All frequencies added.....	24
Figure 20: Calculation using Ray Tracing Method.....	25
Figure 21: Left: Sound speed profile in function of height. Right: Predicted propagation of rays of sound in function of height and distance for this profile ²⁸	26
Figure 22: Attenuation of the sound field using a Parabolic Equation Method under upwind and downwind conditions	27

ABSTRACT

The classical theory of spherical wave propagation is not valid at large distances from a sound source due to the influence of wind and temperature gradients that refract, i.e., bend the sound waves. This will in the downwind direction lead to a cylindrical type of wave spreading for large distances (> 1 km). Cylindrical spreading will give a smaller damping with distance as compared to spherical spreading (3 dB/distance doubling instead of 6 dB). But over areas with soft ground, i.e., grass land, the effect of ground reflections will increase the damping so that, if the effect of atmospheric damping is removed, a behavior close to a free field spherical spreading often is observed. This is the standard assumption used in most national recommendations for predicting outdoor sound propagation, e.g., noise from wind turbines. Over areas with hard surfaces, e.g., deserts or the sea, the effect of ground damping is small and therefore cylindrical propagation could be expected in the downwind direction. This observation backed by a limited number of measurements is the background for the Swedish recommendation (Swedish Environmental Protection Agency report no. 6241), which suggests that cylindrical wave spreading should be assumed for distances larger than 200 m for sea based wind turbines. The purpose of this work was to develop measurement procedures for long range sound transmission and to apply this to investigate the occurrence of cylindrical wave spreading in the Baltic sea. This work has been successfully finished and is described in this report. Another ambition was to develop models for long range sound transmission based on the parabolic equation. Here the work is not finished but must be continued in another project. Long term measurements were performed in the Kalmar strait, Sweden, located between the mainland and Öland, during 2005 and 2006. Two different directive sound sources placed on a lighthouse in the middle of the strait produced low frequency tones at 80, 200 and 400 Hz. At the reception point on Öland, an array of 8 microphones created an acoustical antenna directed towards the sound sources. Wind and temperature data was measured at the source location and during one measurement period (June 2005), wind and temperature profiles were also mapped in the reception area. In order to increase the signal to noise ratio different signal enhancement methods were tested including a Kalman Filter technique and periodic time-averaging. The most accurate results were obtained by combining the Kalman Filter model with a Fast Fourier Transform (FFT). Sound pressure levels as low as a few dB could be detected by using this algorithm. The final results expressed as a transmission loss ("damping in sound pressure level corrected for the atmospheric damping") between the source and the receiver, have been compared to simultaneously measured wind and temperature profiles. The transmission loss data have also been expressed as statistical distributions from which e.g. the average value can be obtained. This average, based on data for the summer period June 2005/2006, has been compared with the Swedish Environmental Protection Agency recommendation⁷. It is found that the breaking point for cylindrical propagation is close to 700 m instead of the 200 m assumed in the recommendation. This is a significant difference and it shows that probably the Swedish recommendation uses a too small value for the expected breaking point. Of course in general the value of the breaking point can depend on the location and for which part of the year one takes the average. How large the variation can be due to such factors is today still unknown. Here only more measurements and perhaps simulations combined with the wind data base available in Sweden can provide an answer.

INTRODUCTION

In the light of the Kyoto protocol development of large off shore wind turbine farms are currently planned or even under construction in large parts of Europe¹. However, to be accepted by the population this development should not add noise disturbances. Therefore the need to establish correct and accurate models for long distance sound propagation over sea is considered urgent.

When the source is placed at a sufficient height above the ground, in a stable atmosphere, the sound waves propagates spherically. However, at long range, the spherical sound wave propagation model can not be applied anymore. The wave refraction effects due to wind and temperature gradients during downwind conditions tend to produce a more cylindrical wave spreading. The waves are curved downward towards the ground due to the gradients, then reflected up and the process is repeated leading to a trapped sound wave and a cylindrical type of wave spreading. In certain cases, the sound attenuation from the ground can nullify this effect and the propagation can appear as in a free field transmission. However, when the ground damping is weak, over areas with high impedance like rocky terrain, deserts and seas, cylindrical spreading could be expected. Present knowledge² shows that there exists a risk for low frequency noise disturbances from sea based wind turbines. This risk is attributed to a cylindrical sound propagation under downwind conditions and that this can be especially pronounced under certain atmospheric conditions, e.g. "low level jets" and to the fact that the low frequency sound attenuation is weak over sea.

In 1991, Hubbard and Shepherd³ reviewed noise propagation measurements for different wind turbines. Long-distance experiments over desert areas and for very low frequency noise (8 to 16 Hz), showed a cylindrical propagation in the case of downwind propagation. In Sweden, sound propagation from wind turbines over the sea at 4-5 km distance was measured in 1998-1999⁴. A higher sound pressure level in spring and early summer has been found and linked to specific wind and temperature gradients.

At the island Saltholm in Denmark, studies⁵ of a military fighter sound propagation have been performed in 1969. The airplane was placed on the ground and microphones were positioned at 7 km from the island. The measurements have been performed in downwind conditions with an average wind estimated at 3m/s at 50 m height and a small temperature gradient. The propagation over 6 km sea and 1 km land was studied by comparing the third octave band sound levels at the airplane and at the microphones 7 km away. Analysis shows cylindrical-type propagation with less attenuation than expected from the spherical propagation theory. In addition, a significantly higher attenuation at frequencies around 200 Hz has been observed but not explained. Moreover a computational simulation⁶ based on the parabolic equation method showed also that the presence of strong winds at low height over a reflecting surface lead to attenuation of 3dB per doubling of distance instead of the 6dB expected already after 200m

Based on these different studies, a model⁷ to calculate noise from off-shore wind farms has been developed by the Swedish Environmental Protection Agency. It gives the maximum value expected of the noise level due to wind turbines. The model is a simplified equation for the transmission loss which does not take into account influences by wind or temperature gradients and uses average coefficients for the atmospheric absorption. It includes an average influence due to the wind and temperature gradients influence and the effect of the ground damping by using 3dB decay attenuation from 200 m away from the source.

There exists one recent investigation by Konishi and al^{8,9} on long term and long range sound transmission over the sea. The sound propagation for frequencies between 250 and 1000 Hz from receivers placed between 5 and 6 km from the source was investigated. A maximum length sequence signal (MLS)

correlation method was used in order to perform measurements with a low signal-to-noise ratio. In the analysis the acoustic data was not linked to the atmospheric conditions, e.g., humidity and temperature. It is therefore difficult to use the results for the total acoustic damping to obtain the damping due to geometrical wave spreading, which is the quantity of interest in this investigation.

This review emphasizes how essential it is to systematically measure long range sound propagation over the sea and to correlate these to atmospheric conditions. In particular, the specific phenomenon of cylindrical propagation and its connection to atmospheric conditions needs to be better understood. The occurrence of this phenomenon can have an important influence on the sound levels from off shore wind farms at residential or recreational areas at the coastline

After having recapitulated the basis of outdoor sound propagation in Part II of this work, the specially developed measurement procedure, using powerful sound sources and a microphone array, which were used during the measurements are described in Part III. Part IV explains signal analysis methods utilized to improve the signal-to-noise ratio and to obtain accurate values for sound pressure levels. The performance and the accuracy of the Kalman filtering technique, the time domain averaging method and Fast Fourier Transform analysis are compared. Finally, the results of the measurements and their relationship with atmospheric conditions are presented in Part V.

BASICS ABOUT LONG RANGE OUTDOOR SOUND PROPAGATION

Sound propagation in the atmosphere is influenced by several factors¹⁰ such as geometric spreading, atmospheric absorption, wind and temperature gradients, ground impedance, topology and atmospheric turbulence.

1.1 ATMOSPHERIC ABSORPTION

The atmospheric absorption is related to the dissipation of acoustic energy into heat. It is proportional to the distance. It depends on the frequency, the temperature and the humidity¹¹. This phenomenon is very well known and described by the attenuation coefficient α (dB/km) as:

$$\alpha = \alpha_{cl} + \alpha_{rot} + \alpha_{vib,O} + \alpha_{vib,N} \quad \text{Equation 1}$$

where α_{cl} is the classical absorption coefficient; α_{rot} is the molecular absorption by rotational relaxation and $\alpha_{vib,O}$ and $\alpha_{vib,N}$ are the molecular absorption caused by vibrational relaxation of oxygen and nitrogen.

Some typical values for the absorption coefficient are given in Table 1.

<i>Air temperature</i>	<i>Relative Humidity</i>	<i>80 Hz</i>	<i>200 Hz</i>	<i>400 Hz</i>
0°C	50 %	0,246	0,644	1,47
	70 %	0,215	0,619	1,21
	90 %	0,187	0,614	1,15
10°C	50 %	0,239	0,843	1,55
	70 %	0,186	0,797	1,60
	90 %	0,151	0,728	1,64
15°C	50 %	0,217	0,93	1,87
	70 %	0,163	0,815	1,92
	90 %	0,130	0,704	1,89
20°C	70 %	0,141	0,776	2,16

Table 1: Attenuation coefficient in dB/km for different cases¹¹.

1.2 GROUND EFFECT

A boundary surface like the ground or the sea affects the propagation of sound by reflecting sound waves as shown in Figure 1.

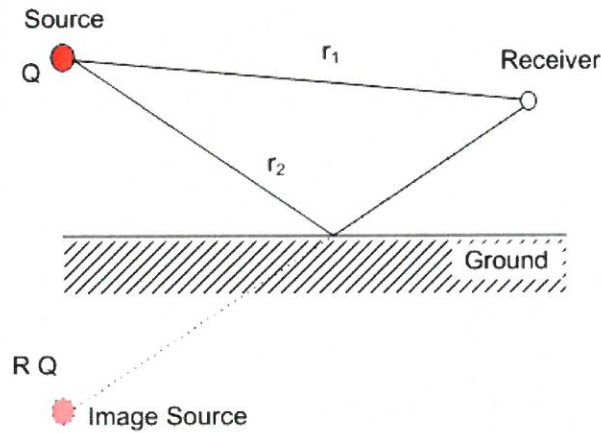


Figure 1: Ground effect.

The ground effect characterizes the attenuation due to the acoustic energy losses at reflection over a surface. This attenuation depends on the impedance of the ground Z_s , the source/receiver geometry and the frequency of the sound source. The interference between the direct and the reflected sound waves are generally noticed after several meters or more. The plane wave interferences can be calculated by¹⁰:

$$p = \frac{Qe^{-ikr_1}}{4\pi r_1} + R \frac{Qe^{-ikr_2}}{4\pi r_2} \quad \text{Equation 2}$$

where p is the complex pressure at the receiver point; Q is the source strength; r_1 and r_2 are the propagation distances of the direct wave and the reflected wave respectively and R is the plane wave reflection coefficient of the ground calculated as:

$$R = \frac{Z_s \cos \phi - 1}{Z_s \sin \phi + 1} \quad \text{Equation 3}$$

The complex reflection coefficient R is a function of the angle of incidence ϕ and the complex surface impedance Z_s which is proportional to the characteristic impedance of the ground Z_c ¹⁰:

$$Z_s = Z_c \coth(-ik_b d) \quad \text{Equation 4}$$

where d is the thickness of the reflecting (ground) layer and k_b is the acoustic propagation constant for the ground.

Different models exist for the calculation of Z_c and k_b . The model proposed by Delany and Bazley in their benchmark studies and the four-parameter model developed for a comparison of sound propagation computational programs are the most commonly used today¹⁰.

In the case of spherical waves reflected to the surface, the reflection coefficient R_s is expressed as a combination of the plane wave reflection coefficient R and a surface wave correction term F ¹⁰:

$$R_s = R + (1 - R)F. \quad \text{Equation 5}$$

The sea surface is generally considered as a hard surface with little absorption whereas grass land reduces the sound level.

The topology of the ground (noise barriers, hills, valleys, building) will also create reflection, diffractions, and shadow zones. This effect will be greater if the source is closer to the ground. However, in the case of sound propagating over sea, the “flat” topology has no influence over the transmission of low frequency sound⁶.

1.3 SHORELINE EFFECT

When the sound waves reach the coast line different phenomena happen. First, the modification of ground boundary conditions, as the surface impedance is changing suddenly, produces a supplementary sound attenuation due to the partial reflection of sound waves. Moreover, the wind and temperature gradients are also modified as the sea and the land are not always at the same temperature and friction are created from the ground surface. These effects transform the sound speed profile and affect the bending of the sound rays.

Few studies have been made of this shoreline effect for acoustical propagation. L. Johansson⁶ made simulations for different cases by changing both the ground impedance and the wind profiles at a certain distance from the source to symbolize the shoreline. The comparison with constant sound profile and ground boundary conditions shows an average attenuation for low frequencies of 3 dB.

1.4 WIND AND TEMPERATURE GRADIENTS

The speed of sound depends on the wind and the temperature. As shown in Figure 2, the wind and temperature fluctuation during the propagation cause variations in the sound speed and curve the sound waves.

The speed of sound propagating in the atmosphere depends first on the temperature of the air. Higher temperatures give higher speeds of sound. Since the temperature of the atmosphere is not uniform there are local variations in the sound speed. When the air is colder than the surface the temperature decreases with the height and the sound waves are refracted upwards. This will result in the formation of a shadow zone where the sound does not penetrate. This situation is typical during the night. On the other hand, if the surface is cold and the air warmer, the temperature is increasing with increasing height, the sound waves are refracted downwards and may be heard over larger distances. Similar phenomena occur in moving air. The sound waves will be refracted upwards or downwards depending on the wind direction as described in the first part of Figure 2.

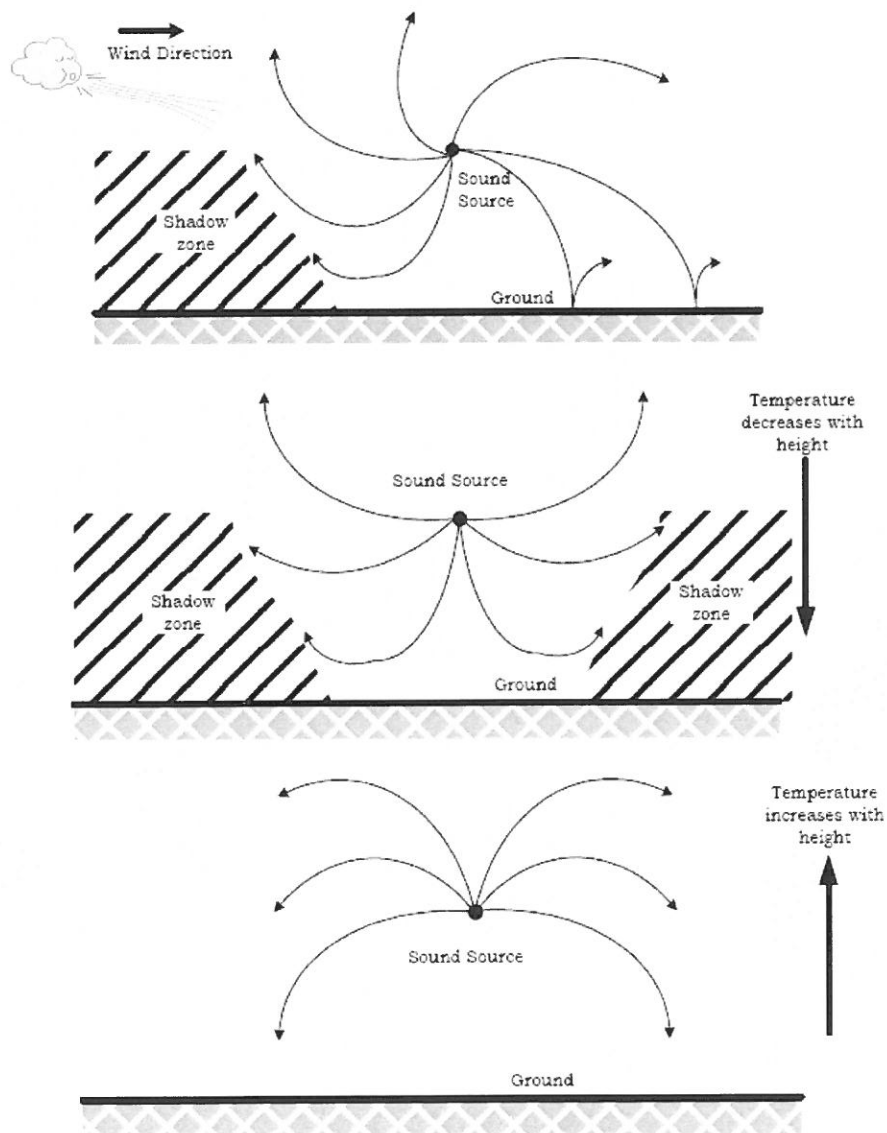


Figure 2: Propagation of sound rays with different conditions of wind and temperature gradients.

1.5 SOUND PROPAGATION OVER SEA AT LARGE DISTANCES

As seen in section 2.2, the ground effect depends on the height of the source or the receiver relative the ground. A special case of interest for the measurement situation presented later in this report is illustrated by Figure 3. In this configuration the effect of ground reflections (or mirror source) is quite different at the source and receiver positions.

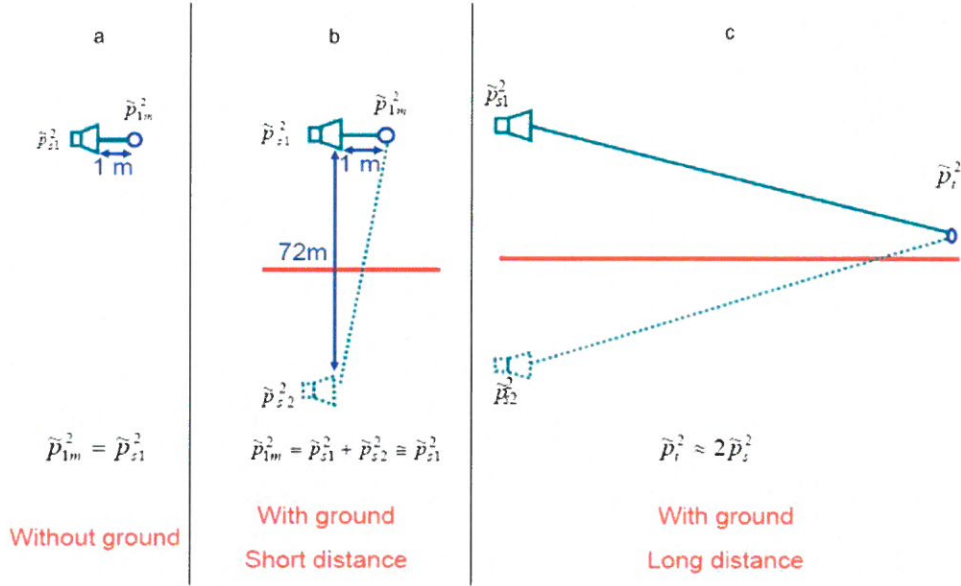


Figure 3: Different cases of ground influence.

In the case a, the receiver is at a reference distance r_0 (say 1 m) from the sound source in a free field. In this configuration there is no effect of ground reflections. The measured sound pressure equals therefore the free field value. In the case b, the sound source is situated above a completely reflecting surface (the sea) at a height $h \gg r_0$ (in our case 36 m) from a completely reflecting surface (the sea). In case c, the sound source is at the same height above the surface, but the receiver is now at a distance $r \gg h$ so that the ratio between height and distance is very small (in our experiments around 10^{-4}). In that situation the influence of the reflecting surface is as important as the direct contribution from the source.

In order to obtain a simple model that describes the effect of downwind refractive effects and a resulting cylindrical wave spreading we now introduce a reflecting layer in the atmosphere at height H . In the case of strong reflecting phenomena such as so called “low level jets”, H can be interpreted as the height of the jet. Low level jets¹² is a phenomena that can occur during certain periods of the year over the Baltic and give rise to rapid changes (gradients) in the wind speed at relative low heights (a few hundred meters). Due to the reflecting layer sound from a source will be enclosed and spherical waves will at distances $r \gg H$ appear (on the average) as a cylindrical wave, see Figure 4.

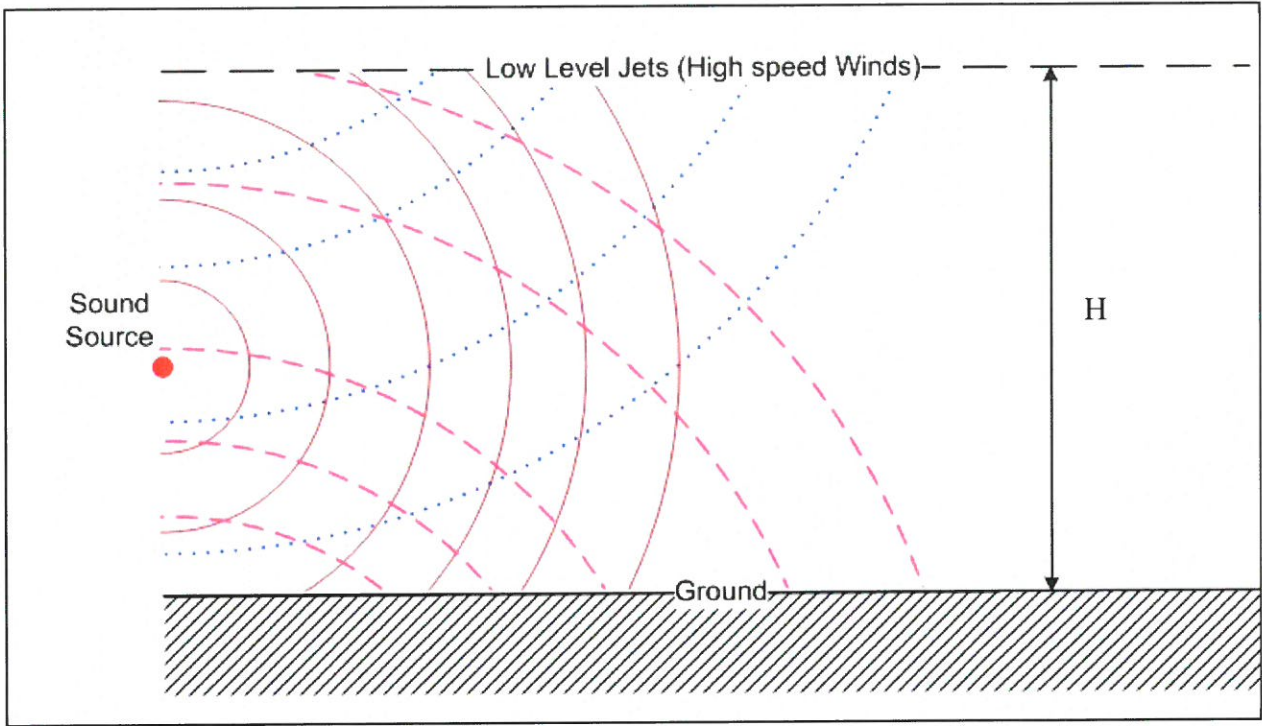


Figure 4: Effect of the LLJ over sea on the sound waves.

For distance $r \gg H$ the sound power W from the source is propagating along a cylindrical surface. This gives:

$$W = \frac{\tilde{p}_r^2}{\rho c} \cdot 2\pi r H. \quad \text{Equation 6}$$

The power is obtained assuming a free field reference position at 1 m as in Figure 3

$$W = \frac{\tilde{p}_{1m}^2}{\rho c} 4\pi \cdot r_0^2 \quad \text{Equation 7}$$

where \tilde{p}_r^2 is the sound pressure at the receiver point, r is the distance of the propagation, H the (average) height of the low level jets, W the sound power of the source, \tilde{p}_{1m}^2 is the sound pressure measured at the reference distance $r_0 = 1\text{ m}$ (in our case), ρ the air density and c the sound speed. It can be noted that equation 7 is the standard formula used for wind turbine power determination, i.e., to pick a reference position, measure the sound pressure, compensate to obtain a free field value and then by assuming an omni-directional source obtain the sound power (IEC 61400-11). Equation 7 is equivalent with the formula suggested by Ljunggren⁷ with $H=200\text{ m}$. However, here the breaking point has been related to the height H of an atmospheric inversion layer trapping the sound waves and thereby creating a cylindrical wave front.

From equations 6 and 7, a model for sound propagation over the sea including the effect of atmospheric gradients trapping the sound below a layer at height H , can be written as:

$$\tilde{p}_r^2 = \frac{2\tilde{p}_{lm}^2 r_0^2}{r^2} \cdot \frac{r}{H} \cdot e^{-\alpha r} \cdot \tau_{shore} \cdot \tau_{ground} \quad \text{Equation 8}$$

where \tilde{p}_r^2 is the sound pressure at the receiver point, \tilde{p}_{lm}^2 is the sound pressure measured at the reference position r_0 , r is the distance of the propagation, α is the atmospheric absorption coefficient τ_{shore} represents the loss due to the shore line effect and τ_{ground} is the attenuation due to the ground damping. From equation 8 the damping of sound or the transmission loss between source and receiver point can be calculated:

$$TL_{tot} = 10 \cdot \log_{10} \frac{\tilde{p}_{lm}^2}{\tilde{p}_r^2} = 10 \cdot \log_{10} \frac{r_0^2}{rH} - 3 + \alpha \cdot \log_{10} r + D_{shore} + D_{ground}, [\text{dB}] \quad \text{Equation 9}$$

where $D = 10 \cdot \log_{10} 1/\tau$.

MEASUREMENTS METHODS

1.6 MEASUREMENT SITE

The measurements started in October 2004 when the siren source was first tested. Then some further test of the procedure took place based on measurements in February 2005. After these initial tests a procedure described below for the signal analysis had been established and was used for the remaining measurements. These were focused to month of June 10 days during 2005 and one week during 2006. The reason to focus on June was that then there is a large probability for low level jets¹². Also risk for annoyance due to wind turbines should be larger in summer when the human outdoor activity is more important and connected to leisure rather than work. The measurements were performed in the Kalmar strait towards the island Öland in the Baltic Sea (see Figure 6). This location has been chosen firstly because the facilities available on the lighthouse permitted strong acoustics sources to be mounted and because a project of 24-wind turbines is planned in this region (www.eon.se).

The emission point was situated 9 km from the shore on a lighthouse (named "Utgrundens fyr"), presently used as a scientific test station.

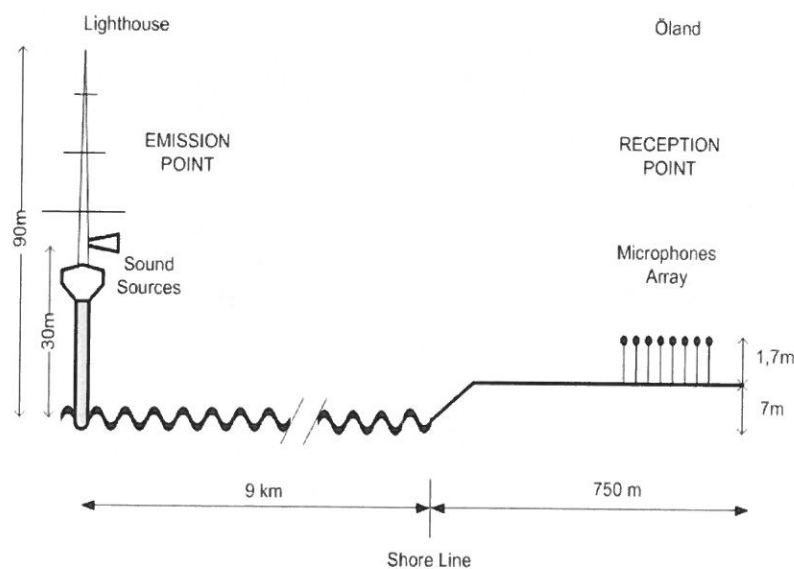


Figure 5: In situ Setup.

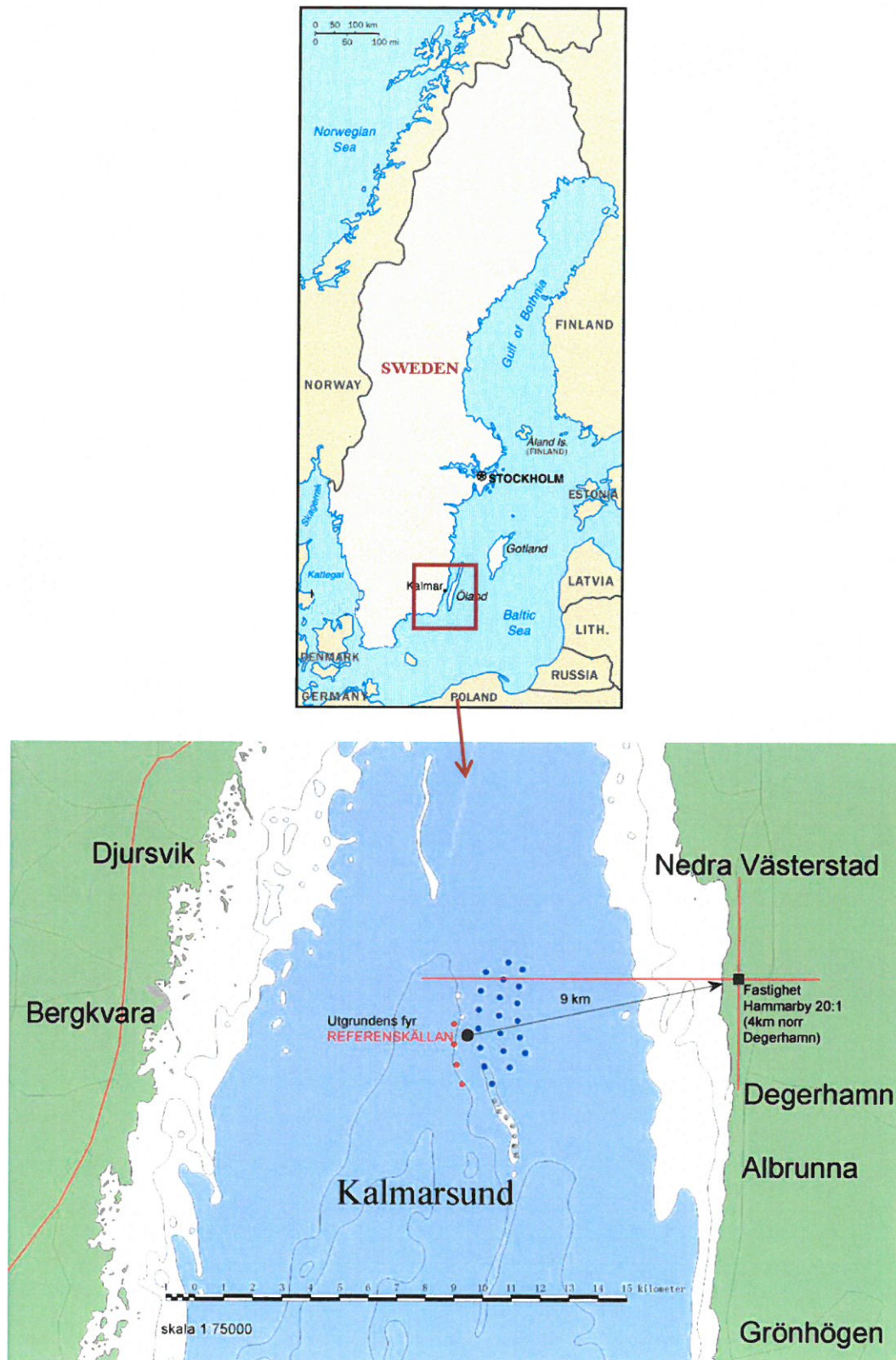


Figure 6: Site for the measurements was the old lighthouse at Utgrunden now converted to a measurement station operated by E.ON.

The receivers were located on Öland at 750 m from the shore and 7 m above sea level (see Figure 5 for the in-situ experimental setup).

1.7 SOUND SOURCES

As depicted in Figure 7, two sound sources were employed simultaneously. The first one was a compressed-air-driven sound source (Kockum Sonics Supertyfon AT150/200 with Valve Unit TV 784) placed at a height of 30 m. A microphone positioned at 1 m in front of the siren was used to measure a 10-second source signal on each occasion. The signal from the source had an average sound pressure level of 130 dB at the fundamental frequency of 200 Hz. Moreover, the first harmonic, at 400 Hz, could also be used. The siren presented variations of the order of 1% in frequency and about 20 dB in level depending on the meteorological conditions. Also the level was not constant during operation possibly due to standing wave effects in the connecting pipes carrying the compressed air. In order to have a constant and more table sound source and to investigate the sound propagation at other frequencies, a second source, consisting of a sound generator coupled to a loudspeaker and a quarter-wave resonator (1.2 m-long) was used. Also in this case, a microphone was recording the signal at 1 m from the source. The loudspeaker produced a 1 minute long signal at 80 Hz giving a constant sound pressure level of 113 dB at 1 m distance.

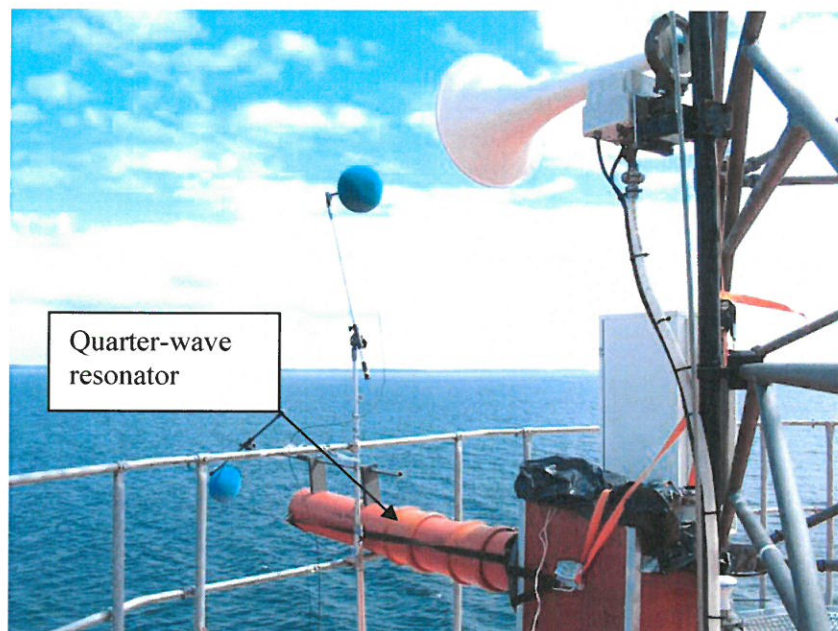


Figure 7: Sound Sources at the Utgrunden Lighthouse. The siren was driven by compressed air and produced a fundamental tone at 200 Hz (130 dB rel. 20 μ Pa at 1 m). The quarter-wave resonator produced a tone at 80 Hz (113 dB rel. 20 μ Pa at 1 m).

1.8 RECEIVERS

At first, the aim was to be able to measure the sound pressure level from the sound source at 200 Hz. As the expected sound level transmitted could be weak, a microphone antenna was designed to increase the signal-to-noise ratio. The receiver point was situated at the houses closest to the shoreline, in a very quiet residential area. Eight $\frac{1}{2}$ -inch microphones were placed on a line parallel to the direction of the emission point to create an end-fire microphone array (See Figure 8).



Figure 8: Microphone array at the receiver point.

The microphones were placed at 1,7 m height accordingly to ISO 1996. The distance between the microphones was set to 40 cm to optimize the directivity pattern pointing towards the sound source at 200 Hz. The signals were transmitted through a preamplifier to an UA100 analyzer and then processed in Matlab as explained below. The signals $x(t)$ of the N microphones were added with their respective time delays τ as shown by Eq. 10

$$s(t) = \frac{1}{N} \sum_{n=1}^N w(n) x_n(t - \tau_n) \quad \text{Equation 10}$$

where $w(n)$ are the binomial coefficients defined by $\frac{N!}{n!(N-n)!}$, N is the total number of microphones,

$\tau_n = \frac{(n-1)d \cos \phi}{c}$ is the time delay of the n -th microphone, x_n the signal recorded by the n -th microphone, d the distance from the source to the microphone, ϕ the angle between the direction of propagation and the direction of the array and c the speed of sound. The directivity patterns for 200 Hz is shown in Figure 9. Unfortunately, this antenna was not sufficient enough to distinguish the signal from the noise when atmospheric conditions were not favorable. Signal analysis techniques which are discussed in Chap IV had to be implemented. These post-processing methods produced good results for all the frequencies and appeared to be sufficient. The antenna was then not used for the measurements after 2005. Moreover, post-processing the measured data verified that the background noise was negligible at 80 Hz, 200 Hz and 400 Hz even when the sound source was not audible.

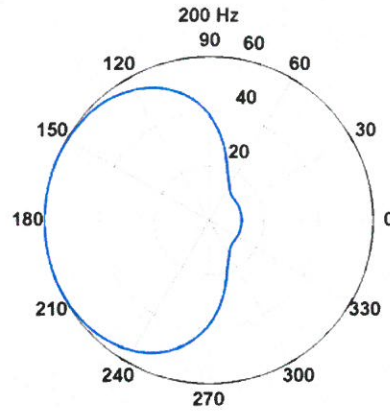


Figure 9: Directivity pattern of the microphone array for 200 Hz.

The advantage of using a microphone array compared to a single microphone is that the directivity pattern of the array allows canceling of the disturbances due to background noise coming from other directions. For instance, influence of the noise coming from a small road situated 100 m inland from the measurement position can be avoided.

Moreover, to prevent the effect of the pseudo noise from wind blowing into the microphones special elliptical shaped windshields were used. Tests in a wind tunnel at the Marcus Wallenberg Laboratory were performed. See Figure 10 for the test setup.

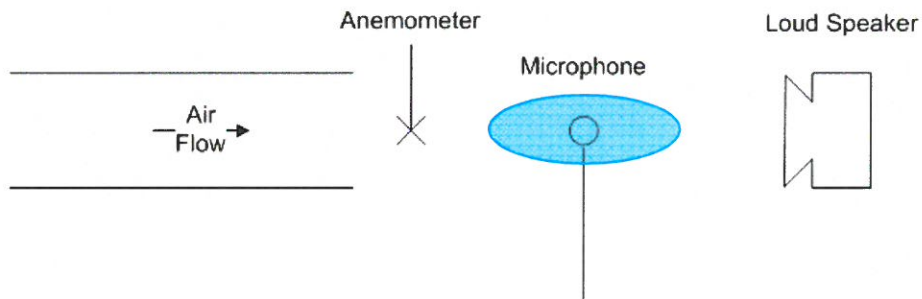


Figure 10: Setup for measurement of wind protection performances. The modified wind protection was made of foam plastic similar as the one used in the standard B&K protection. The shape was elliptical with a diameter of 200 mm in the horizontal plane and a vertical thickness of 100 mm (see also Figure 8).

The measurement showed that this wind protection was up to 5dB more efficient at 200 Hz than the normal round (B&K) one at a wind speed of 10m/s.

1.9 METEOROLOGICAL MEASUREMENTS

The wind speed was measured at 38, 50, 65, 80 and 90 m above sea level on a meteorological mast at Utgrunden. We used 10 min average automatically recorded at 38 m height for our calculations. The wind direction was determined with wind vanes at 38 m and 80 m heights. The temperatures were measured at five heights: 6, 38, 50, 65 and 80 m. The temperature closest to the sound sources was used for calculations. Finally, the relative humidity was measured at 38m height. During the measurements performed in June 2005, wind profiles at the receivers point were measured during the day using single

theodolite tracking of free flying balloons¹² Results from these measurements are presented in part IV and in more detail in Ref. 13, see also Appendices.

POST-PROCESSING TECHNIQUES

The expected propagation time between the source and the receiver can be calculated by:

$$\frac{\text{distance (m)}}{\text{sound speed (m/s)}} = \frac{9750}{343} \approx 28,4s$$

However, due to the large distance and the unpredictable wind effects, it was not possible to predict exactly when the sound would reach the microphones. Thus, the noise was recorded during 2 min which provided a good knowledge of the background noise. The first aim of the post processing was then to isolate the sound source signal (10s for 200 and 400 Hz, 1 min for 80 Hz). Moreover, as mentioned in Part I, the siren was not constant in frequency. A FFT analysis could not offer us accurate levels for the transmitted sound pressure. Therefore, specific signal-processing techniques as Time Domain Averaging and Kalman filtering were used in order to separate the signal from the noise and to acquire the exact frequency and levels.

1.10 TIME DOMAIN AVERAGING

The first method developed to extract the signal is based on a synchronized time Domain averaging (TA). The time signal recorded is divided in different segments $1/f_1$ in size, as shown in Figure 11, where, f_1 is the frequency of the sound source e.g. 200 Hz. Then all the segments contained in a $\Delta T=0.5$ second long record are added together. The components of the signal at the studied frequency and its harmonics will always add in phase to each other (Figure 11 a, b, and c), whereas components at other frequencies will be reduced (Figure 11 d, e and f). The method is simple and fast, giving valuable information about the sound pressure level of the signal and its position in the recorded track. This method was very useful to reduce the calculation time of the FFT and the Kalman analysis method.

However, the time domain averaging method has some limitations. First, it includes all the harmonics of the studied frequency. Although the higher harmonics are supposed to have little contribution to the main signal, in our case we found that the first harmonic at 400 Hz had a level comparable to the main frequency. The second limitation is that in the way it has been used here it introduces a ΔT s error for determining the beginning and the end of the signal. A typical result from the time averaging method is depicted in the second curve of Figure 12

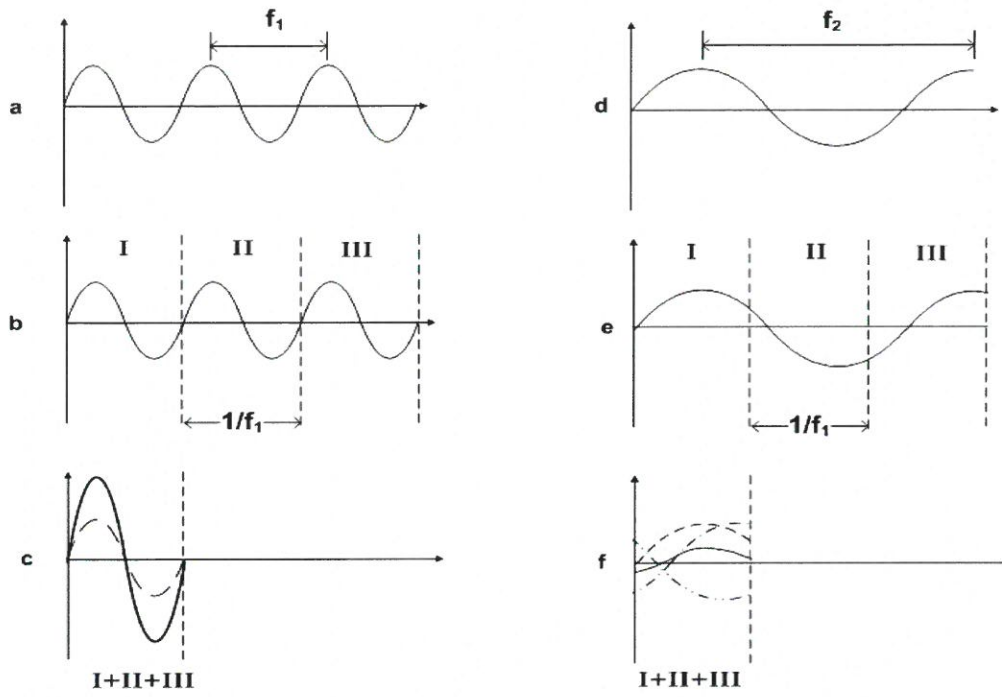


Figure 11: Time averaging method: 4a, 4b, 4c for the studied frequency f_1 ; 4d, 4e, 4f for another frequency f_2 .

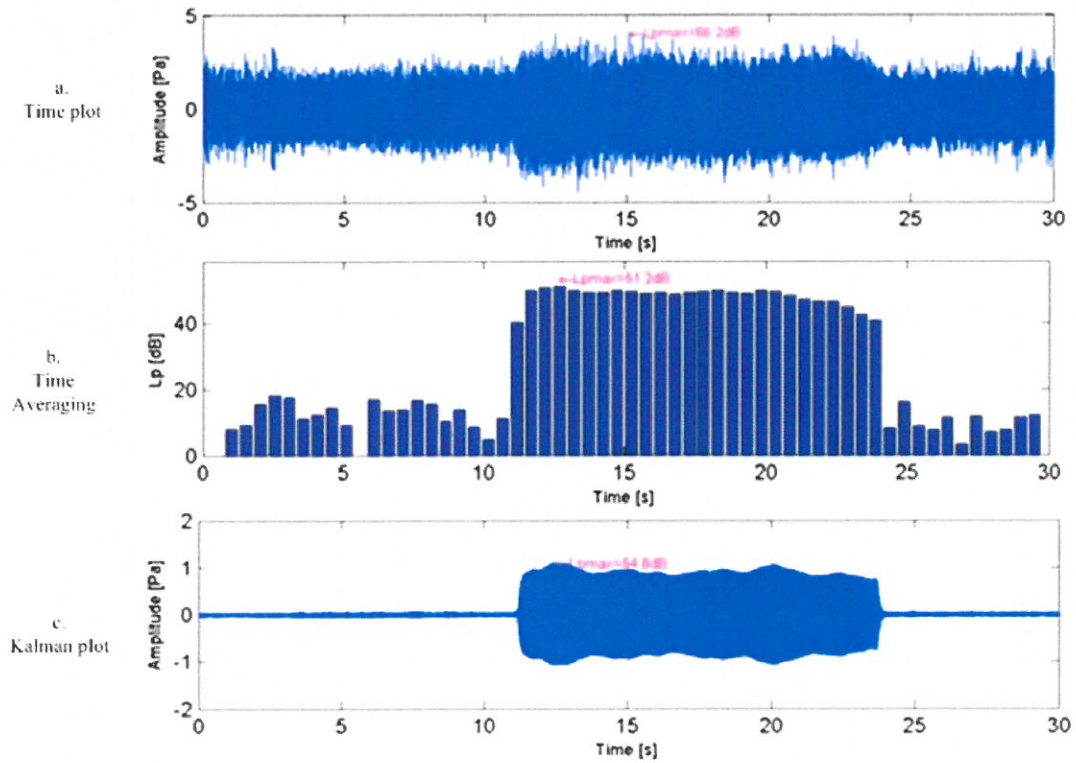


Figure 12: a. Time signal; b. Signal after Time Domain Averaging; c. Signal after Kalman Filtering.

1.11 KALMAN FILTERING

Another method to extract the signal is to use a Kalman filter¹³. In 1960, R.E. Kalman¹⁴ presented a new approach to linear filtering and provided a new way of solving the problem of separation of random signals from random noise introduced by Wiener. A Kalman filter combines all available information about the measurement in order to find an estimate of the desired variable with a minimal error. In our case, as the frequencies of the sound source signals are known, they can be implemented in the Kalman Filter. This was done using a code developed at KTH by Ulf Carlsson.

The Kalman method is more accurate than the time averaging technique. Since no averaging is computed over a time sequence in the Kalman filtering, the result is more precise in time. Another advantage is that no contributions from higher harmonics are introduced. The beginning and end of the signal can also be accurately determined. The signal to noise ratio is higher than with the time averaging method. The Kalman method is slower than the time averaging. For a 30 s signal the analysis by Kalman filtering required approximately 100-120 s to converge on a standard PC, whereas only a few seconds were needed for the time averaging method.

1.12 FAST FOURIER TRANSFORM

The last method used is a classic Fast Fourier Transform (FFT) over the part of the measurement containing the signal from the source. As it was not possible to distinguish the sound source signal in the 2 min measurement period, a first analysis through the Kalman filter and the Time Averaging method has been performed. It allows us to know exactly the start and stop of the studied signal. Then by computing an FFT we could know the exact frequency of the signal. Moreover, by computing a FFT just few seconds before or after the signal, the level of the background noise could be determine and compared with the level of the sound source. When the two levels present a difference of less than 10 dB, the measurement was dismissed.

Furthermore, two FFT's have been calculated: the first was performed over the time signal directly from the array, the second over the time signal after the Kalman filter. Both gave essentially the same result, which proves that the Kalman Filtering does not add any gain to the signal.

1.13 CONCLUSION

The three methods have been used simultaneously for the each measurement. The algorithm is depicted in Figure 13. First, an analysis by the time averaging technique and Kalman filter method with a rough estimation of the frequency is performed to locate the signals from the sources in the measurement. Then, when the location is know, a FFT is performed in order to get the exact frequency of the sound source. The Kalman filter method is then implemented using this frequency in order to obtain the sound pressure level at the receiver points. This procedure is repeated for each frequency of interest.

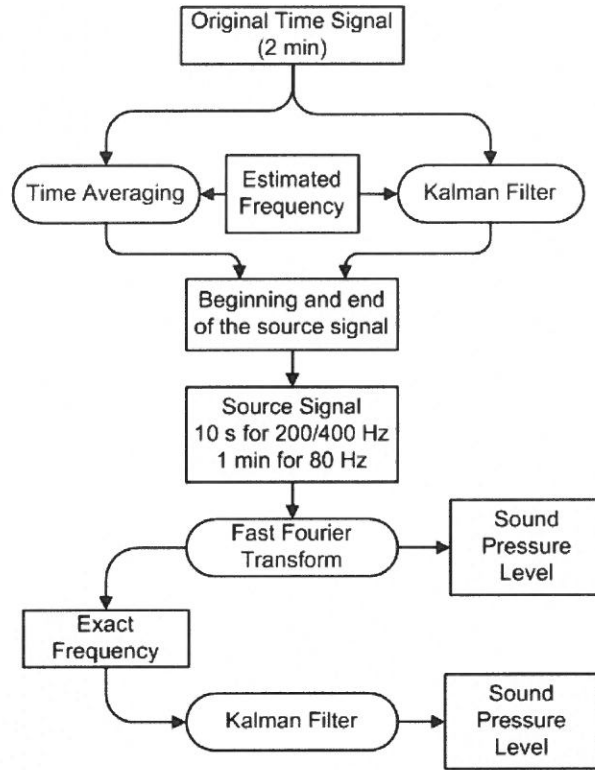


Figure 13: Algorithm of the Post processing Techniques.

RESULTS AND ANALYSIS

Previous atmospheric studies in the Baltic Sea have shown that the most interesting phenomena from an acoustical point of view occur in late spring and early summer⁴. Thus two measurements periods in June 2005 and June 2006 were performed. Wind speed, wind direction, humidity and temperature have been measured at the source at the same time as sound pressure level. Furthermore, measurements¹² of wind profiles at the receiver point have been performed in June 2005.

1.14 METEOROLOGICAL MEASUREMENTS RESULTS

1.14.1 Wind speed and direction

The wind speed and the wind direction are two important factors for long distance sound propagation problems. Modern wind turbines start producing energy for wind speeds over 5m/s. In Sweden, acousticians are recommended¹⁵ to measure noise in downwind directions only, .i.e., when the angle between the wind direction and the sound propagation direction is $\pm 45^\circ$. This corresponds to the dark area in Figure 15. However, as shown in Table , in our case, that situation did not occur often enough to be able to draw valuable conclusions. But as shown in Figure 15 most of the measurements in upwind conditions occurred when the wind direction was very close to downwind conditions. Thus, the results are expected to be similar and in the analysis all the data have been used.

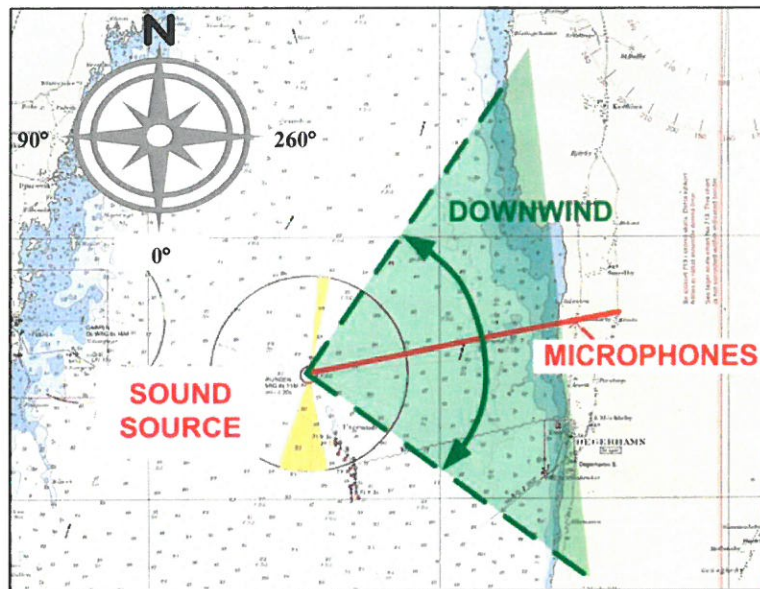


Figure 14: Direction of propagation (plain line) and downwind conditions (between the dashed lines) according to Swedish recommendation.

	200 Hz	400 Hz	80 Hz
ALL	160	160	93
DOWNWIND	42	42	23
UPPWIND	118	118	70
UPPWIND and > 5m/s	76	76	48
UPPWIND and < 5 m/s	42	42	22
DOWNWIND and < 5m/s	20	20	20
DOWNWIND and > 5m/s	22	22	3
< 5m/s	64	64	25
> 5m/s	96	96	68

Table 2: Number of acoustic measurements for different wind conditions.

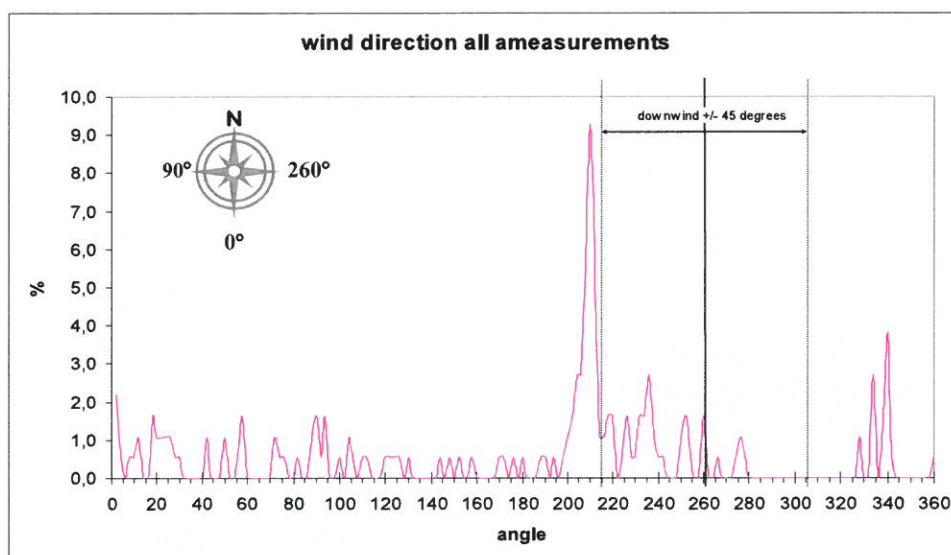


Figure 15: Relative occurrence of wind directions measured at Utgrunden during the acoustic testing.

1.14.2 Sound Data

From equation 9 we obtain the transmission loss due to the geometrical spreading (gs):

$$TL_{gs} = 10 \cdot \log_{10} \frac{r_0^2}{rH} = TL_{tot} + 3 - \alpha \cdot \log_{10} r - D_{shore} - D_{ground}, \text{ Equation 11}$$

From the measured data TL_{tot} is known. The atmospheric damping was calculated using the meteorological conditions at the source and ISO 9613-1¹¹. Then in accordance with the Swedish Environmental Protection Agency model⁷ the effects of shore and ground damping are neglected. In the figures below the resulting statistical distributions for the transmission loss due to geometrical spreading are presented. In the data analysis all wind directions are included since a detailed analysis (see Appendix 1 and Ref. 12), shows that a good transmission do not always correlate with a downwind condition. The purpose of the analysis is to produce estimates for the average transmission for the most interesting period of the year which as argued above was chosen to be the month of June.

Figure 16 shows the relative occurrence of a specific transmission loss value based on Equation 11 for the three frequencies 80 Hz (dotted line), 200 Hz (blue line) and 400 Hz (dashed line). Figure 18 shows the cumulative distribution, i.e., in what percentage of the measurements the transmission losses are higher than a certain value. In both graphs, the bold line at 80 dB marks the theoretical transmission loss due to spherical spreading giving 6 dB damping per doubling of distance and 63 dB marks the case of a cylindrical spreading (3 dB per doubling of distance after 200 m) according to the Swedish recommendation⁷. The assumed propagation distance is 9750 m.

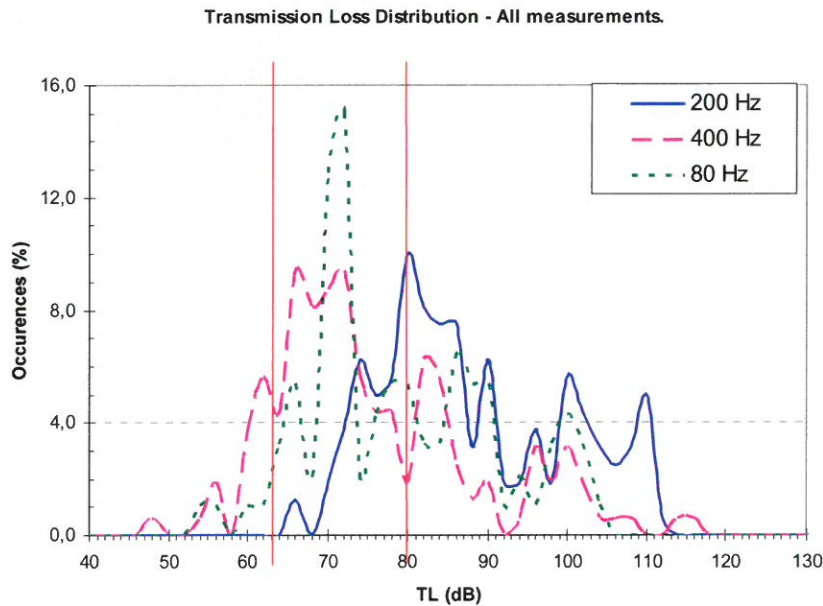


Figure 16: Relative distribution of transmission loss due to geometrical spreading.

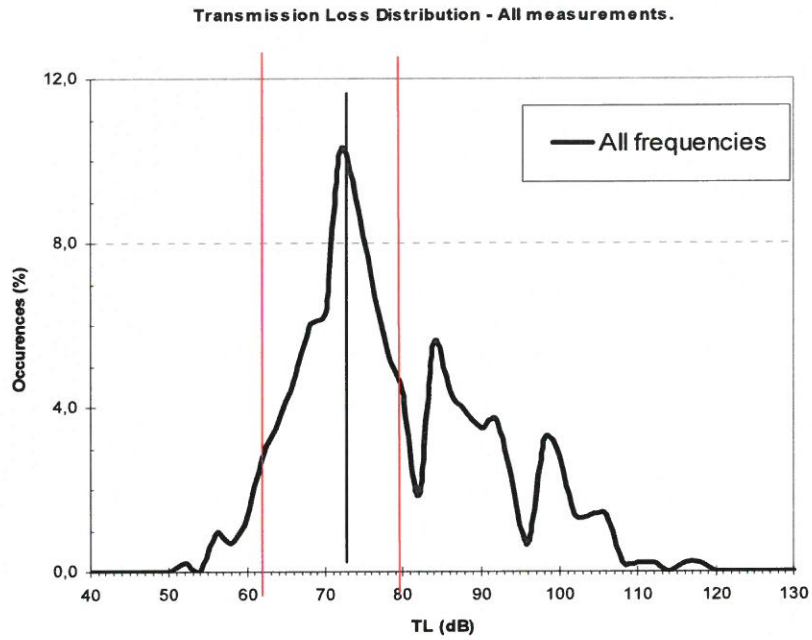


Figure 17: Relative distribution of transmission loss due to geometrical spreading.
All frequencies added and with the ground damping at 200 Hz removed.

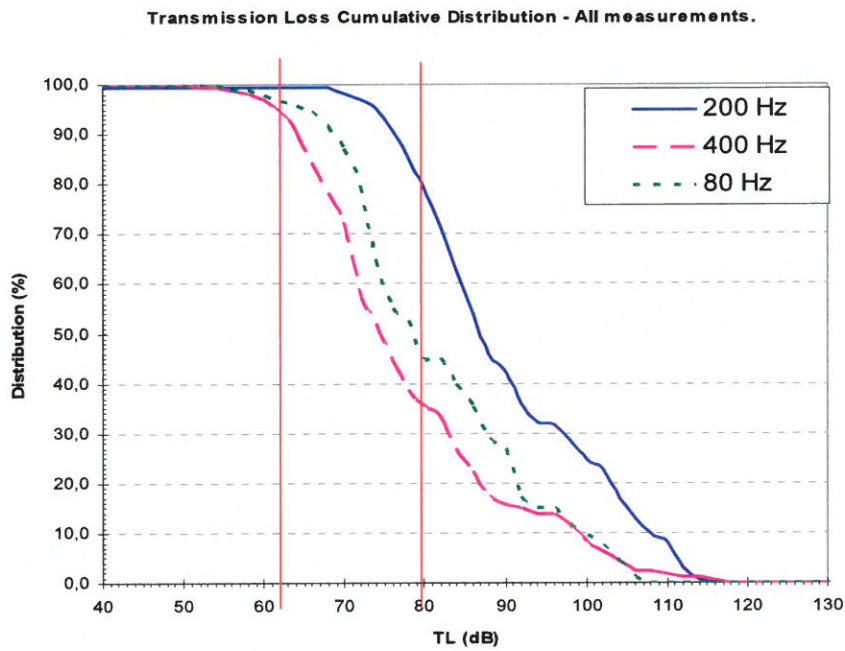


Figure 18: Cumulative distribution of transmission loss due to geometrical spreading.

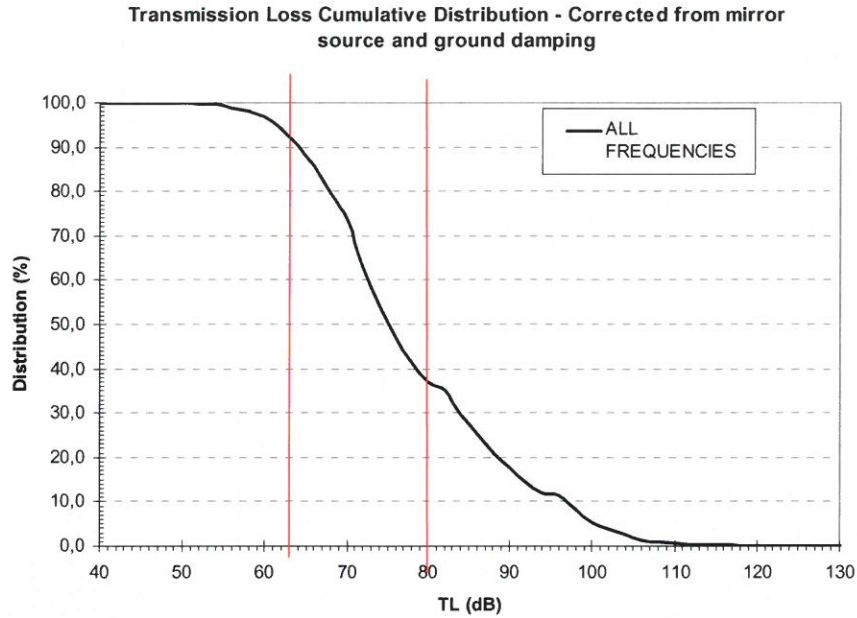


Figure 19: Cumulative distribution of transmission loss due to geometrical spreading. All frequencies added and with the ground damping at 200 Hz removed.

The fact that the transmission loss sometimes is larger than for spherical propagation can be explained by factors such as the effects of the shore line, the sea, the waves, the wind and temperature gradients which were not taken into account in the calculations.

It can be noticed that the transmission loss are higher at 200 Hz than for the 2 other frequencies. This difference is almost certainly due to attenuation of the acoustics waves over ground at that frequency¹⁰. As the frequencies at 200 Hz and at 400 Hz come from the same source signal (the siren), they travel together and are submitted to the same conditions. They could therefore be expected to have the same average damping due to wave spreading. Assuming this one finds that the ground damping effect at 200 Hz is close to 14 dB. This is in remarkable agreement with an old Danish measurement² at Saltholmen performed with similar set up, i.e., a long sea distance (~ 7 km) and a short distance on land. Once the ground damping for 200 Hz is corrected, we can plot all the frequencies together to find an average transmission loss. Figure 17 and Figure 19 depict the transmission loss with all the frequencies added and the ground damping removed. Table 3 summarizes some different transmission loss estimates obtained from the experiments. The values given for 200 Hz have been corrected for the ground damping as described above. TL10 represents the transmission loss exceeded 10% of the time. In the same way, TL90 represents the transmission loss exceeded 90% of the time.

	80 Hz	200 Hz	400 Hz	All frequencies
Average TL = $\frac{1}{N} \sum_n 10^{-TL_n/10}$ (dB)	70	67	67	68.4
TL10 (dB)	97	94	95	97
TL90 (dB)	65	62	62	64

Table 3: Summary of transmission loss values (geometrical spreading only) based on measurements in Kalmarsund June 2005 and 2006. Note the values at 200 Hz are corrected for the ground damping effect.

PREDICTIONS MODELS

1.15 F.F.P.

The Fast Field Program has been first developed for underwater acoustics and applied later for atmospheric propagation^{16,17,18,19}. The method assumes that the geometry and medium parameters are range-independent and consists of using a Hankel transform to transform the Helmholtz equation in cylindrical co-ordinates to an ODE boundary value problem with the vertical co-ordinate as independent variables. A Fast Fourier Transform is then used as an approximation to the Hankel transform. In FFP the continuous variation of sound speed with height is replaced by a stratified variation.

A large amount of articles deals with predicting outdoor sound propagation by using FFP programs. They mostly address two problems, first the influence of wind and temperature gradients, second the effects of ground impedance and ground discontinuities. It is beyond the scope of this report to describe the matter in detail but a very precise description can be found in two tutorials^{20,21} and a comprehensible summary²² has been already published by the author.

1.16 RAY TRACING

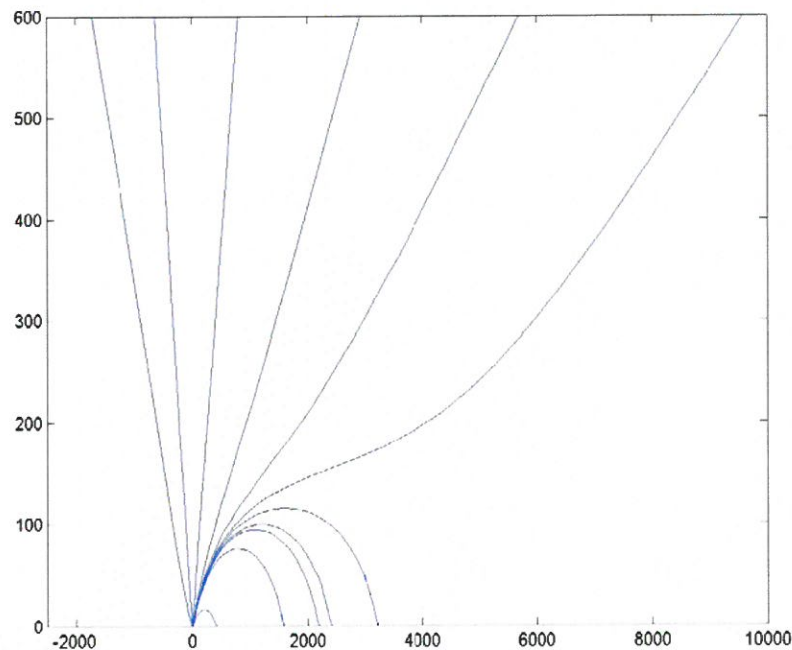


Figure 20: Calculation using Ray Tracing Method.

Ray tracing²³ is a technique widely applied to approximately calculate wave propagation in optics and in acoustics. If the wavelength of the sound is small compared to the dimensions of surfaces in the medium (as the ground or walls) and small as well compared to the scale of variations in the density, sound speed or flow speed then we can use the theory of ray tracing. Indeed, using the assumptions of geometrical acoustics, a sound ray can be considered to represent the normal direction to a wave front propagating away from a source. The path of such a ray can be traced using simple three-dimensional geometry. The ray theory is relative simple and intuitive and often used as a first approximation for high frequencies.

As an example of the results that can be obtained using ray tracing techniques, a Matlab code has been built. Eleven different angles θ have been chosen in order to illustrate the behavior of the ray paths as function of ray elevation angle at the source. The wind speed at the ground level was chosen to be 20m/s and exponentially increasing as function of height. Figure 20 shows the ray paths in the x-z plane when the source is placed at the point (0,0). We can clearly see the formation of a shadow zone in the downwind direction. We need to point out that in this figure the ray paths are terminated at the ground surface, the reflections are not taken into account.

In Sweden, a more complete and accurate model called XRAY has been developed by Ilkka Karasalo at the Swedish Defense Research Agency²⁴. Using this model preliminary analysis and modeling using the data collected at Utgrunden have been carried out and promising results indicate that good quality predictions of the sound levels are possible, also in presence of a complicated sound speed profile, see Figure 21.

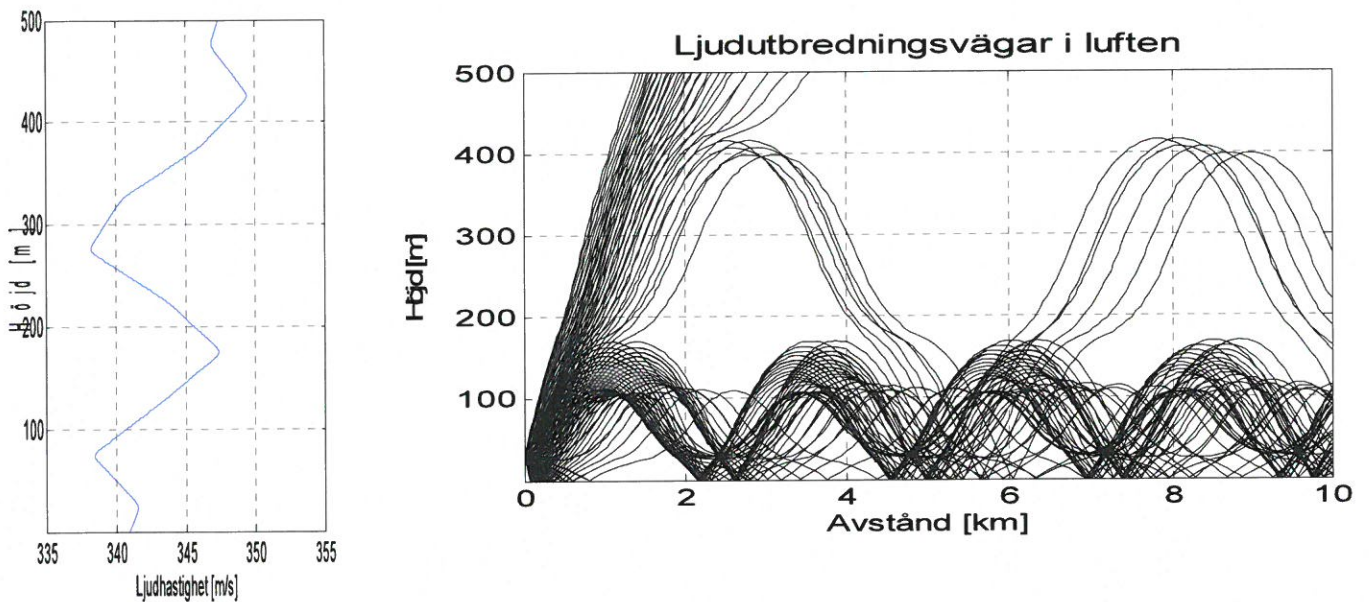


Figure 21: Left: Sound speed profile as function of height. Right: Predicted propagation of rays of sound as function of height and distance for this profile²⁴.

1.17 PARABOLIC EQUATION

Like the Fast Field Program, the Parabolic Equation (PE) method has first been developed for underwater acoustics. PE methods are applicable when the geometry and/or the medium parameters are weakly range-dependent. The original PE method by Tappert²⁵ was accurate at propagation with small elevation angles ($\leq 14^\circ$) only.

In the beginning of the nineties, wide-angle approximations have been developed and it is now one of the most used methods. As an example of the results that can be obtainable using PE methods, the equations proposed West, Gilbert and Sack²⁶ giving a wide-angle approximation, was coded in Matlab giving the results depicted Figure 22. The source had a Gaussian distribution in space and was centered at 2m of height. The calculations were done for a frequency of 50hz and a ground flow resistivity of 120 kR/m. The sound speed gradient was constant and either 0.2 1/s positive or negative.

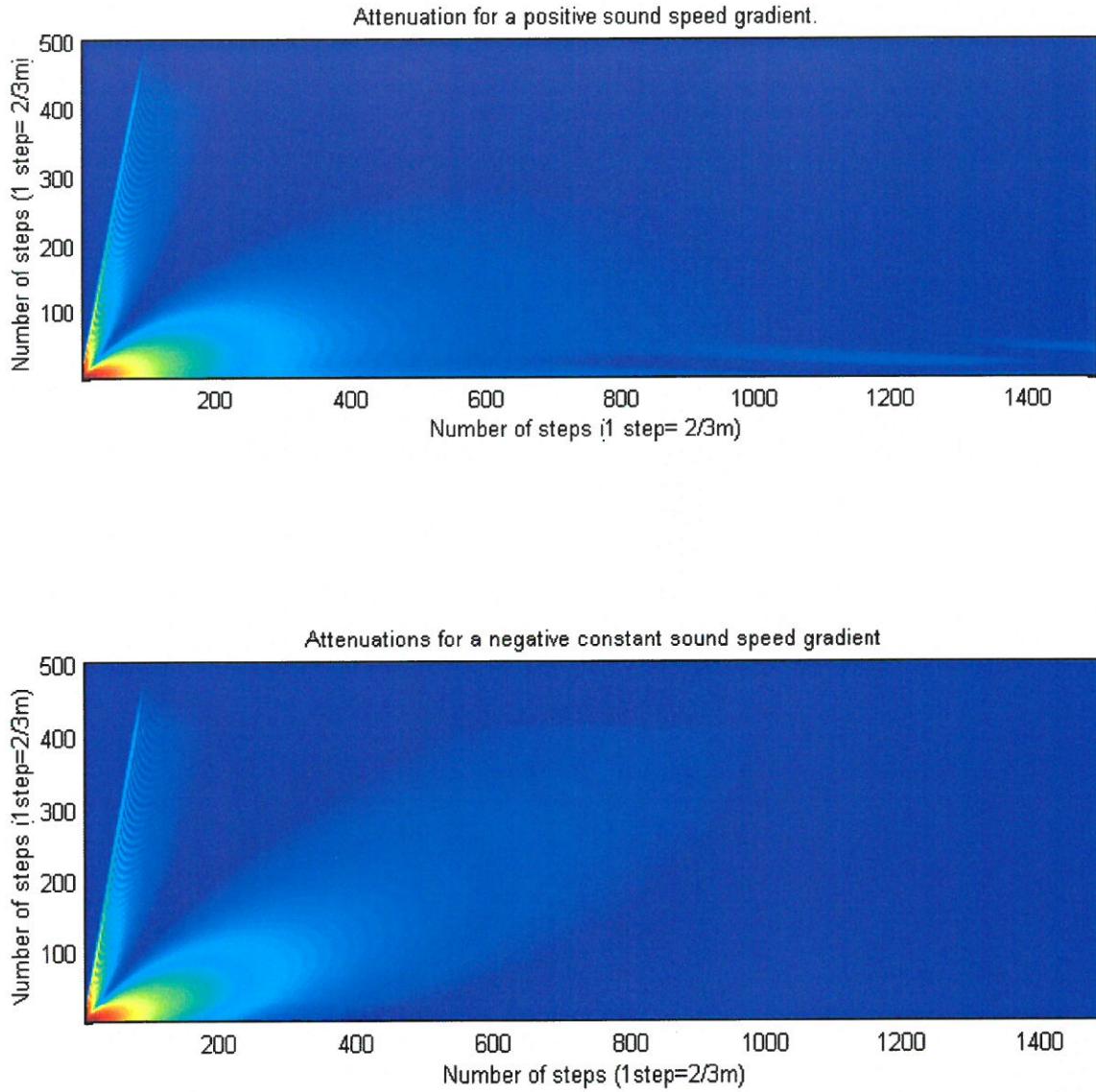


Figure 22: Attenuation of the sound field using a Parabolic Equation Method under upwind and downwind conditions.

Recently, a new approach of the parabolic equation method has been initiated. Salomons²⁷ Gilbert and Di²⁸ used a Green's function method for calculating the Parabolic Equation instead of the Crank-Nicholson algorithm. This method support a calculation step which can be very large compared to the wave length. The starting point is to express the sound field at one point ($r_1=r_0 + \Delta r$; z_1) as an integral over the vertical line at the previous point ($r=r_0$) by using the Kirchhoff-Helmholtz integral equation. By using a Fourier transform, the field at $r + \Delta r$ can be calculated from the field at r . The sound pressure field is expressed as a product of an exponential factor and the sum of three terms which represent the direct wave, the reflected wave and the surface wave. Besides the fact that the horizontal steps can be much larger, this method permits to include directly the boundary conditions for the finite ground impedance. In practice, the Fourier transforms are completed by a FFT algorithm. In this project efforts were made to

code this method and this work is still ongoing and a final version of the code ready for use has not been finished.

SUMMARY AND CONCLUSIONS

One of the first long term measurements of transmission of sound over the sea have been performed in the Baltic region. One purpose being to obtain better data for judging the validity of the Swedish recommendation for estimating noise from sea based wind turbines⁷. This recommendation which is unique in the world assumes cylindrical wave spreading after a distance of 200 meters. Since cylindrical wave spreading compared to spherical only gives a reduction of 3 dB/distance doubling compared to 6 dB, this has large consequences on the predicted noise imission from wind turbines. Furthermore the work was intended to explore the relationship between good sound transmission and meteorological phenomena such as low level jets. This work was performed in co-operation with MIUU at Uppsala and is reported in detail in Ref. 12. One important observation from this part is that the good transmission conditions for long range propagation do not necessarily correlate with downwind conditions. Part of the work was also to develop procedures for the measurement of long range sound transmission and to develop modeling based on the parabolic equation. Regarding the measurement procedure it is described in detail in Sec. IV. For the modeling it was decided to use a parabolic equation method based on a Greens function approach. The modeling part is still not finished and work on this will continue at KTH in co-operation with FOI. Concerning the results from the measurements they are summarized as statistical distributions in sec. 5.1.2. Based on the distributions one can calculate various averages and expected values for the transmission loss or TL (compensated for atmospheric damping so that only the geometric spreading is included) as summarized in the table below.

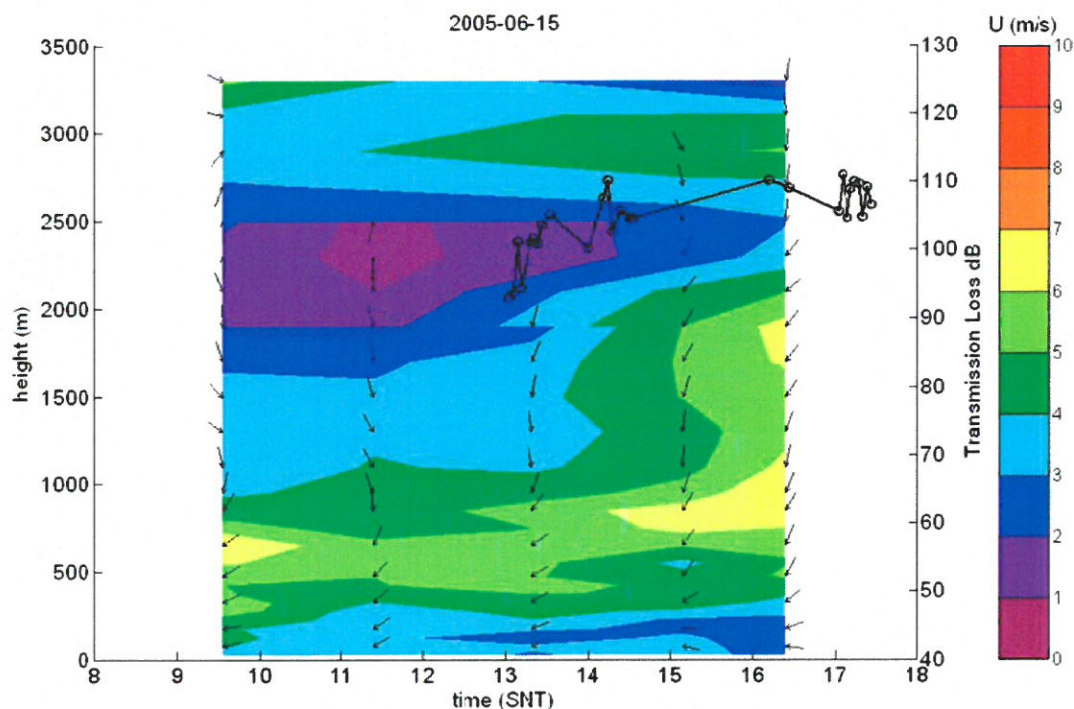
Data from Utgrunden June 2005/2006	80 Hz	200 Hz	400 Hz	All frequencies
Average $TL = \frac{1}{N} \sum_n 10^{-TL_n/10}$ (dB)	70	67	67	68.4
TL10 (dB)	97	94	95	97
TL90 (dB)	65	62	62	64

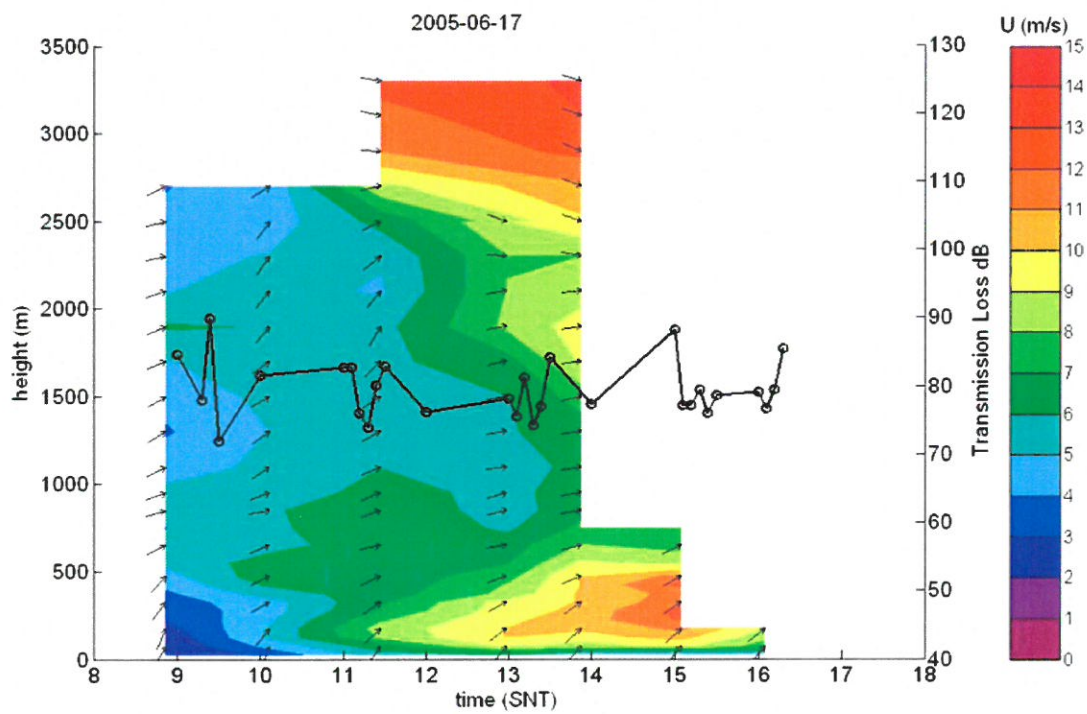
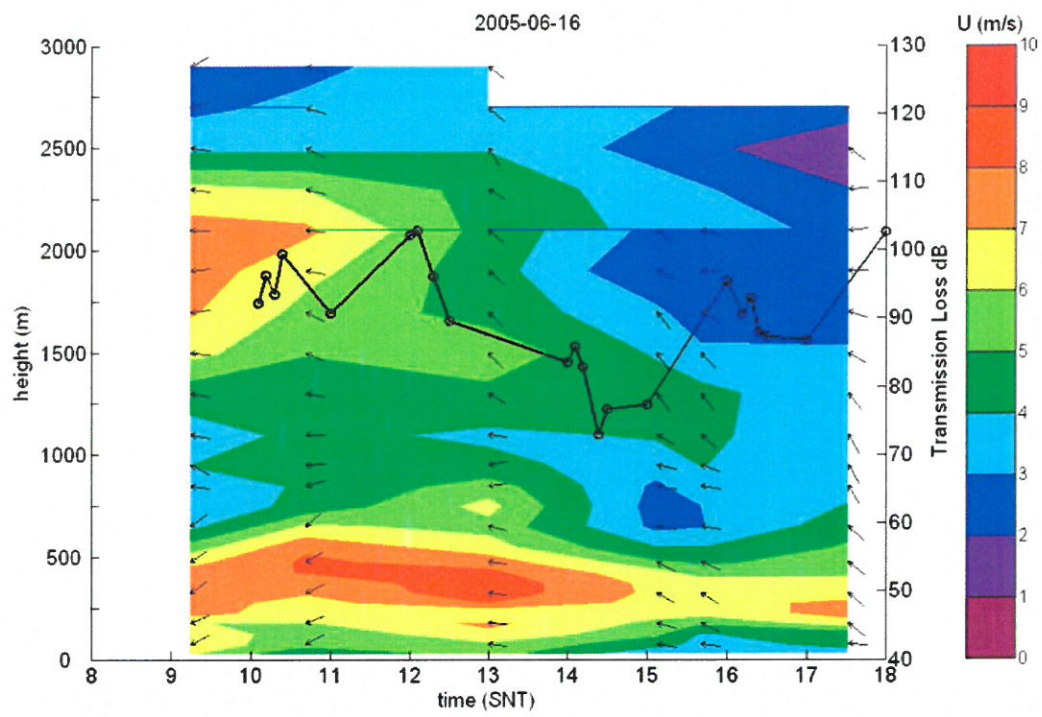
The TL (average) value for the propagation (geometric spreading) part only based on the Swedish model⁷ and a distance of 9750 m is 63 dB. In this model the breaking point for cylindrical transmission is set to 200 m. Our data gives a value of 68.4 dB for the average transmission. Using this and equation 11 gives a value around 700 m for the breaking point. Or as we define it here (see sec. 2.5) the average height H of the inversion or reflecting layer trapping the sound and thereby causing a cylindrical wave spreading. It can also be noted from the table that TL90 (the TL value exceeded 90 % of the time) rather than the average is closest to the value predicted by the Swedish model.

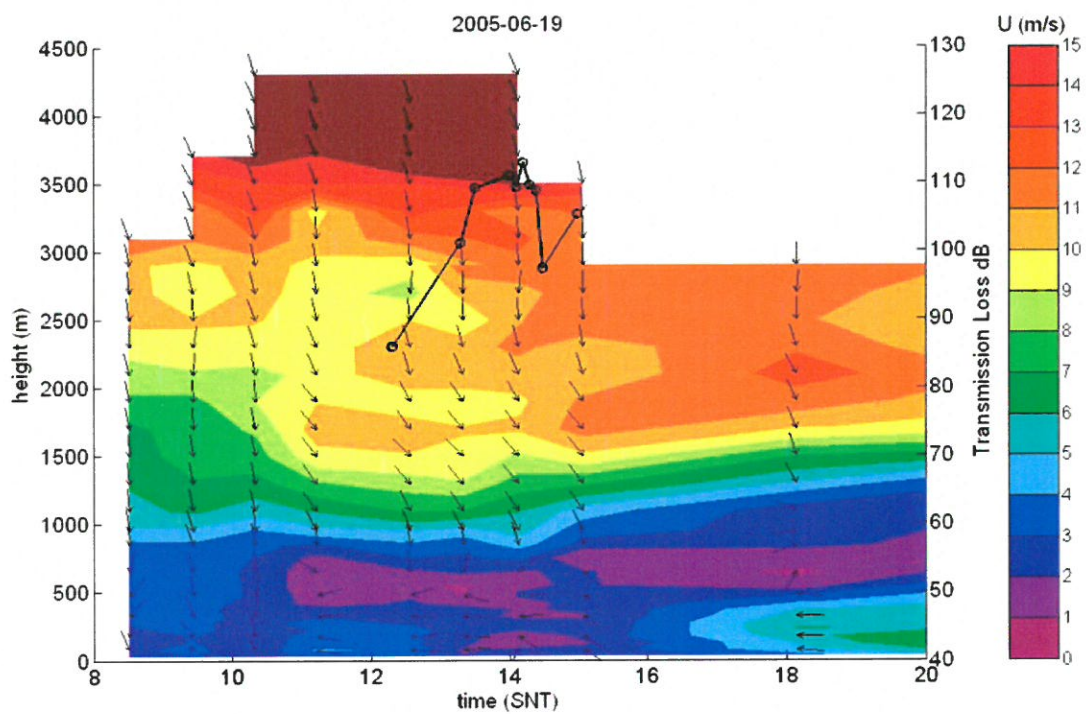
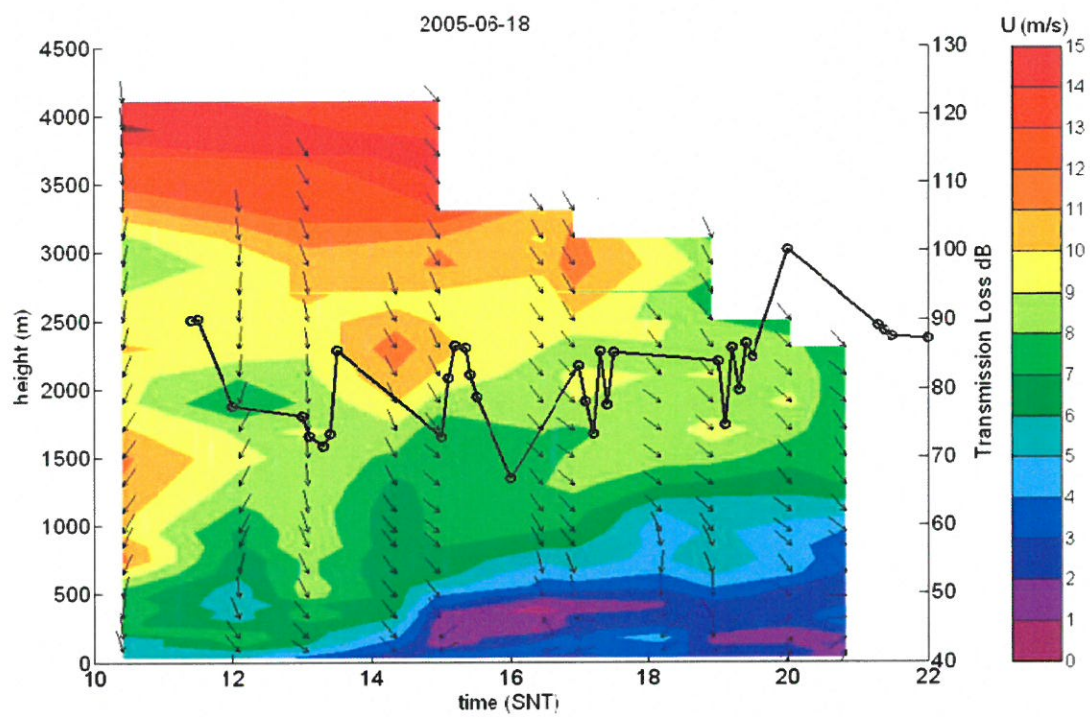
It is difficult to state how general the results are. More measurements are needed also at other locations. This is now possible using the procedures developed in this work. However, an alternative to such long term efforts would be to combine fast simulation techniques, e.g., mainly ray-tracing, with the meteorological data base existing at MIUU to simulate the transmission statistics.

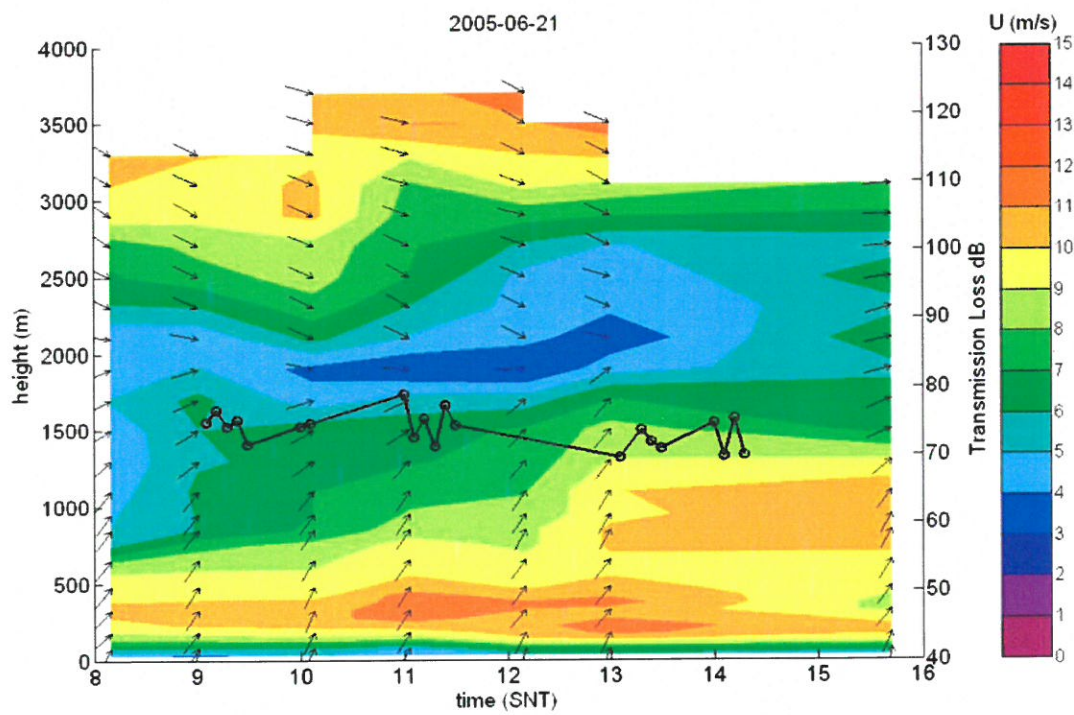
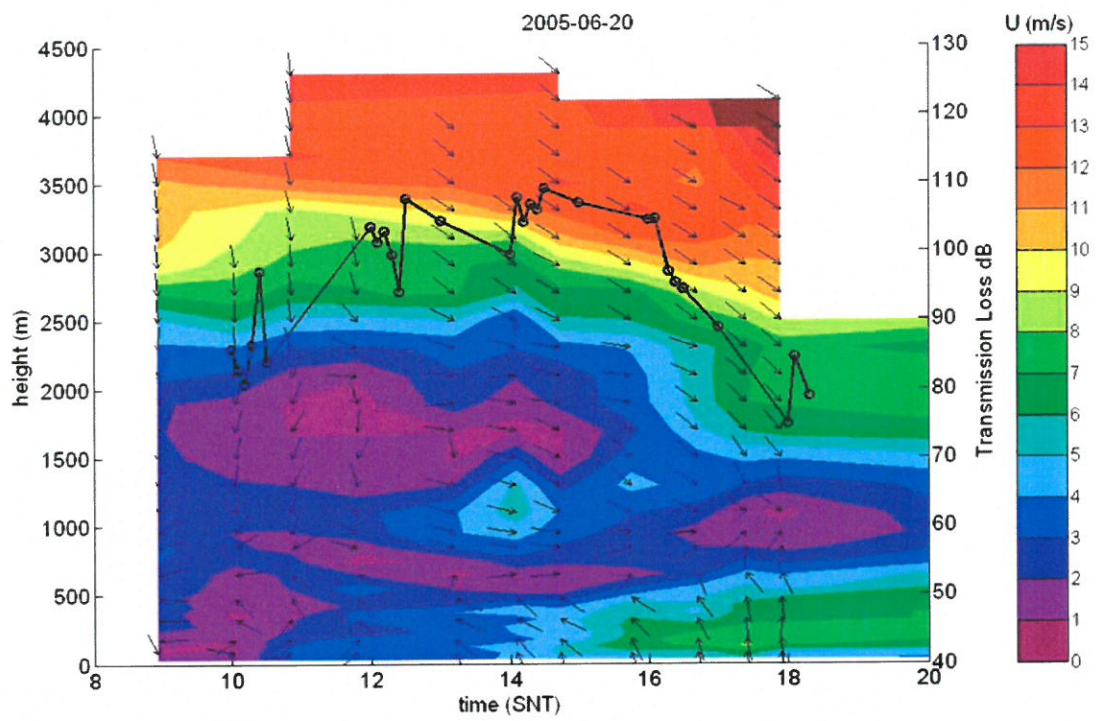
APPENDIX 1: EXAMPLES OF WIND SPEED, WIND DIRECTIONS PROFILES AND TRANSMISSION LOSS DATA AT 200 HZ, JUNE 2005 ÖLAND

The variation of the transmission loss due to geometric spreading at 200 Hz measured at Hammarby in June 2005 is plotted against time (Swedish Standard Time, SNT) together with the wind measured by theodolite tracking of free flying balloons at the same time and place¹². The data is not compensated for the ground damping which was observed at 200 Hz. The colors in the plot show the wind speed, while the arrows give the direction of the wind, where a downward pointing arrow indicates northerly winds and an arrow pointing to the right indicates westerly winds, i.e., towards Öland and the receiver side. In general the figures show a lower transmission loss when the wind is towards Öland. Compare for instance the results from 2005-06-16 with 2005-06-17. Not also the low level jet (LLJ) structure that exists during 2005-05-16, which probably explain why low transmission values also occur during this “upwind” condition. A good example of a LLJ structure combined with wind towards the receiver is 2005-06-21. This combination also exhibits the lowest transmission loss values of the cases presented below.



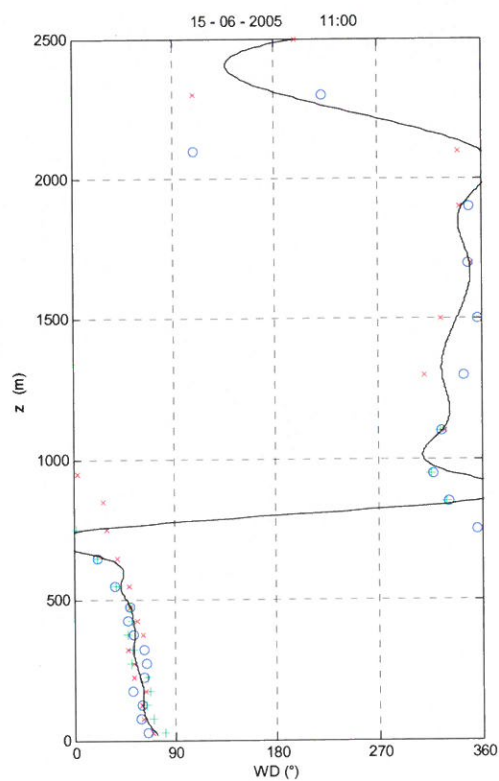
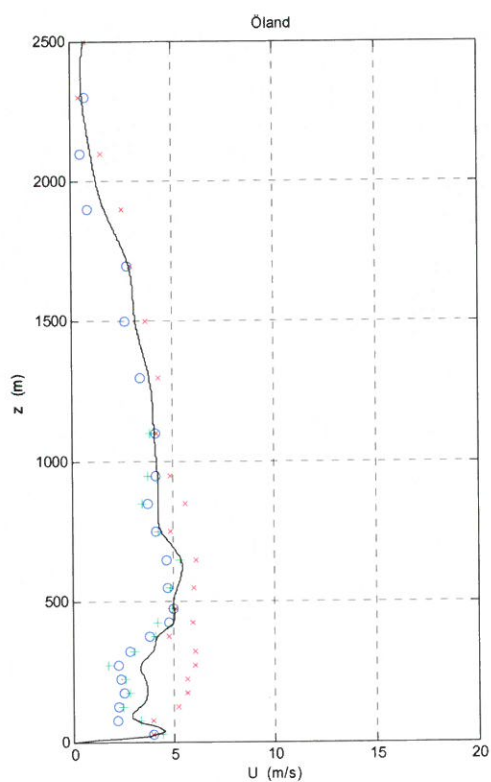
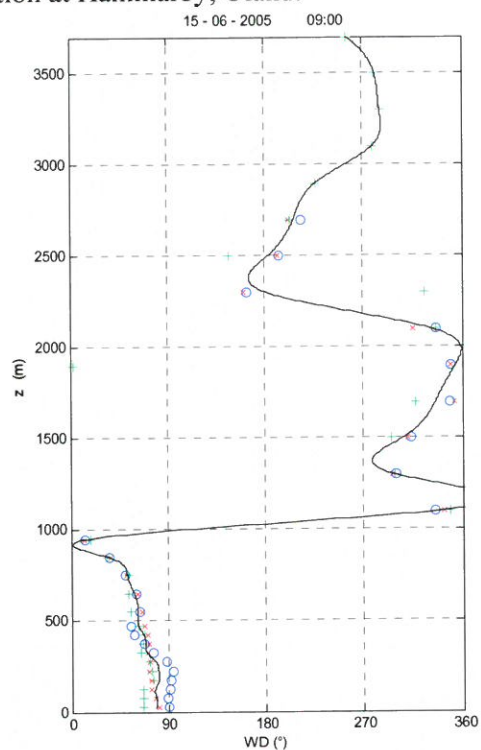
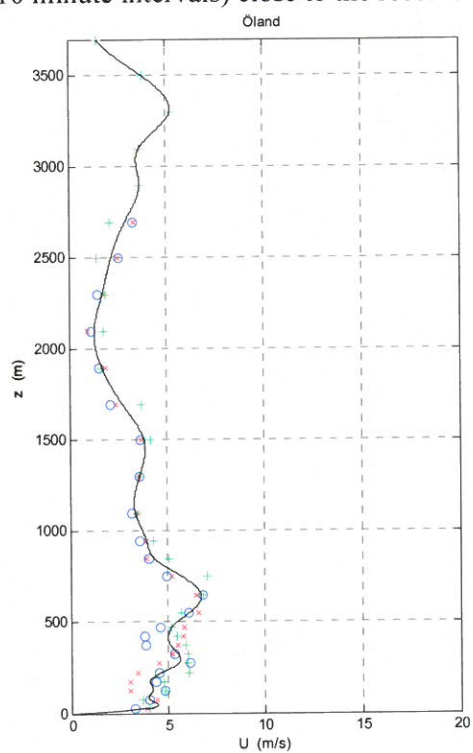


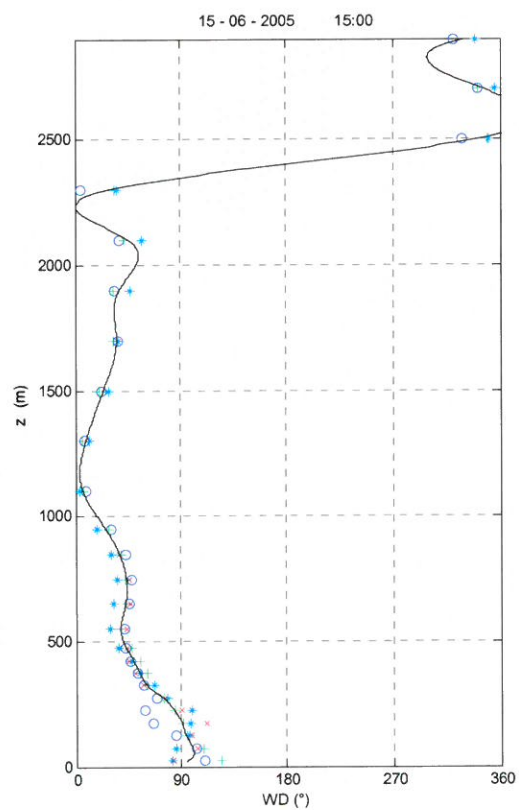
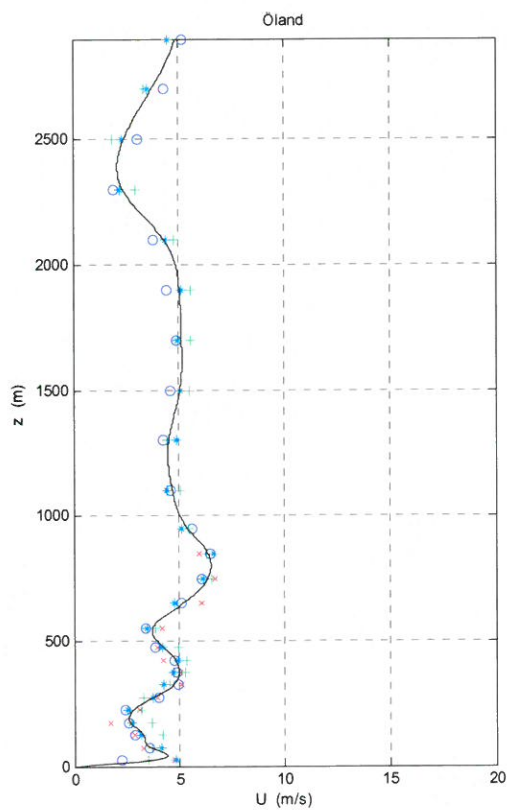
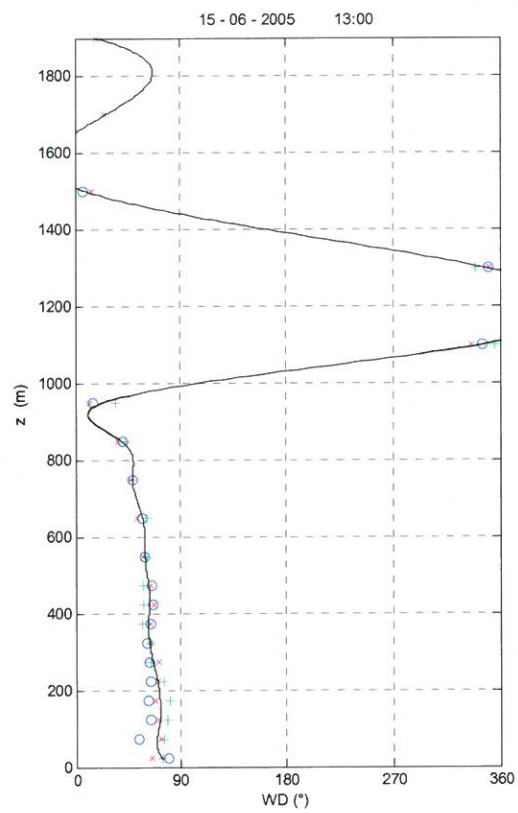
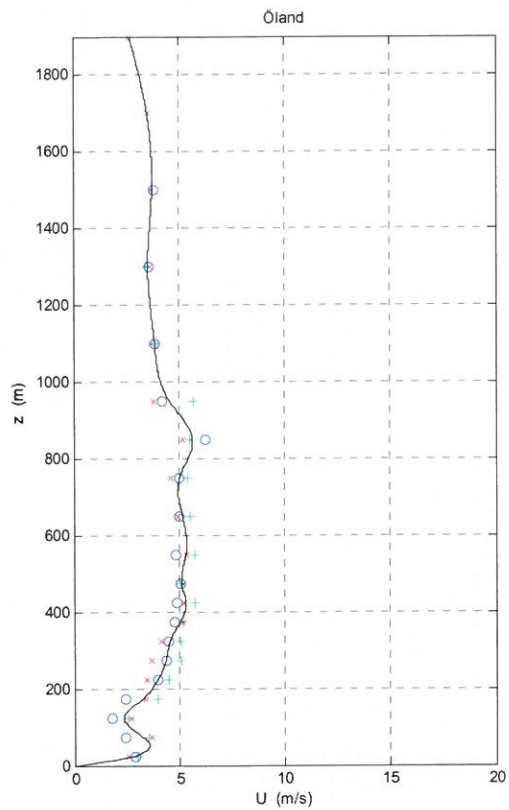


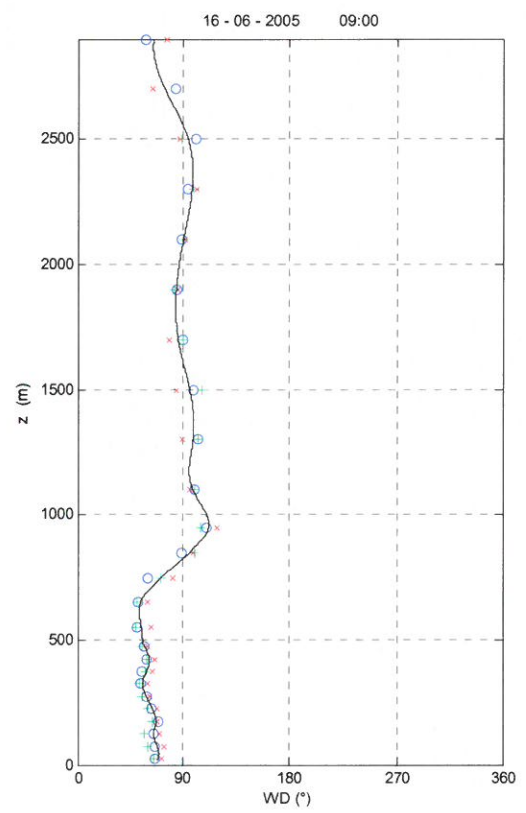
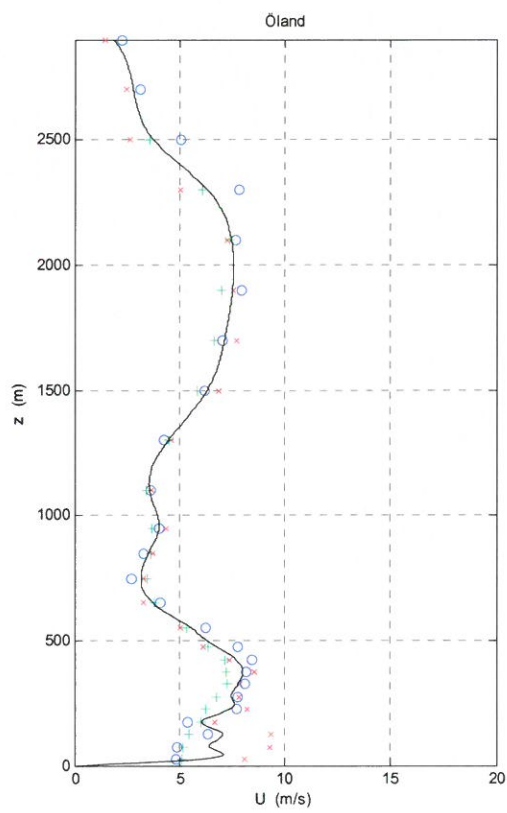
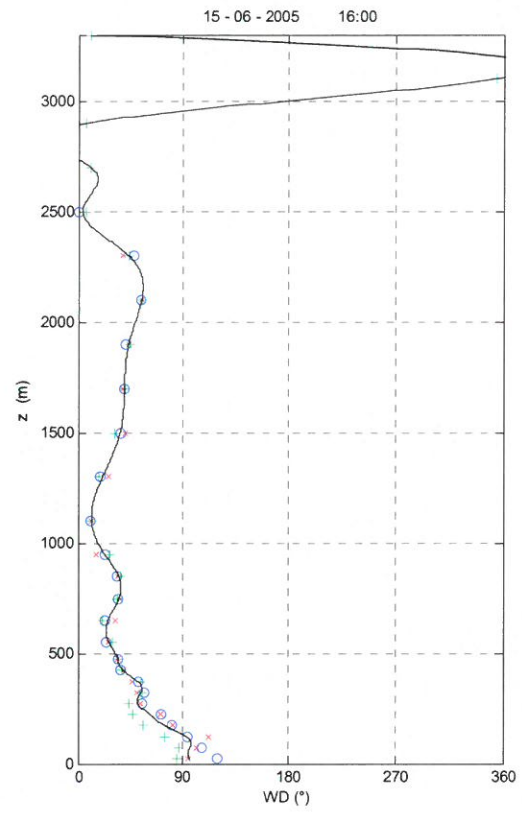
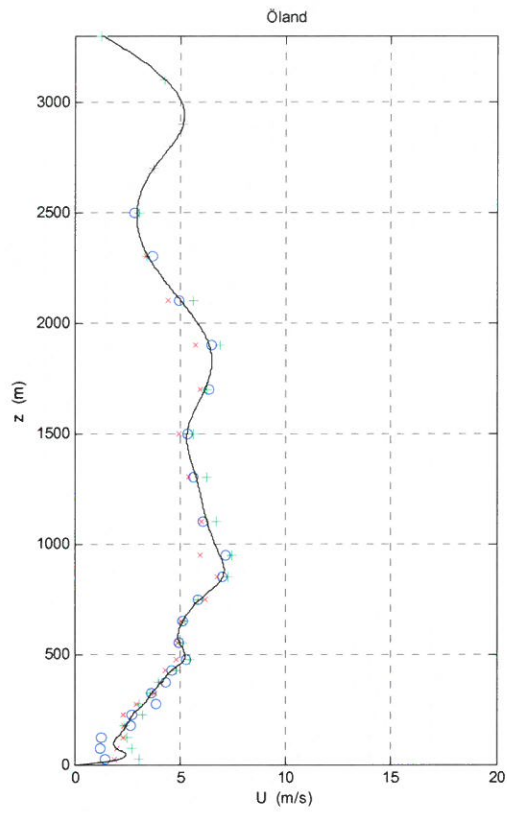


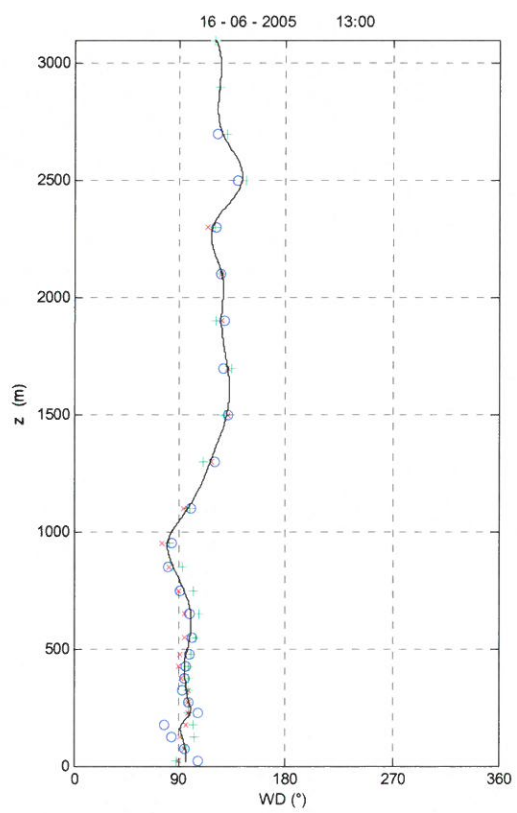
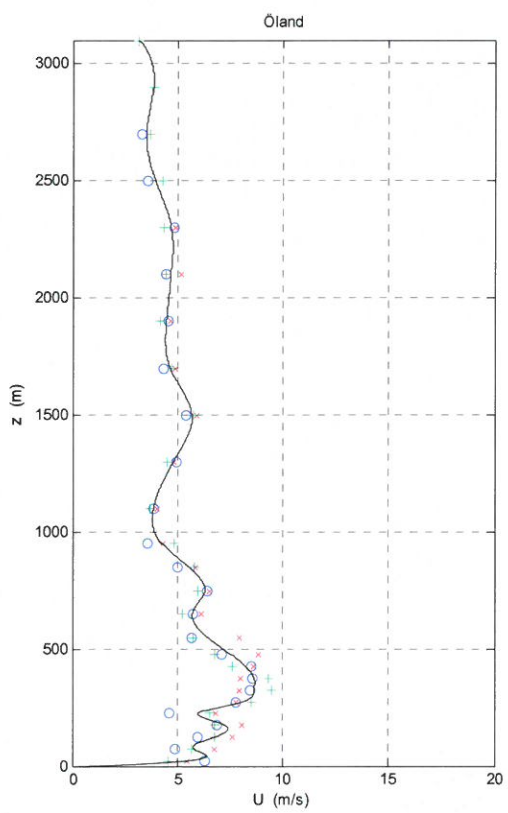
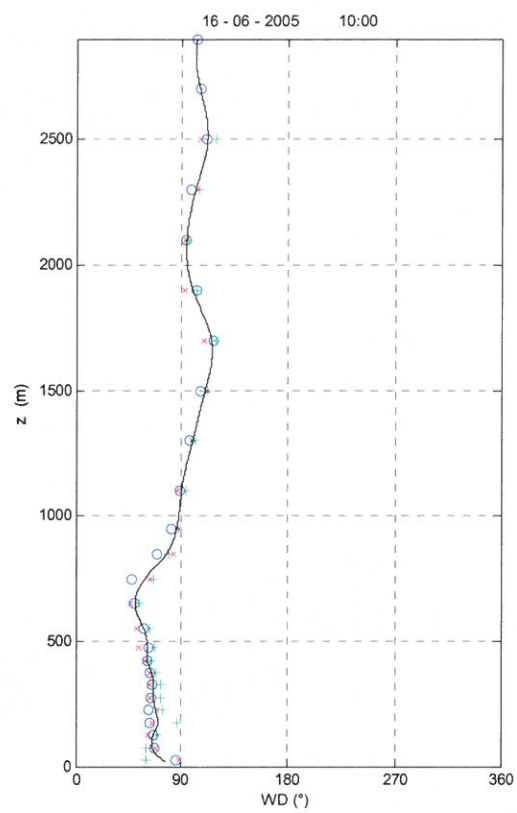
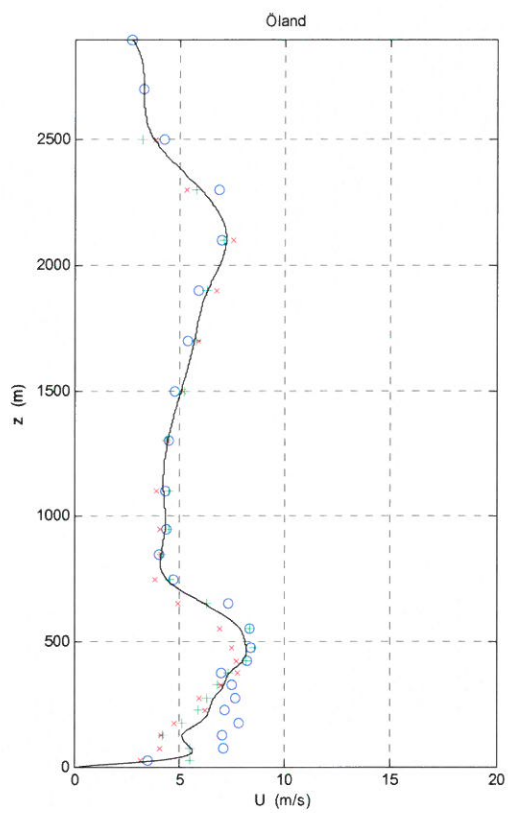
APPENDIX 2: WIND SPEED AND WIND DIRECTIONS AT ÖLAND IN JUNE 2005

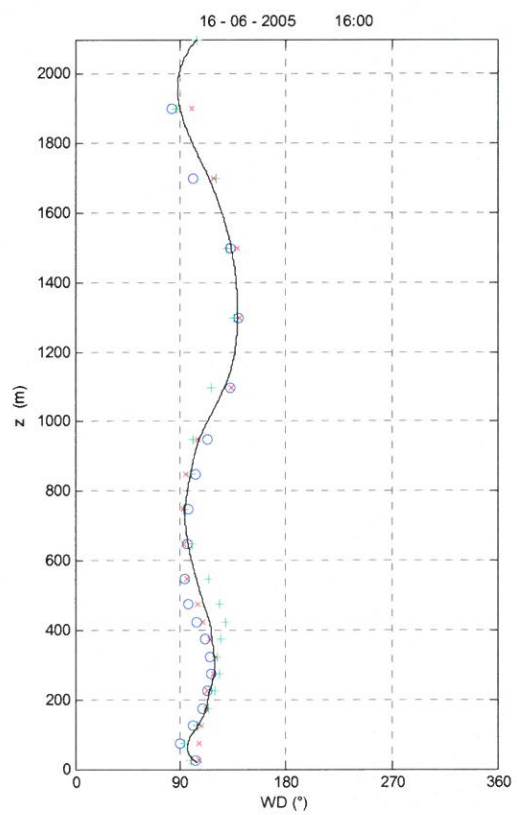
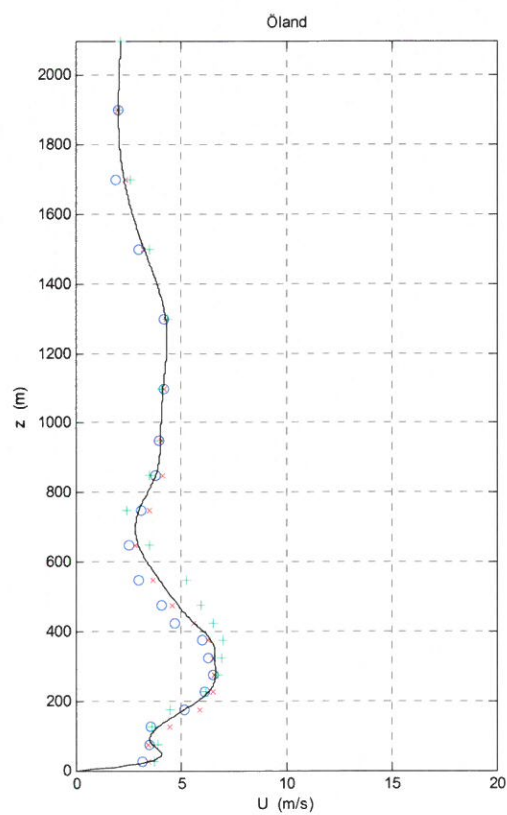
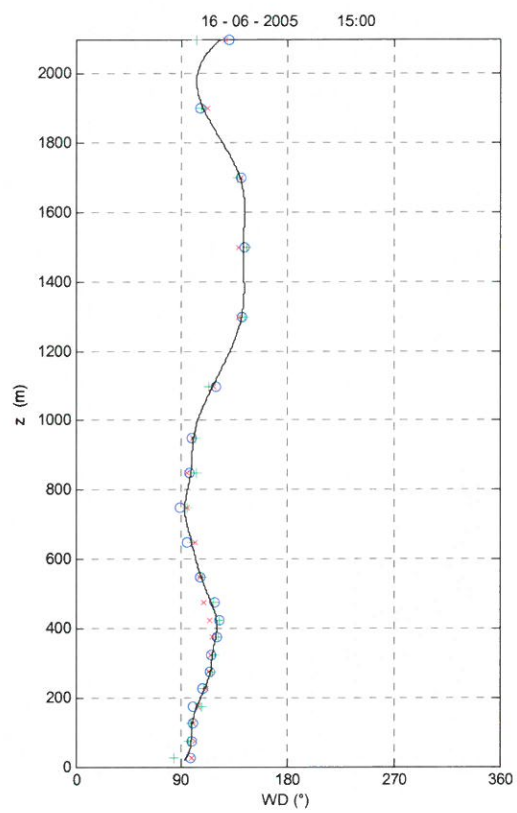
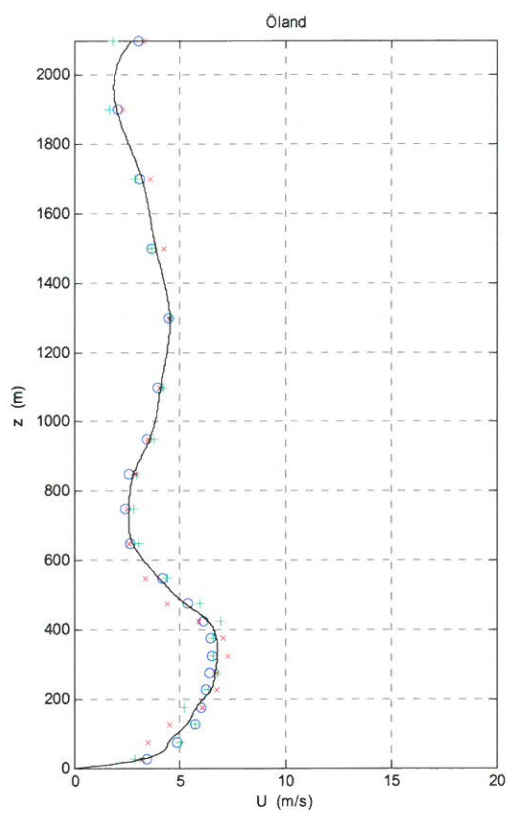
The data are based on theodolite tracking of free flying balloons. The solid lines represent the best curve fit to the discrete measurement points obtained from two- three balloons sent up after each other (~10 minute intervals) close to the receiver position at Hammarby, Öland.

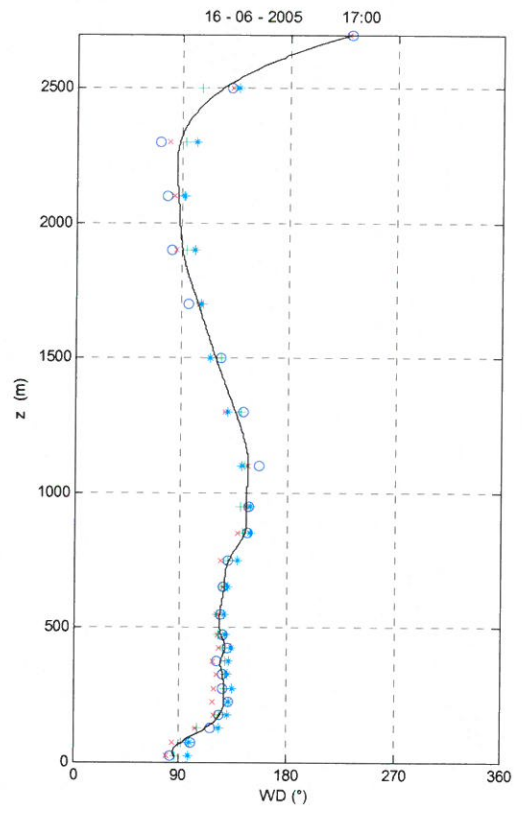
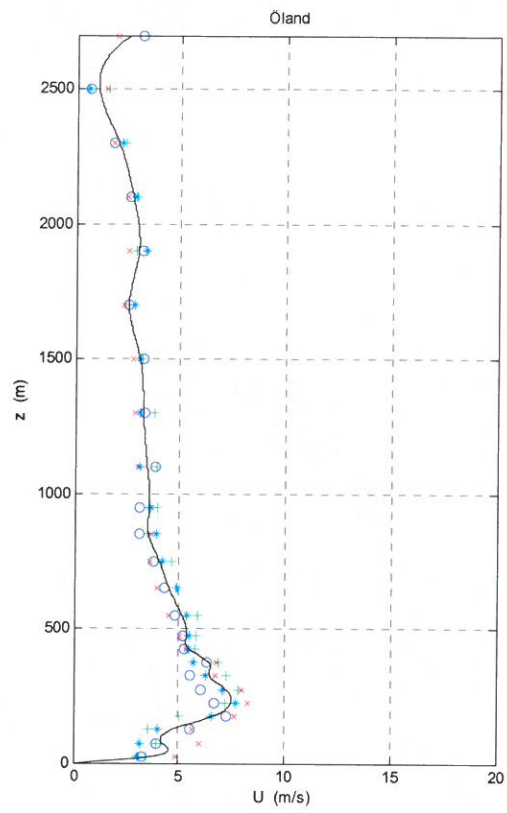


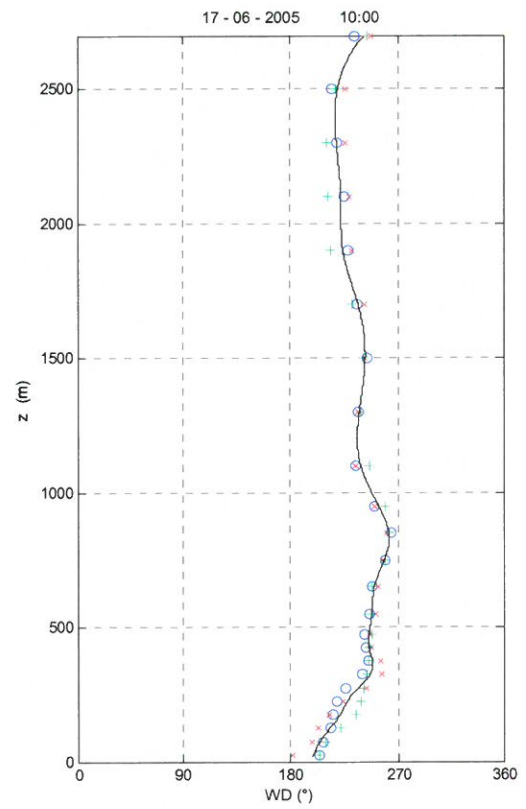
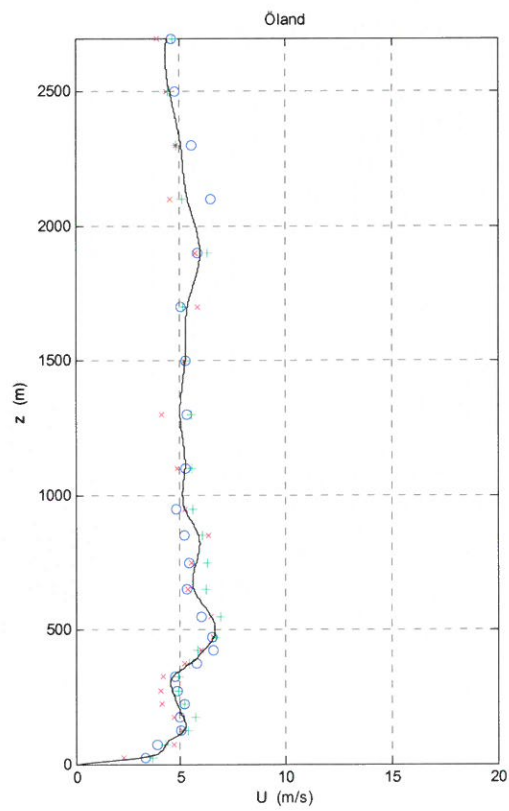
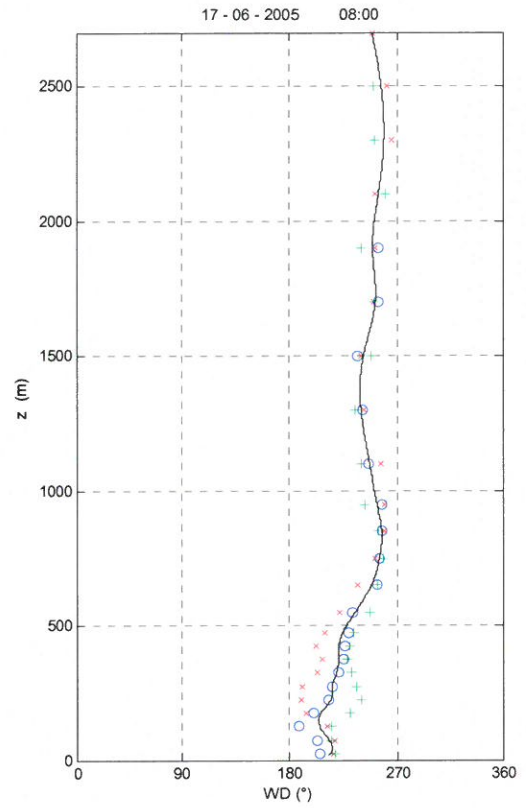
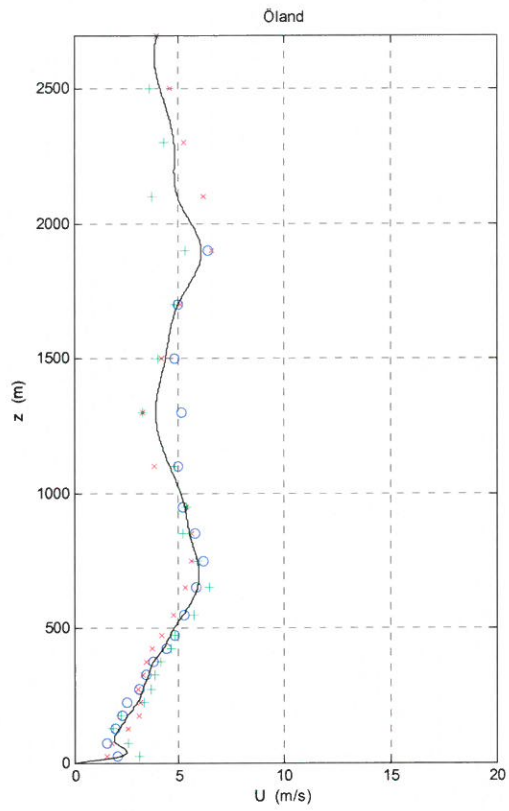


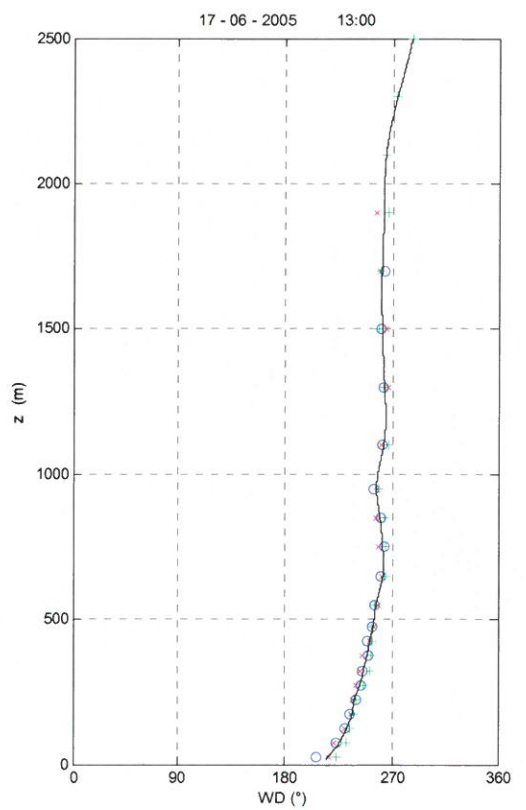
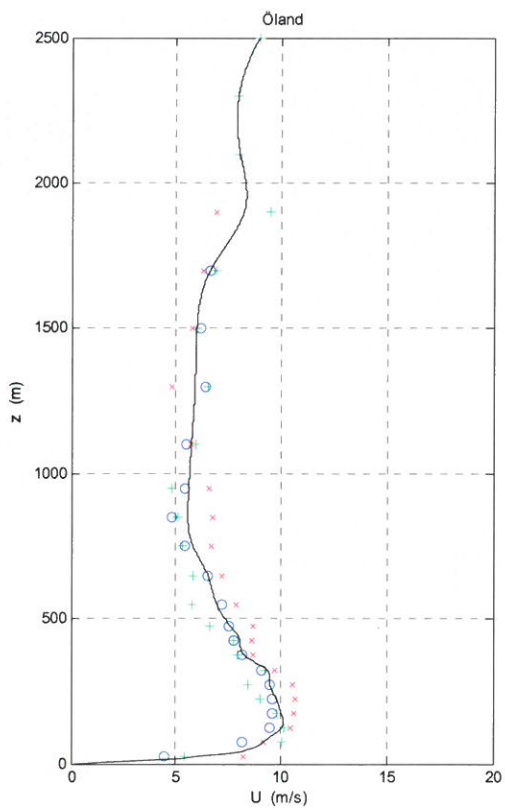
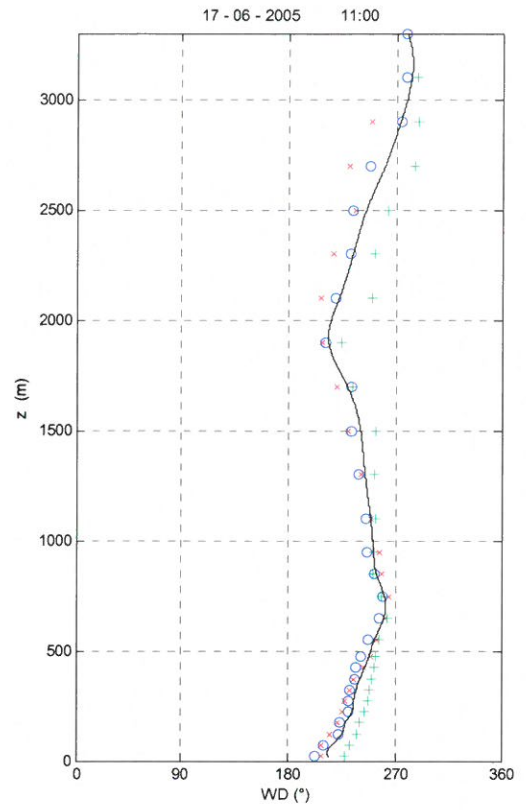
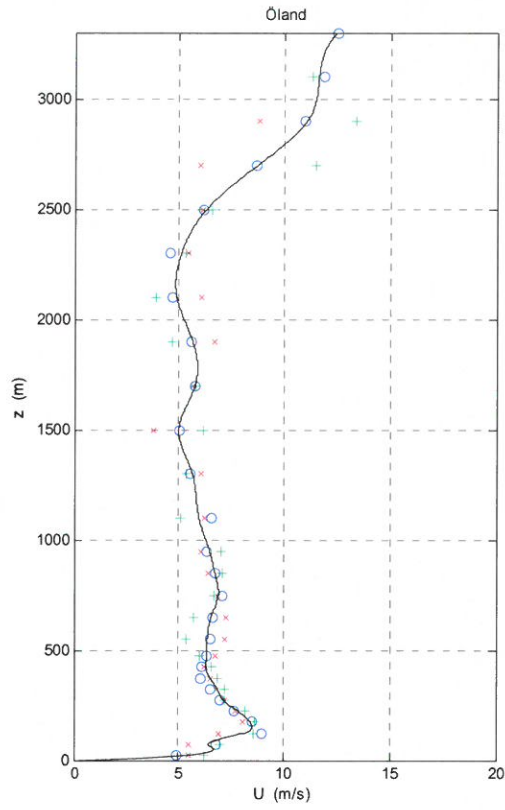


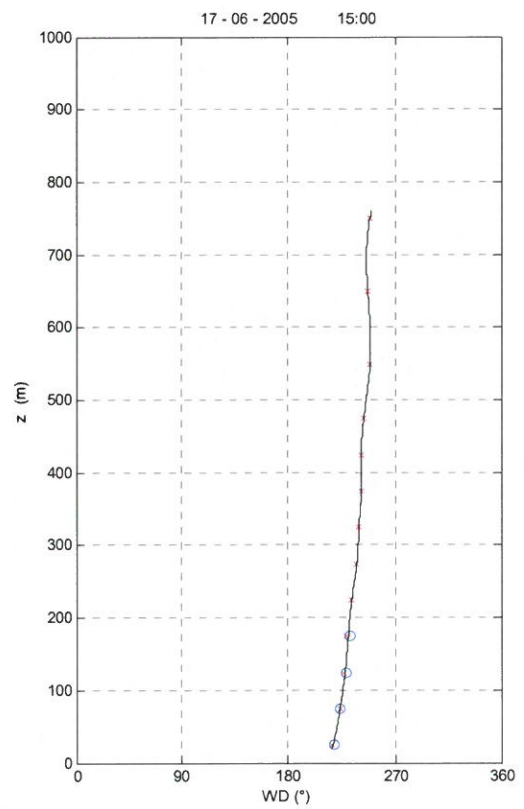
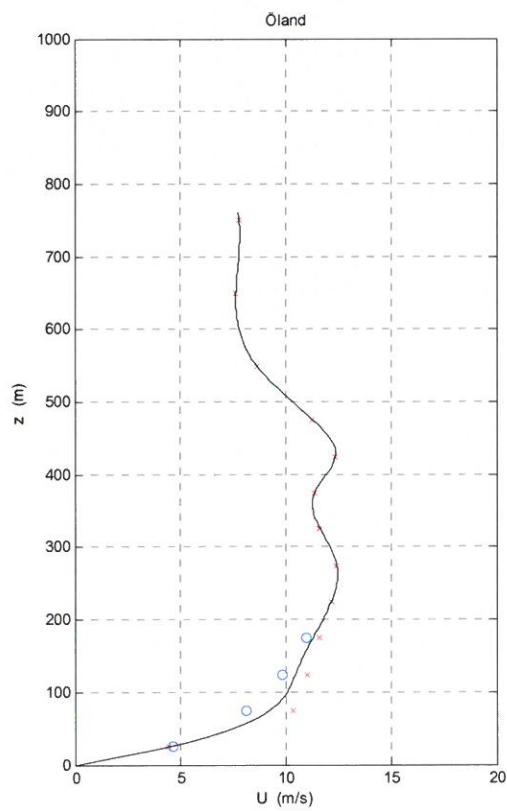
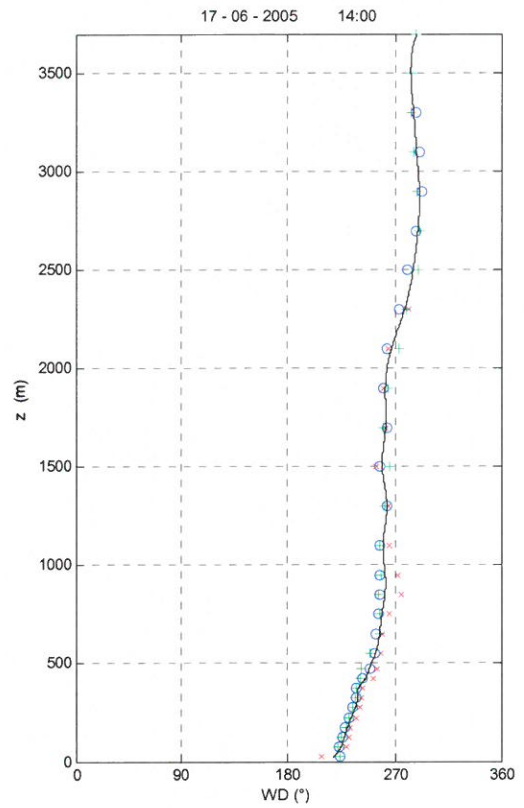
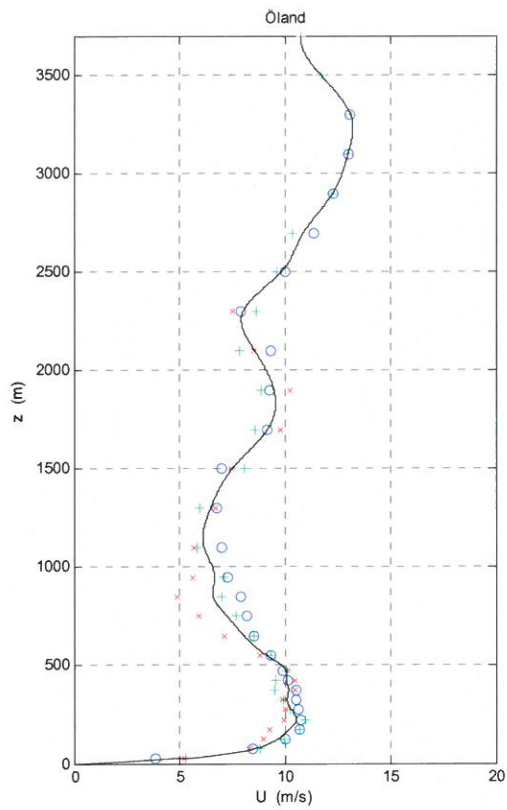


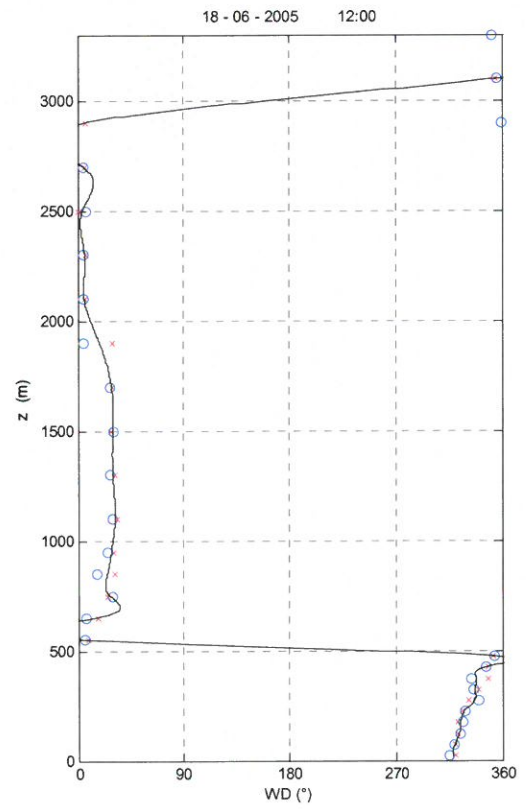
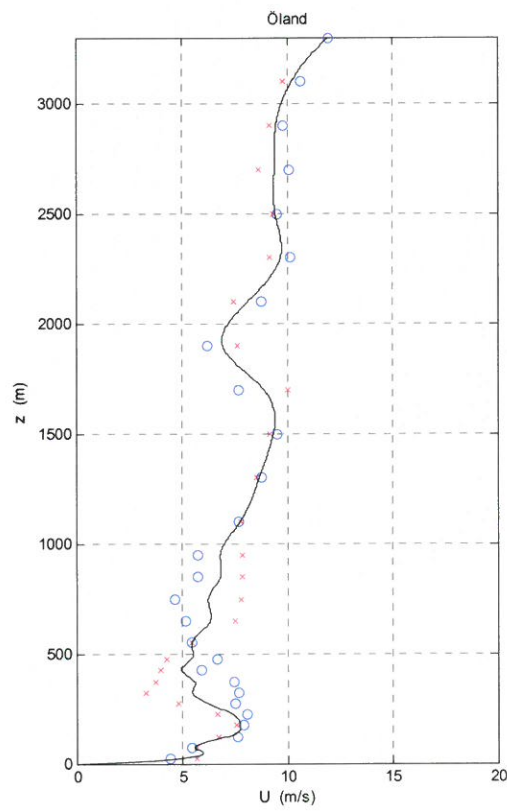
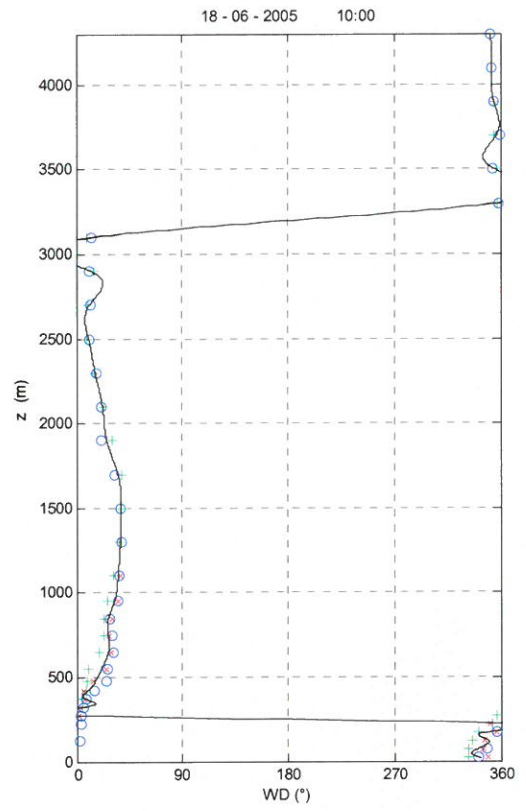
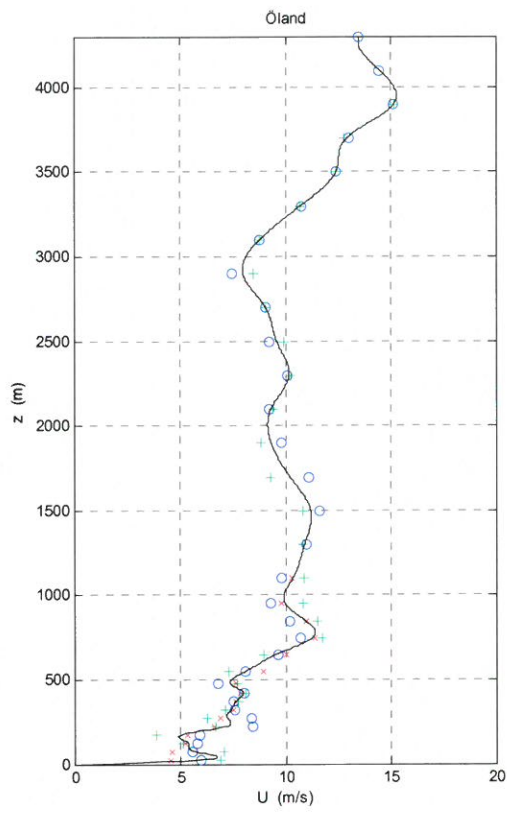


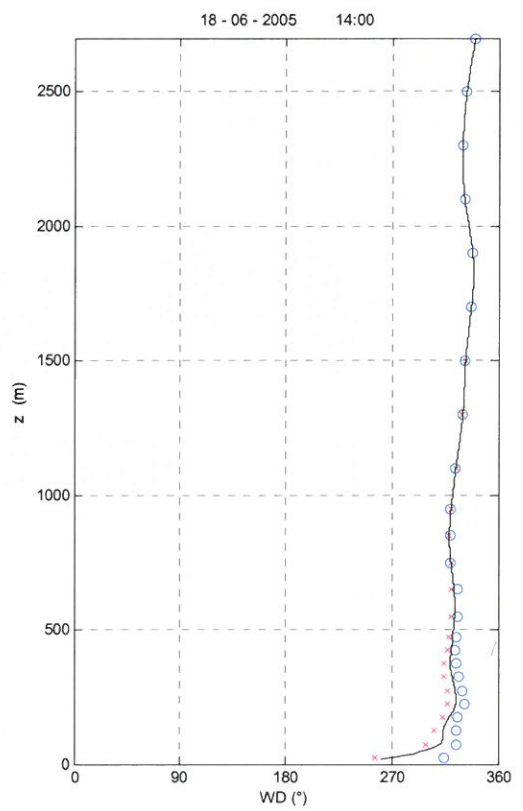
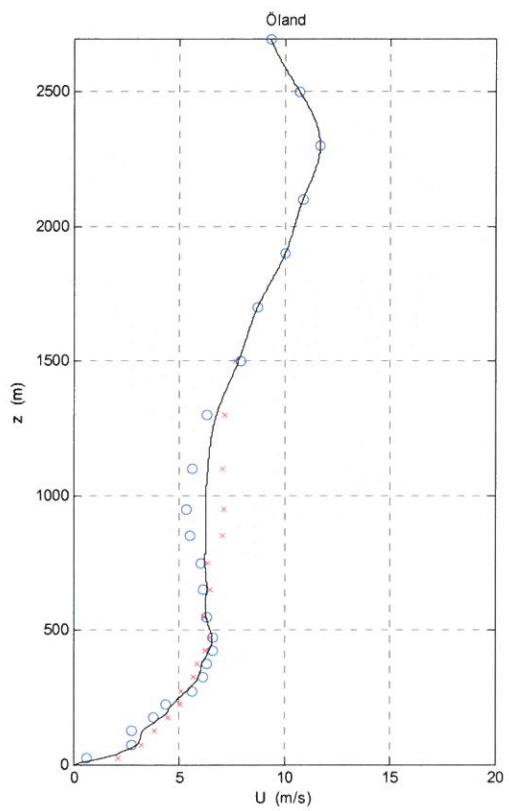
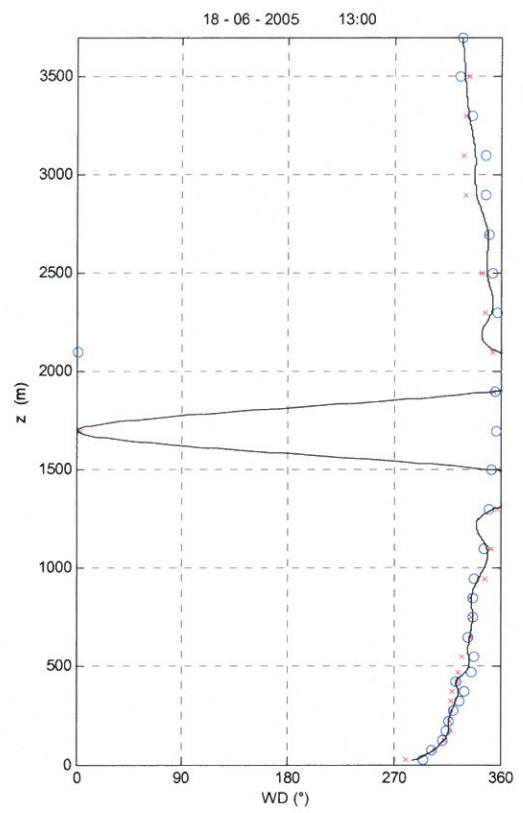
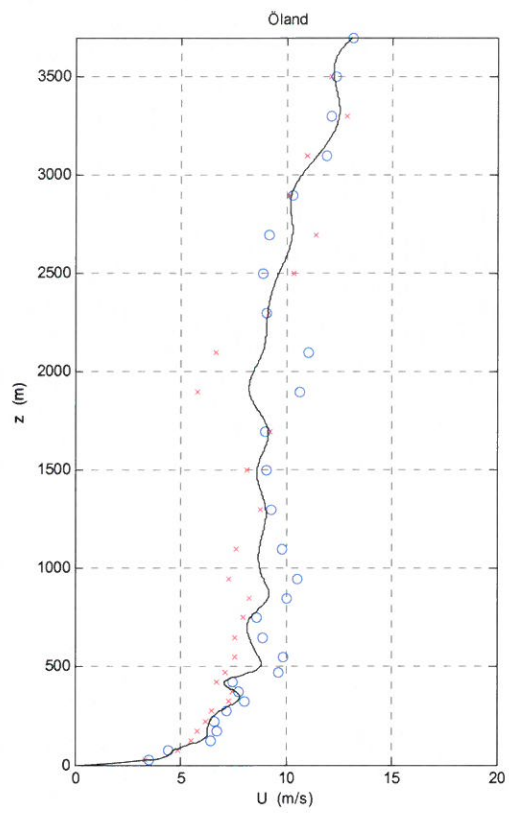


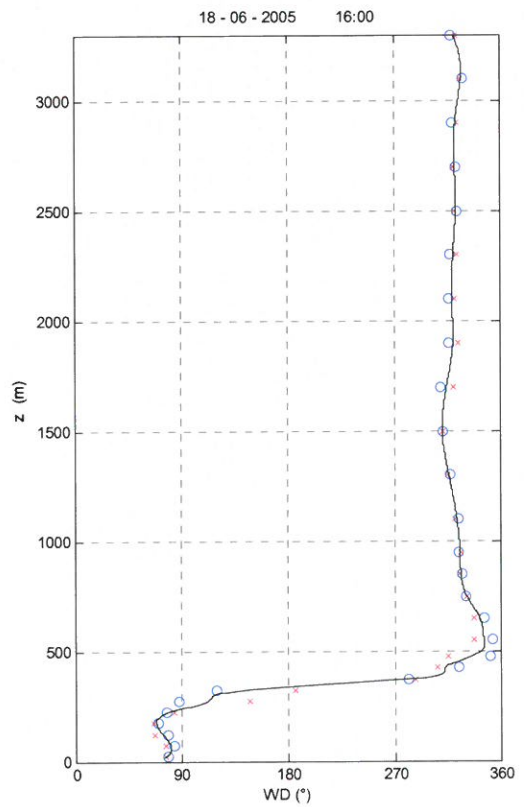
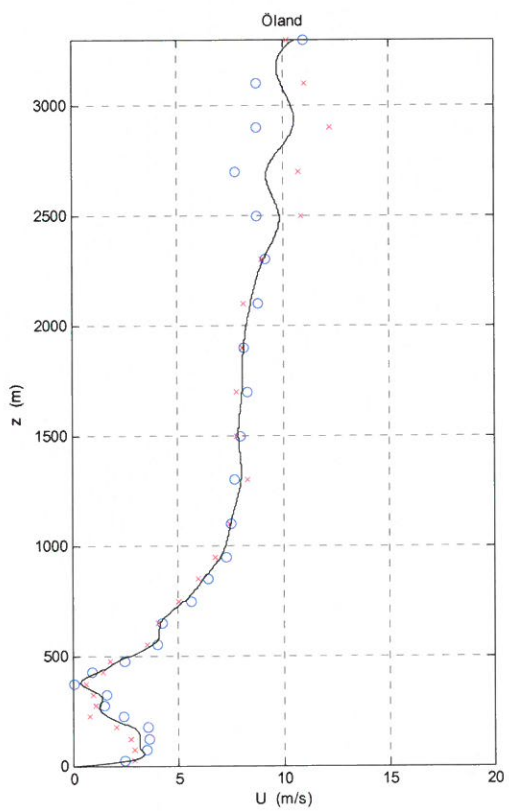
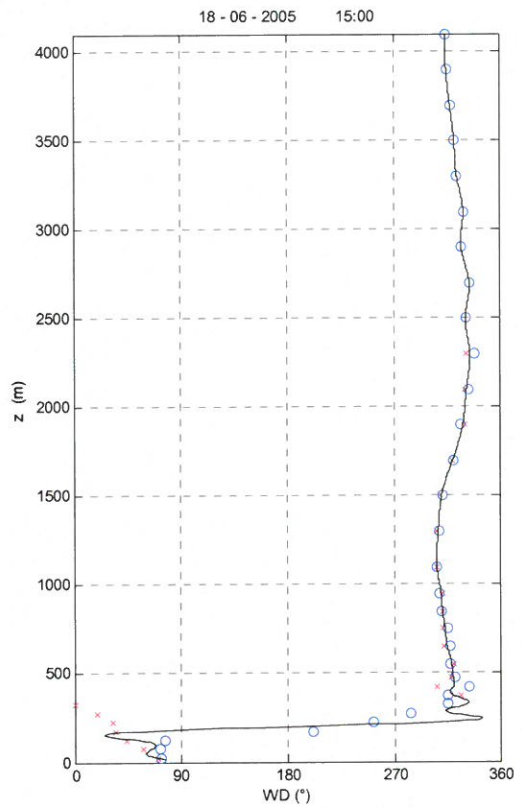
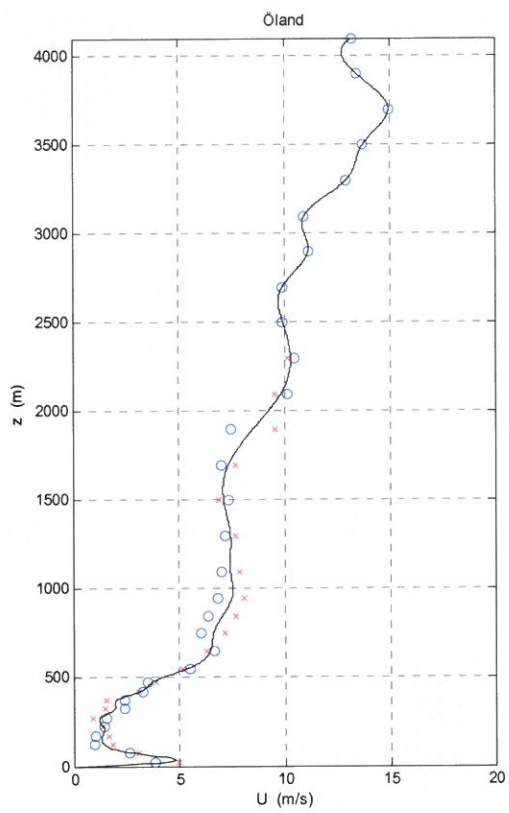


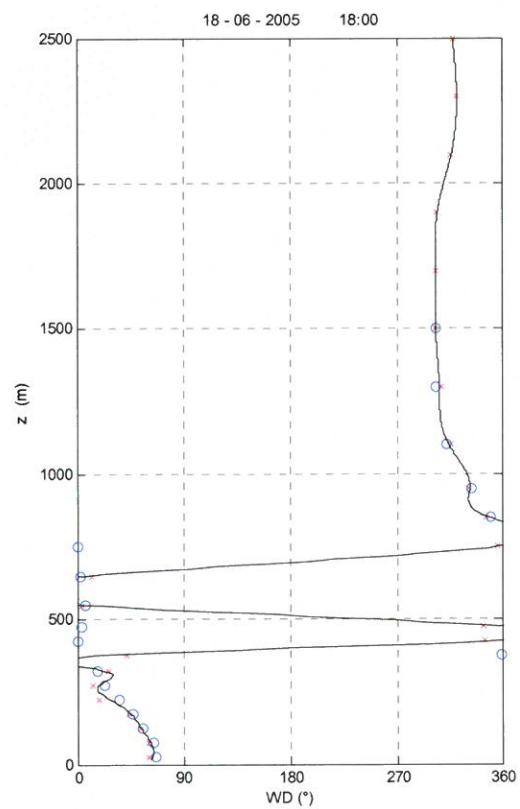
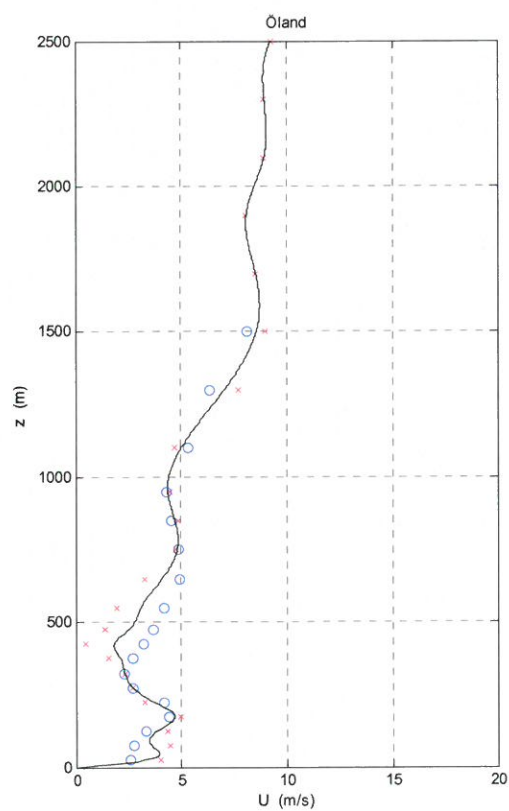
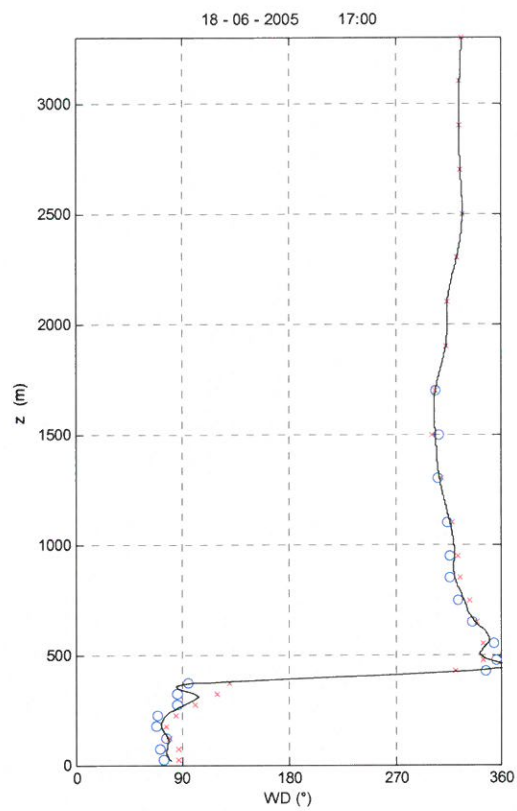
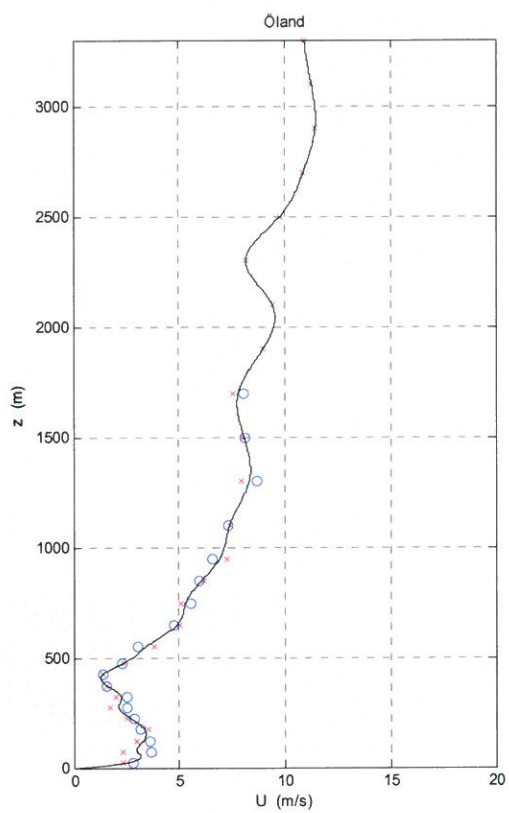


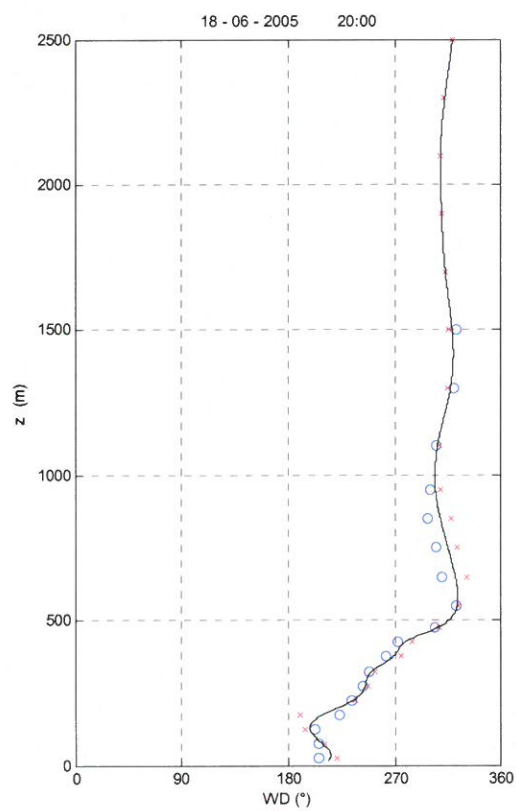
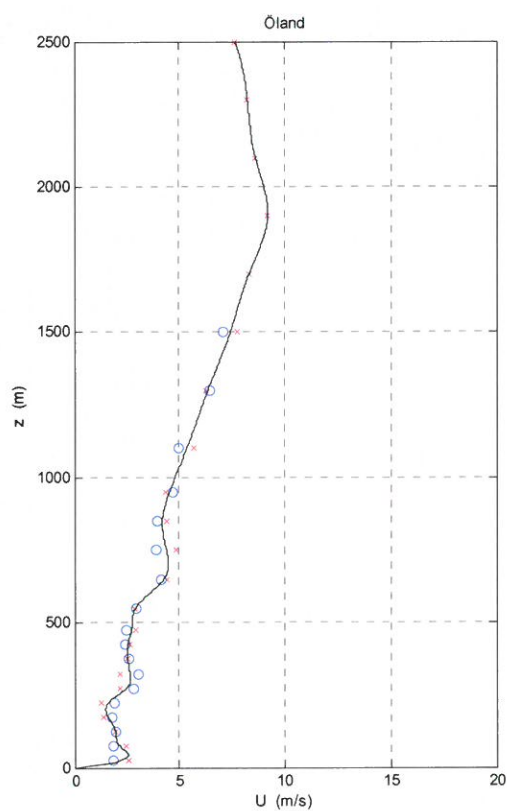
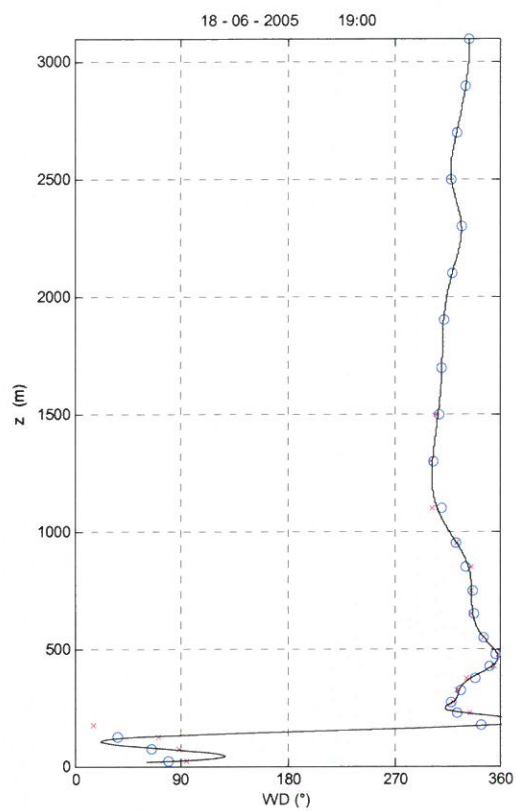
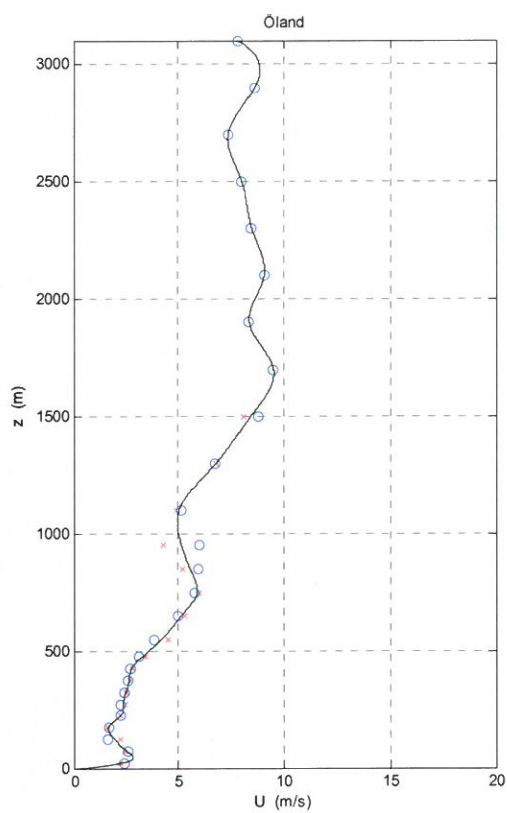


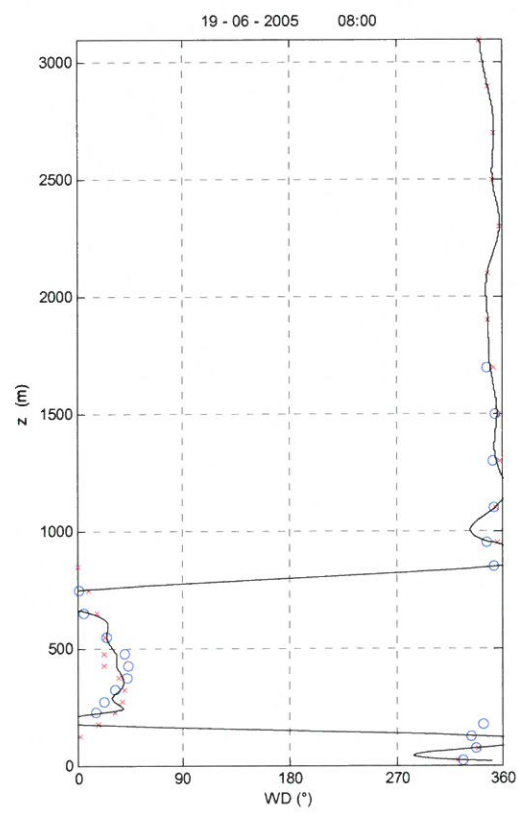
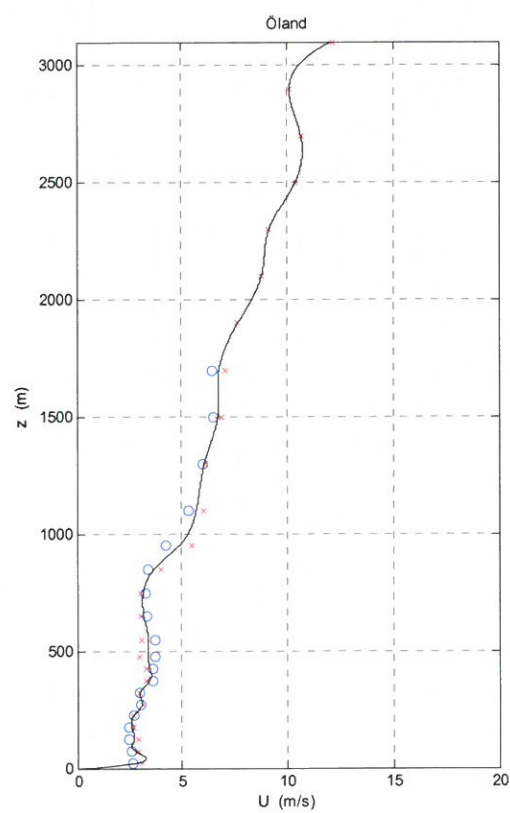
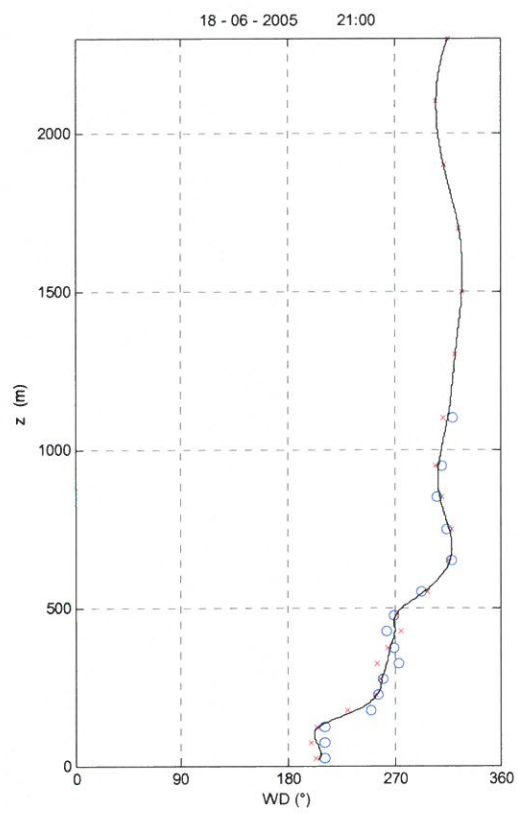
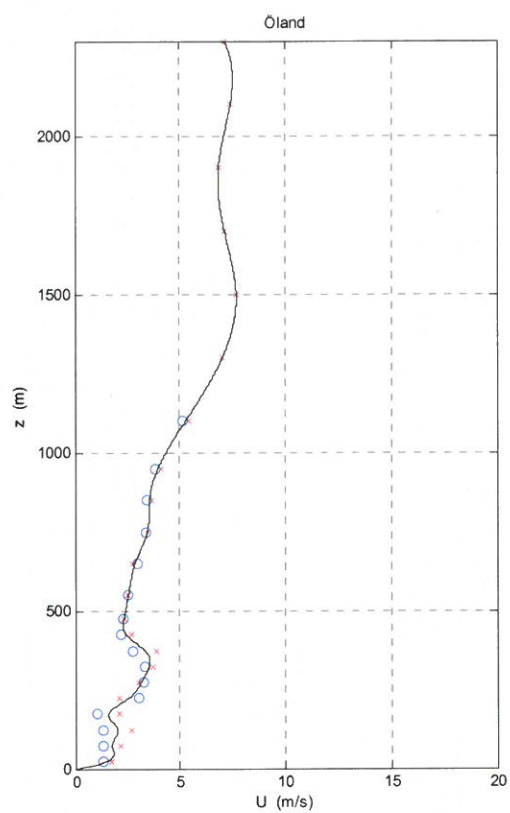


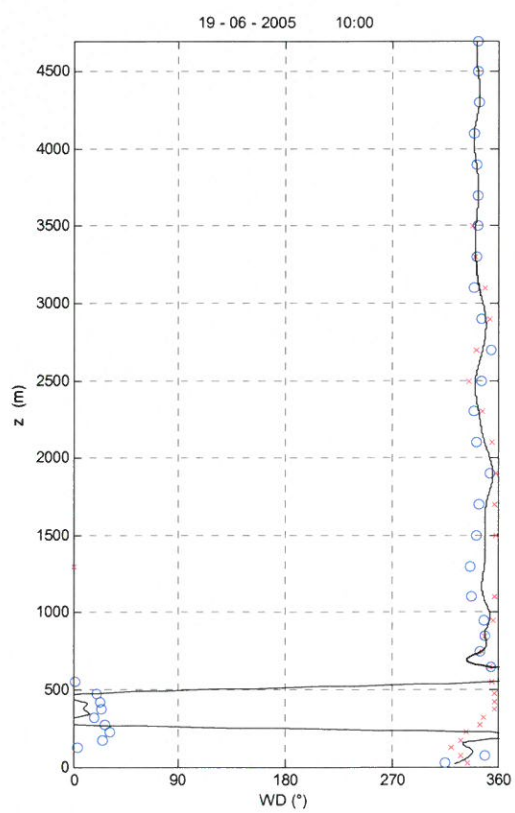
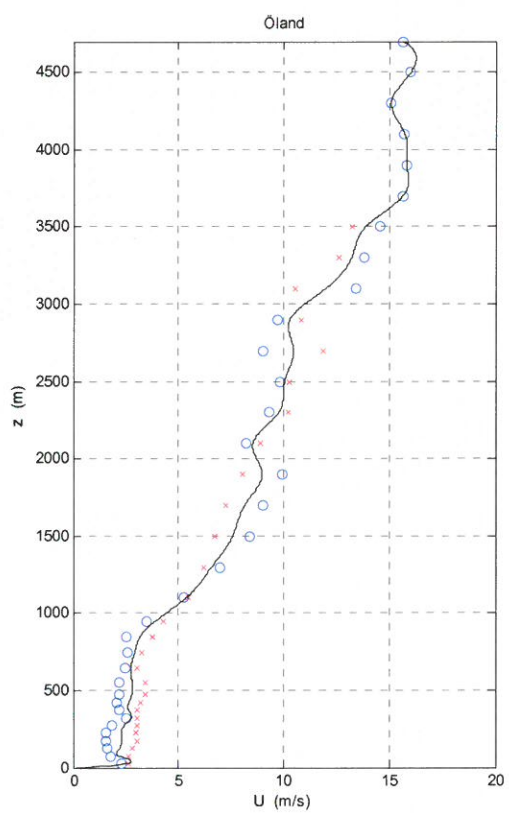
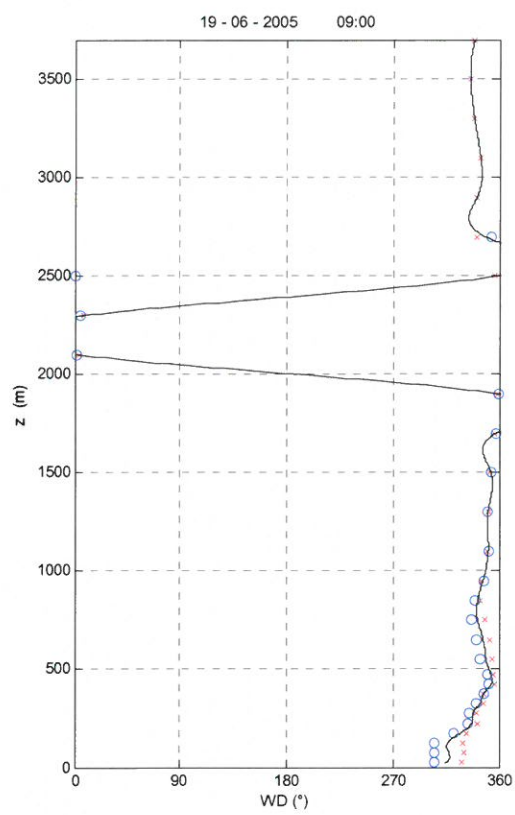
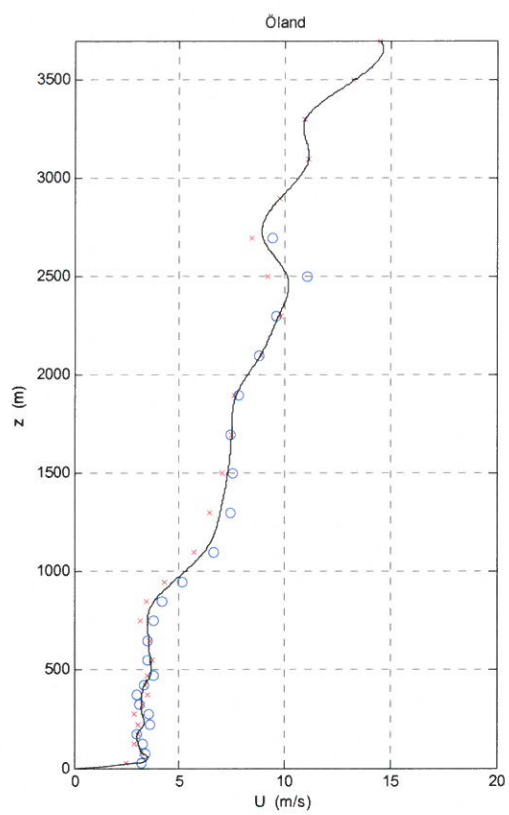


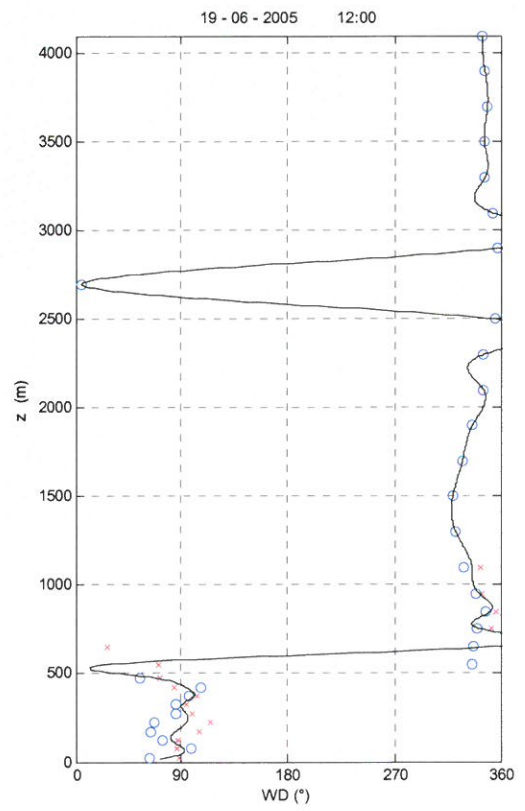
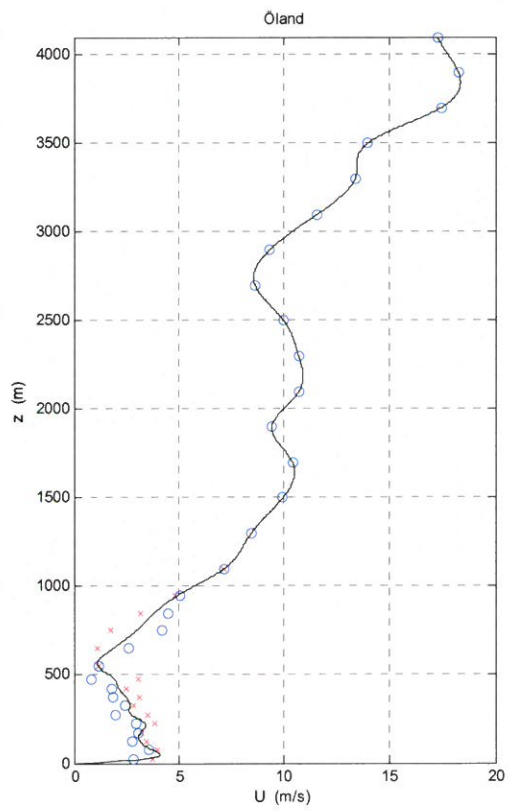
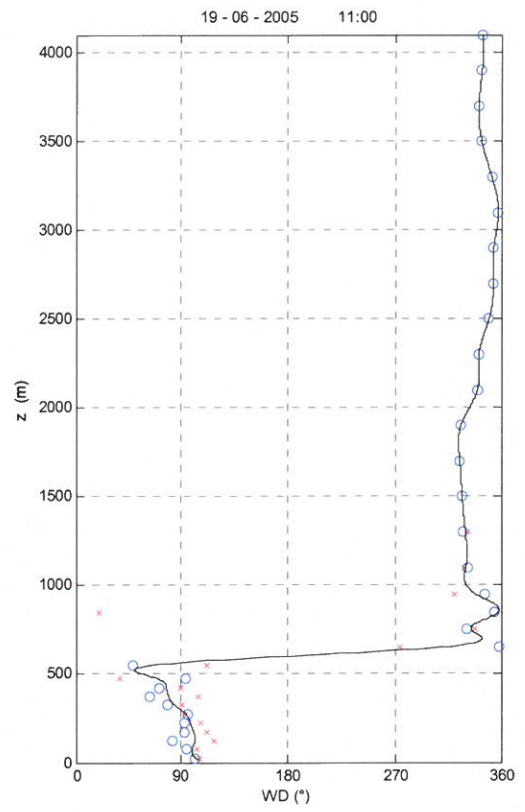
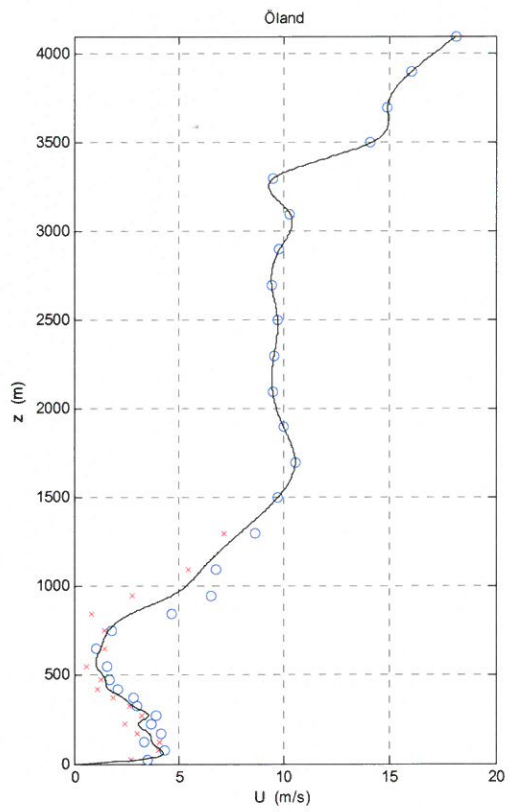


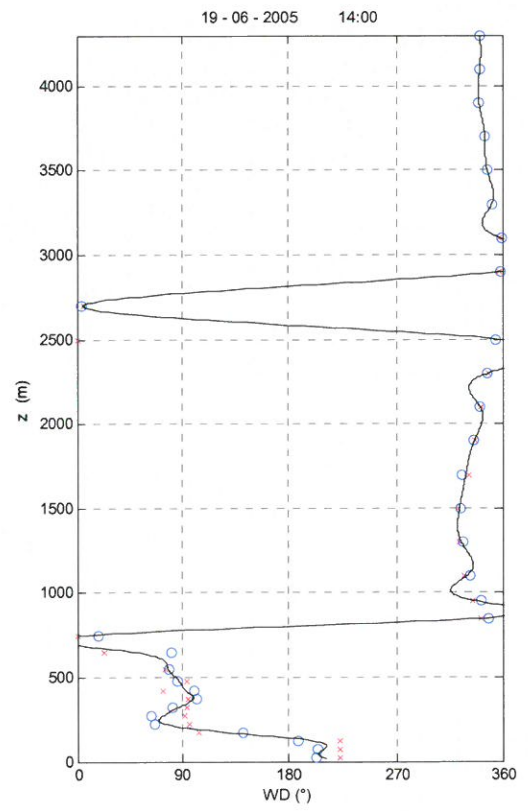
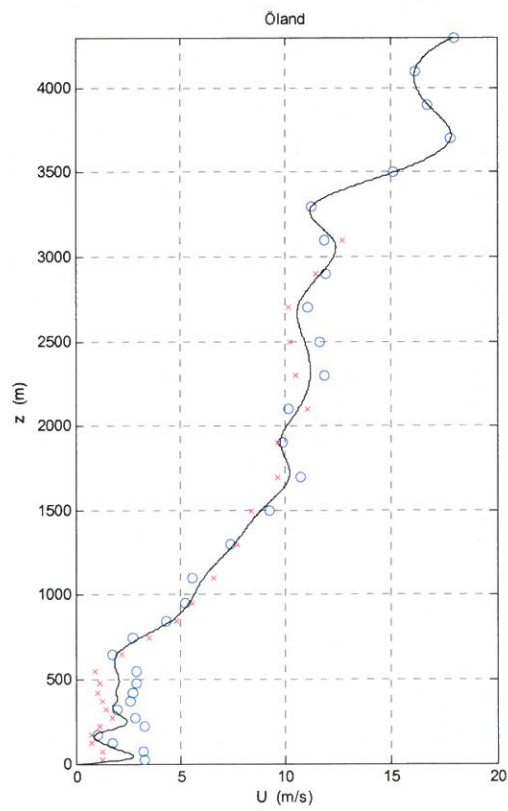
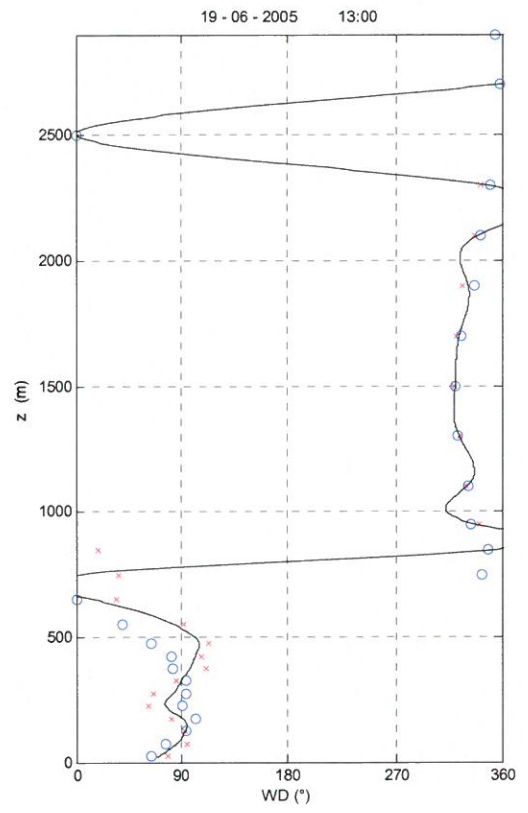
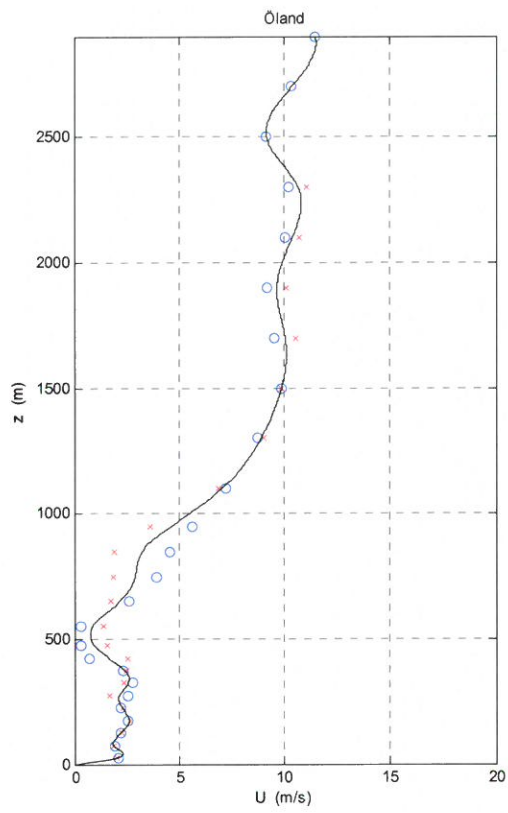


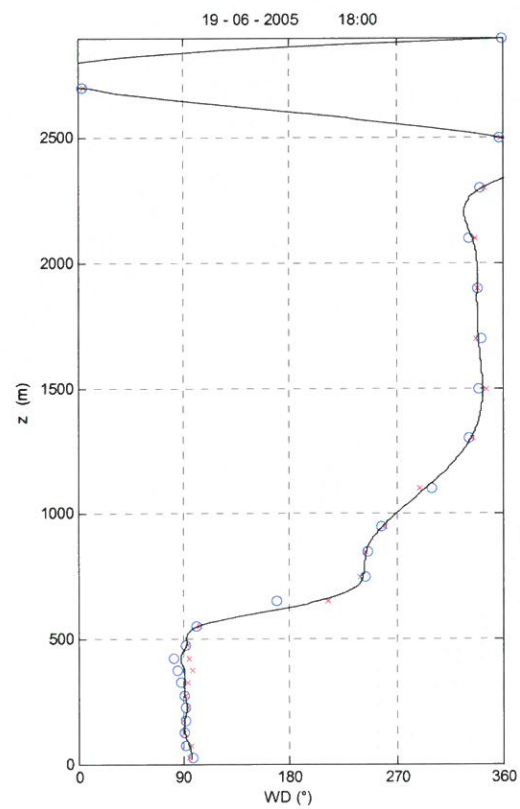
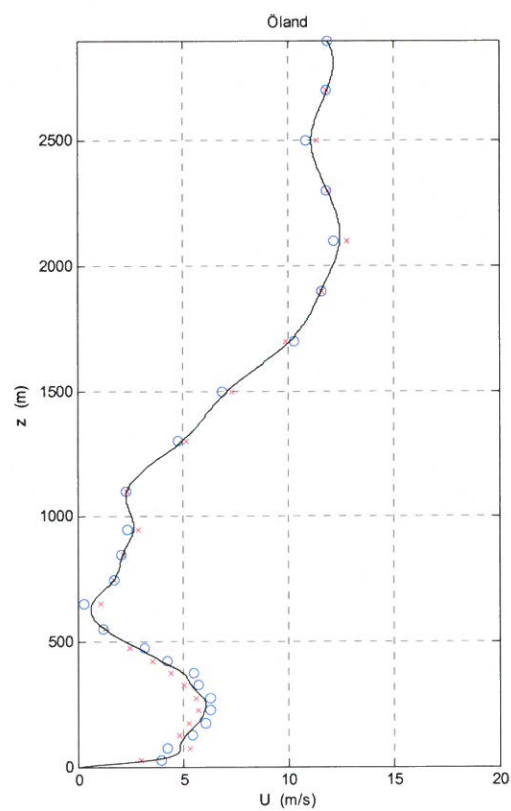
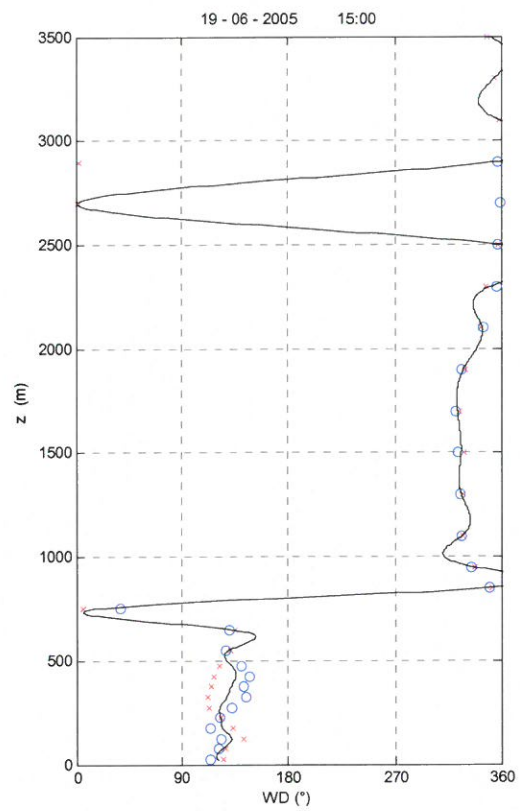
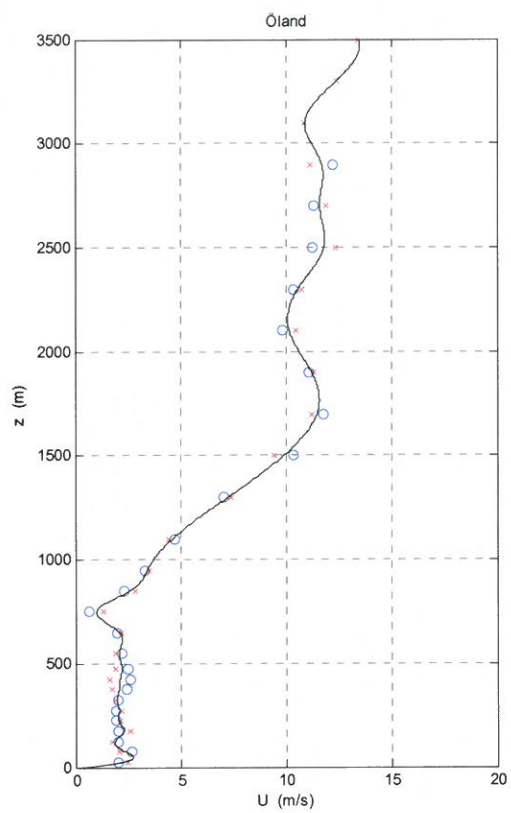


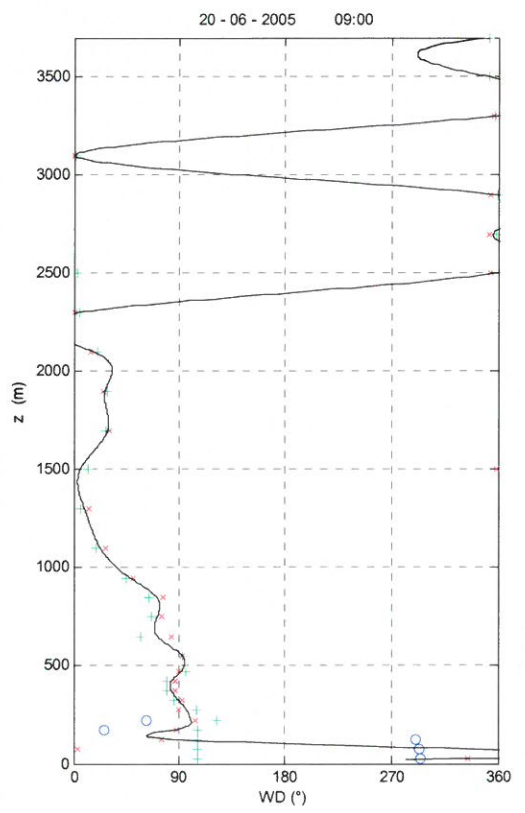
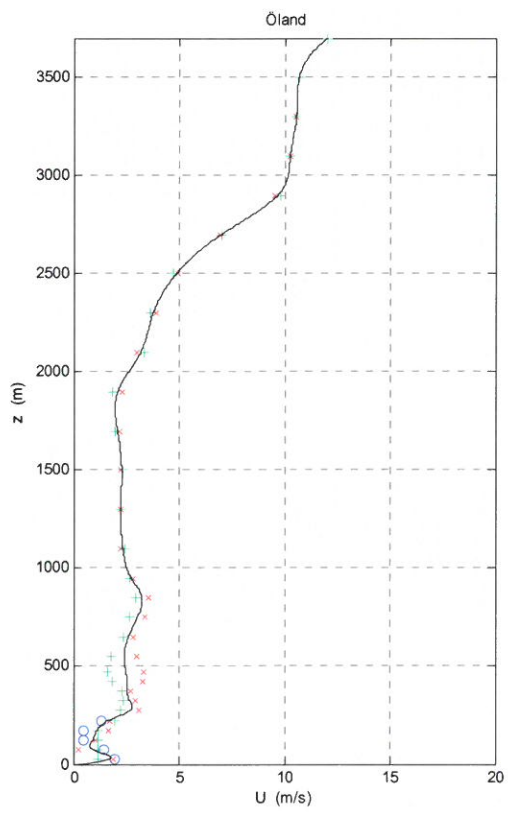
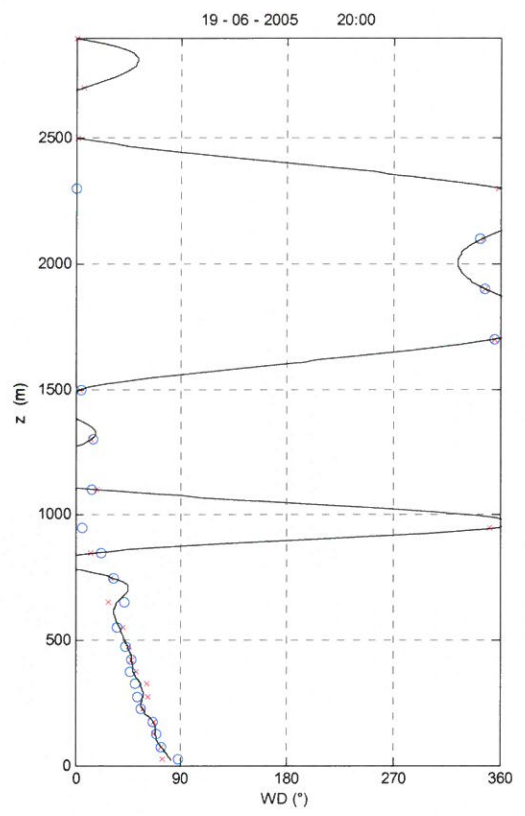
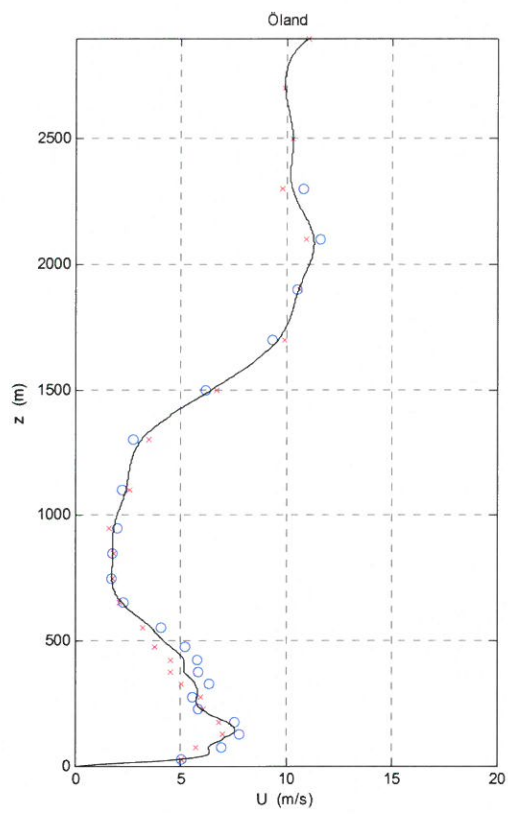


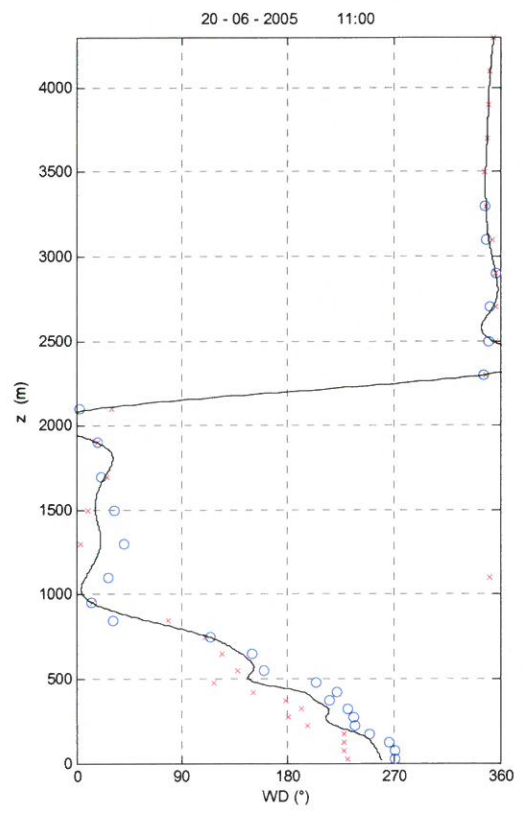
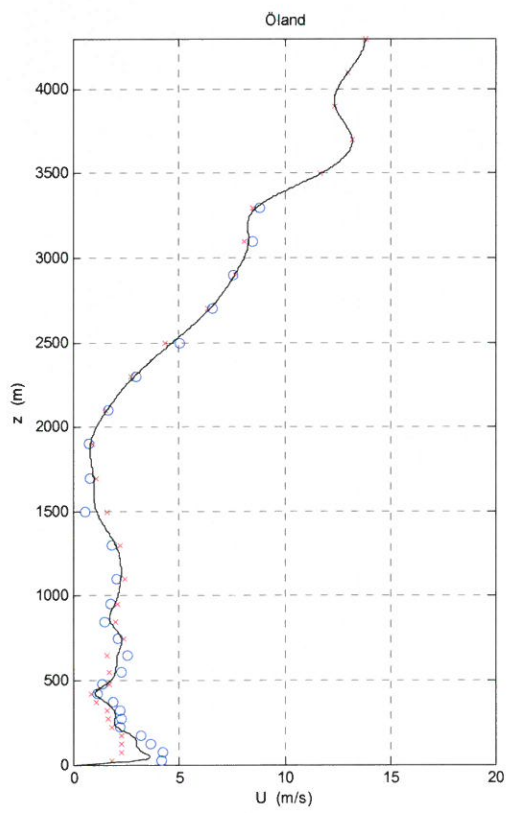
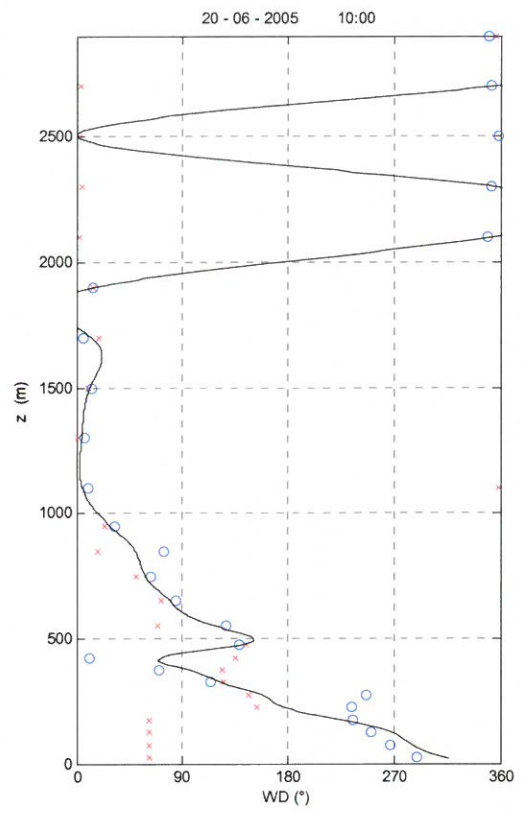
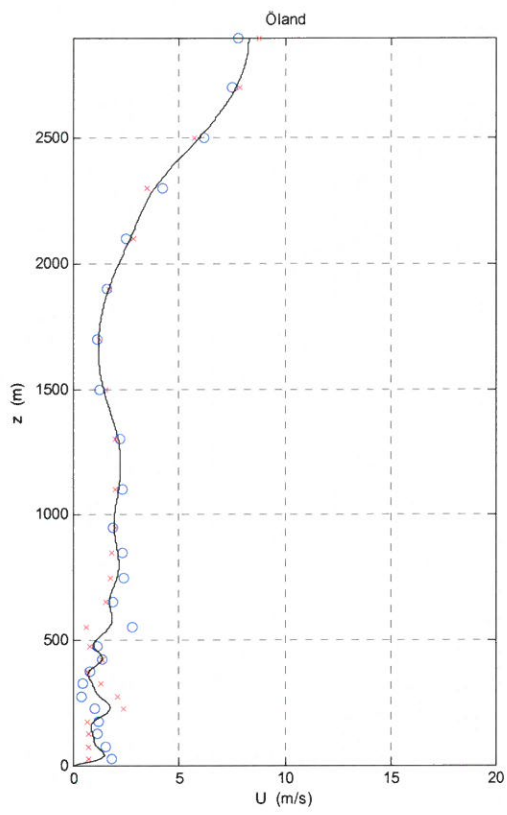


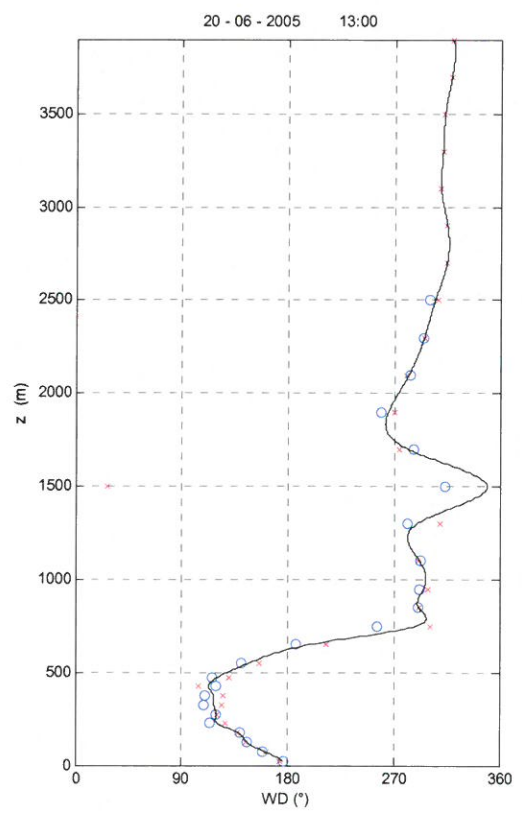
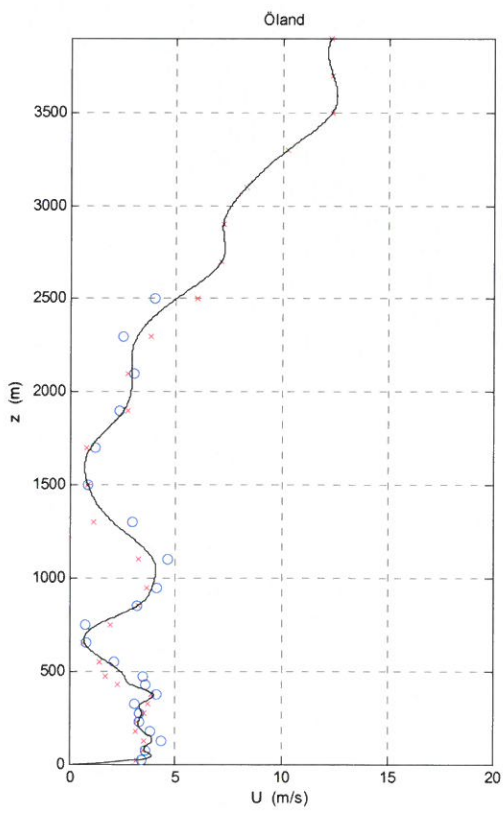
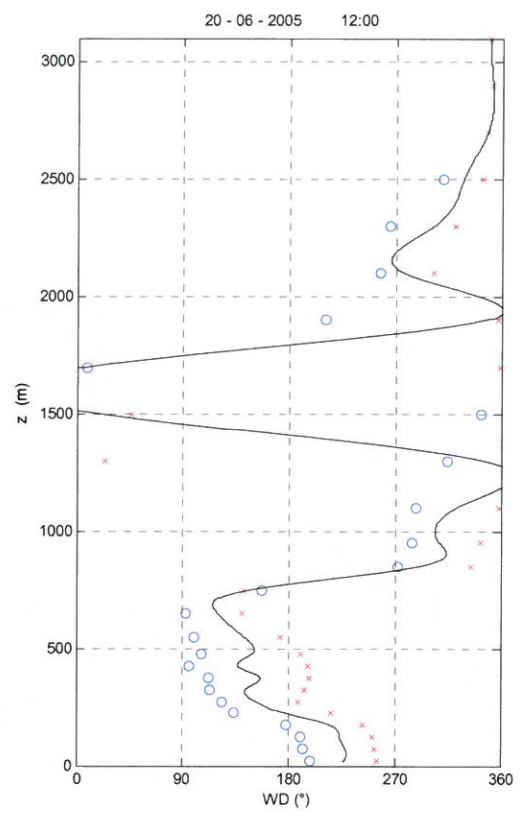
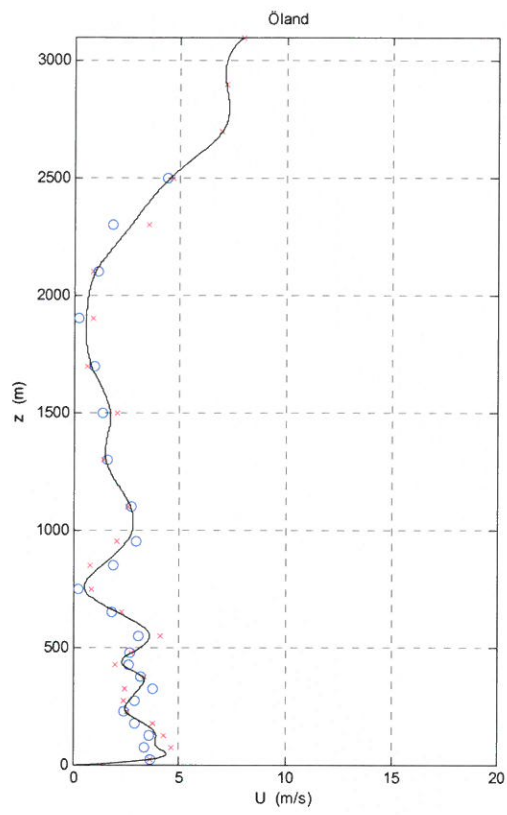


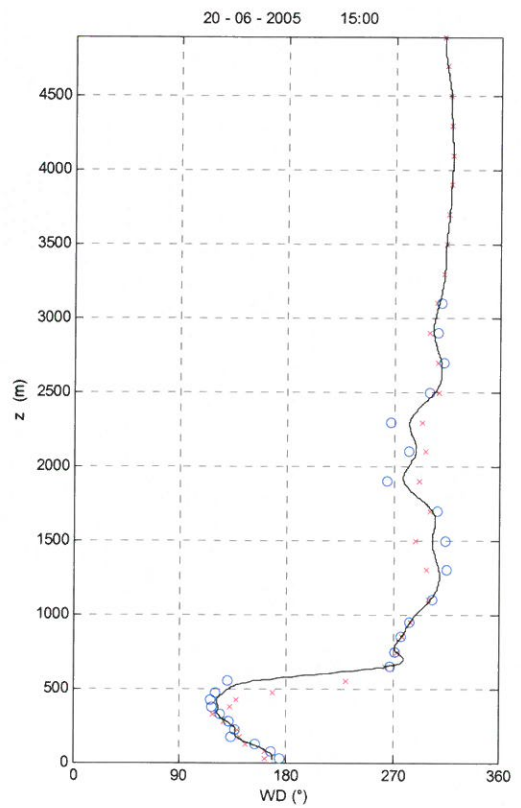
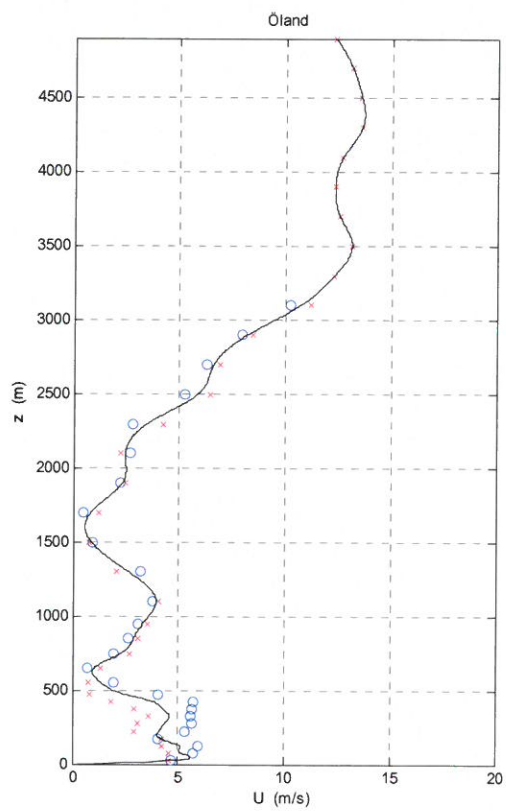
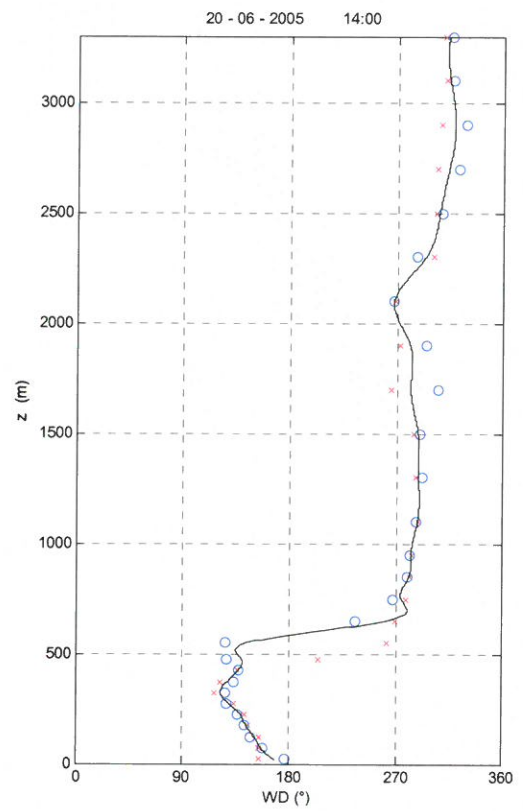
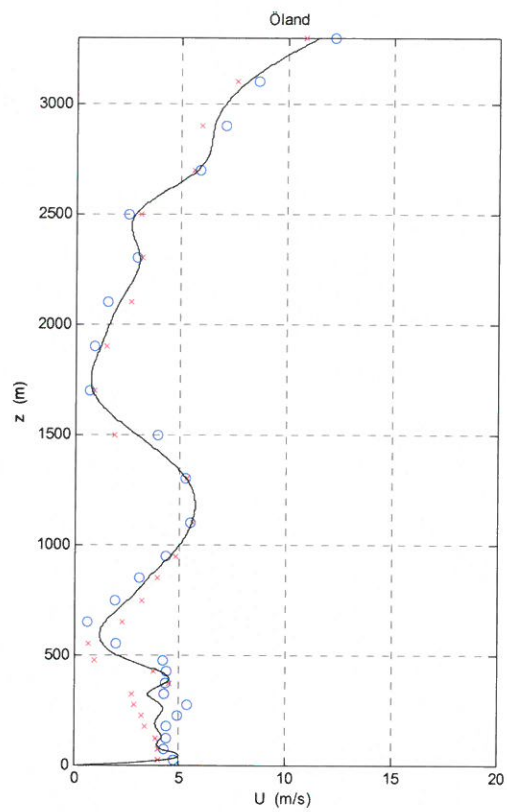


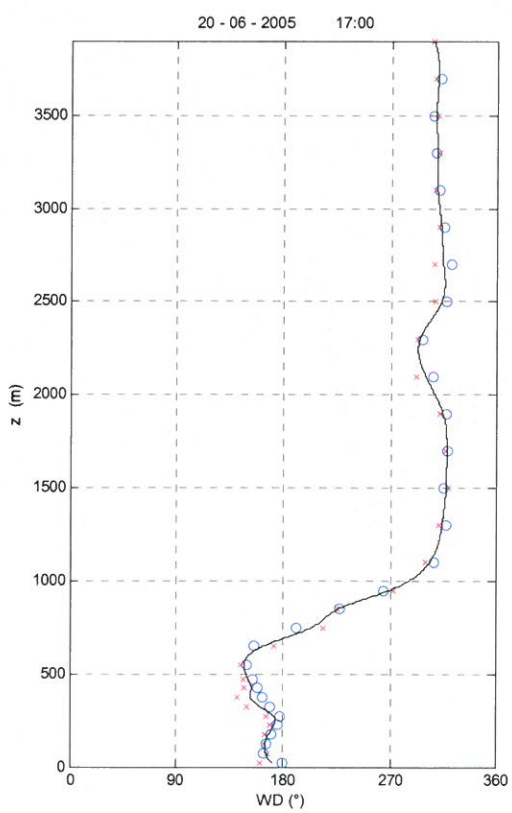
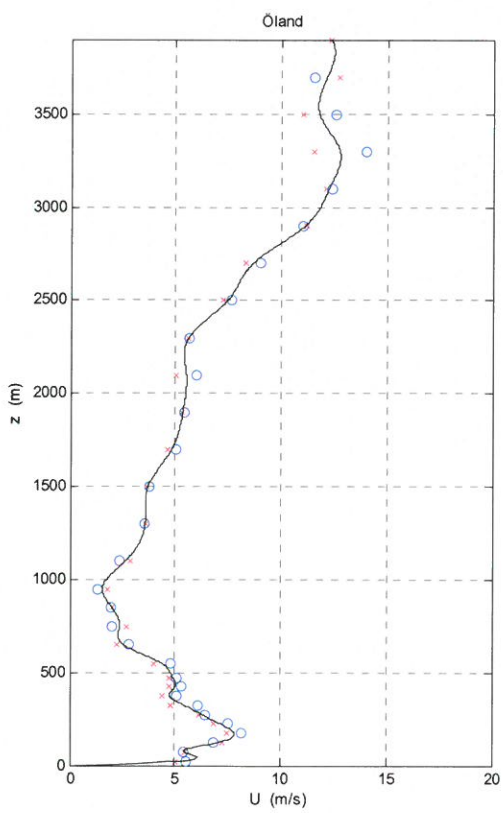
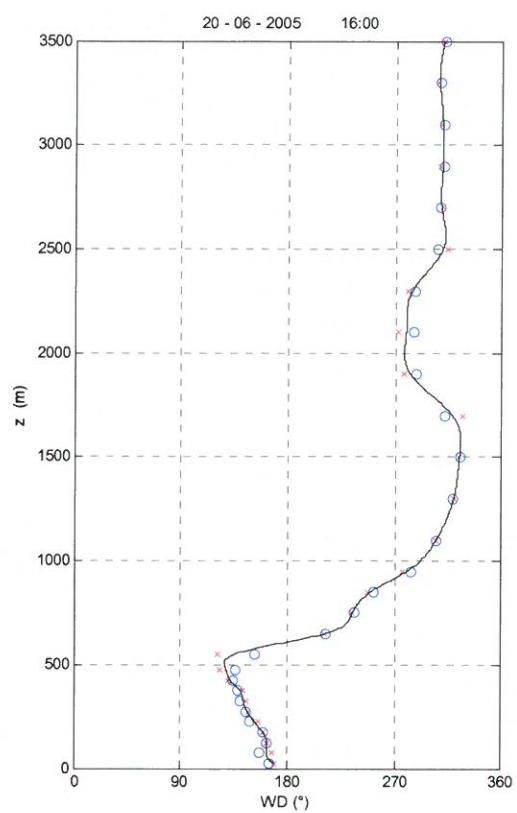
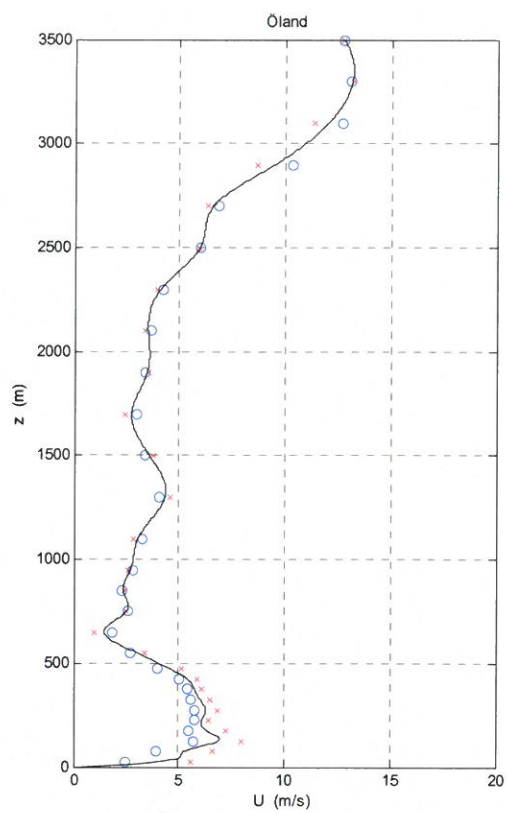


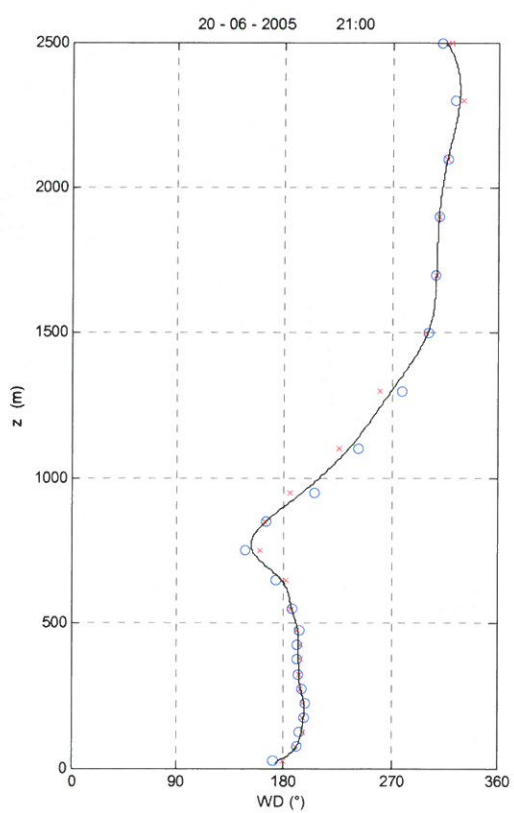
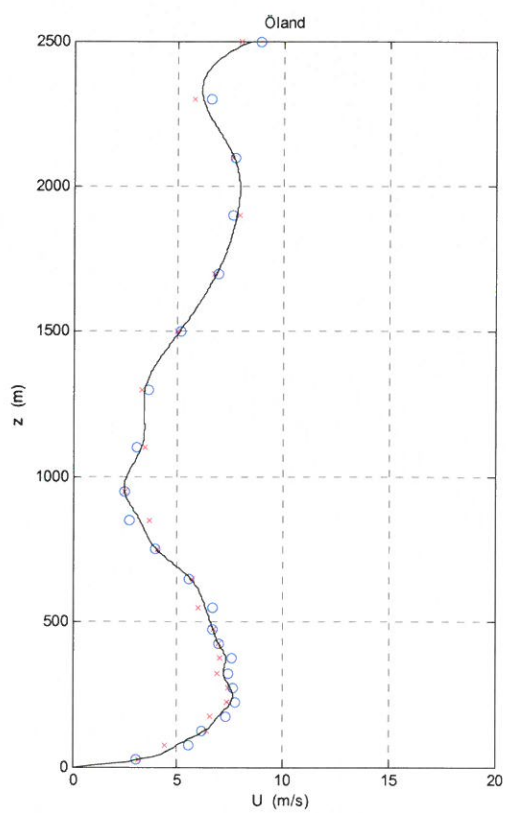
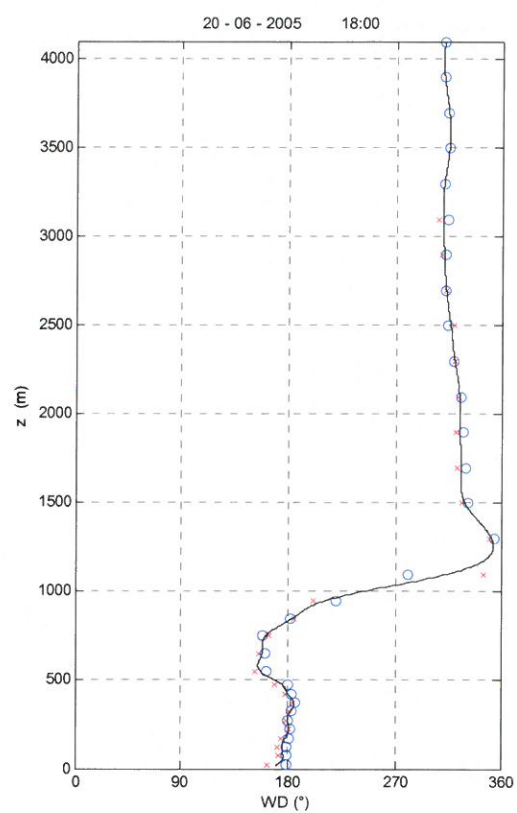
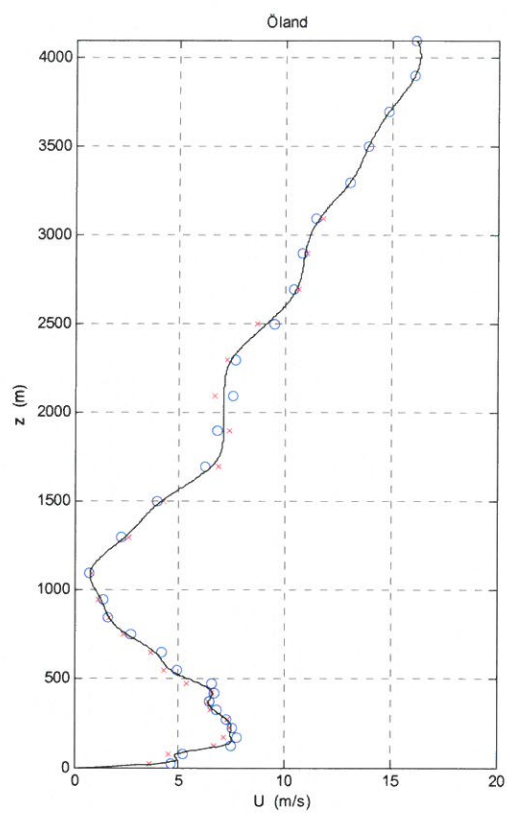


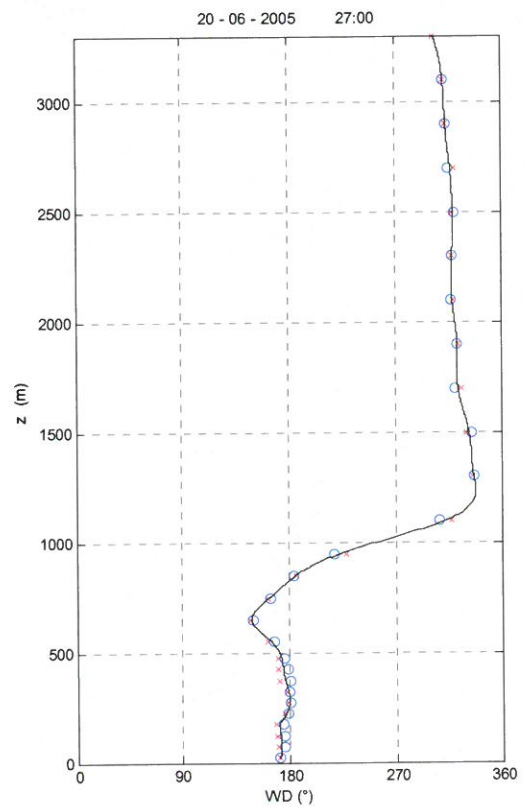
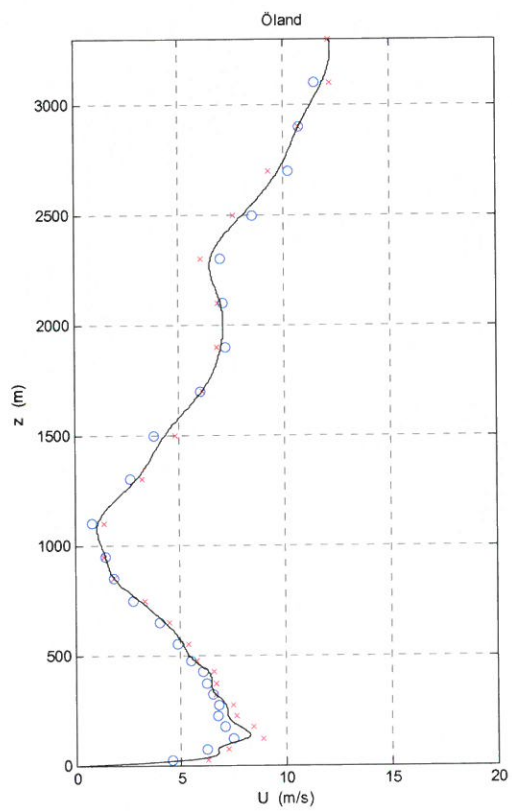
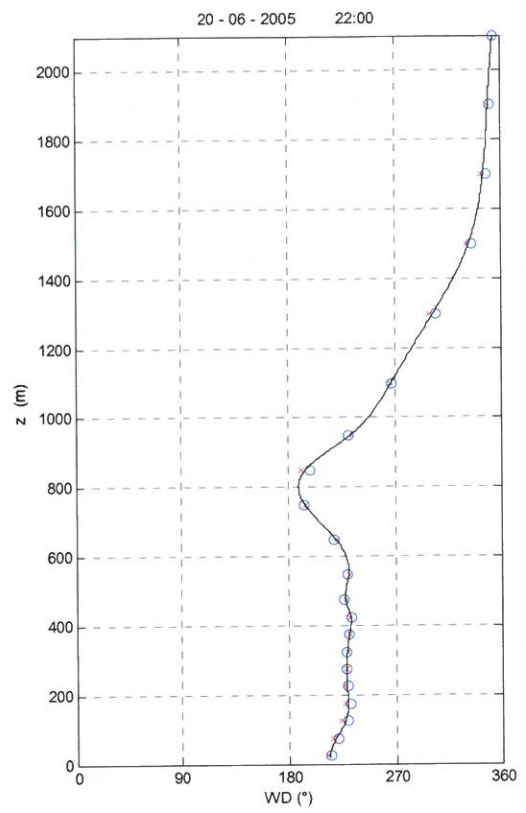
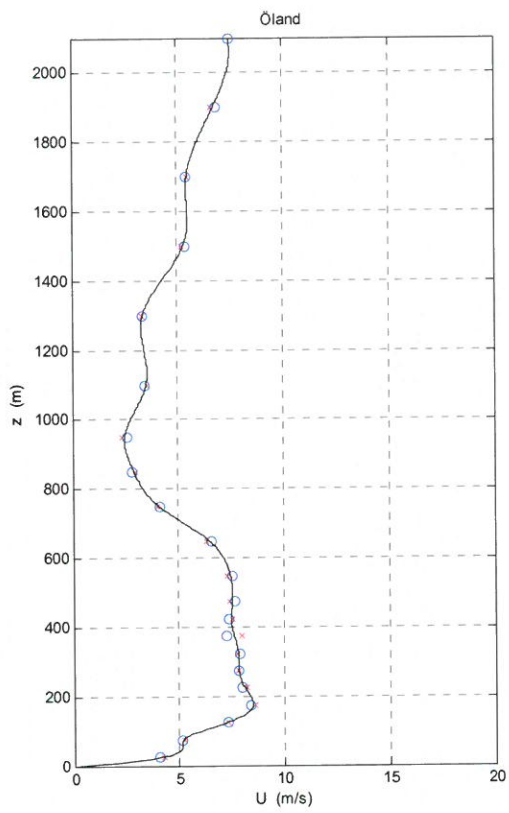


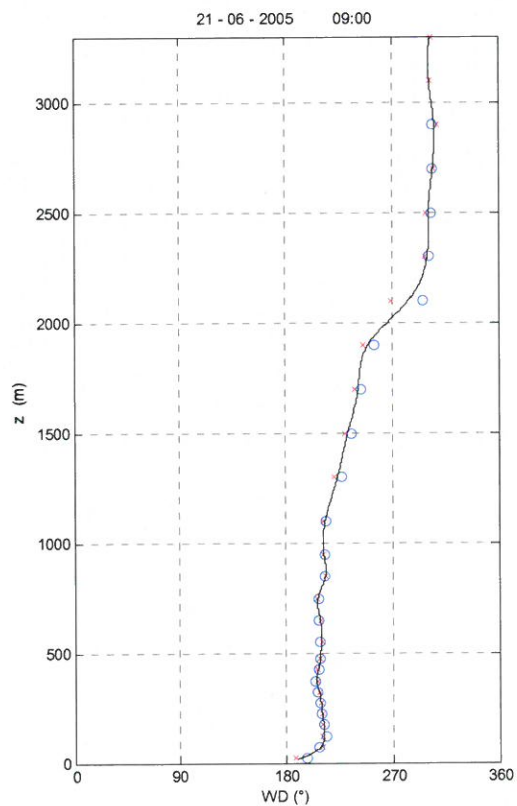
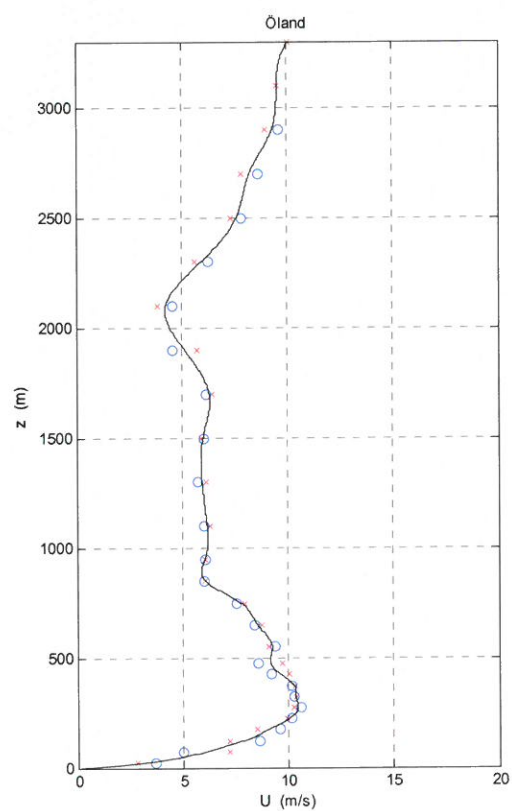
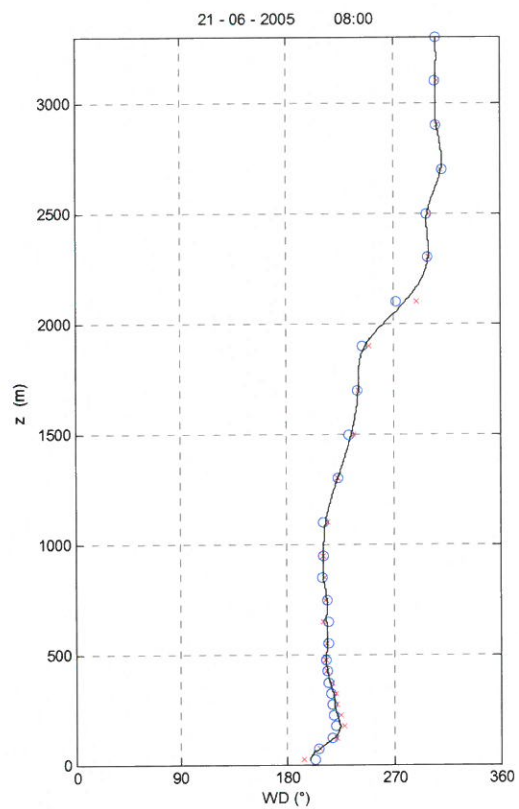
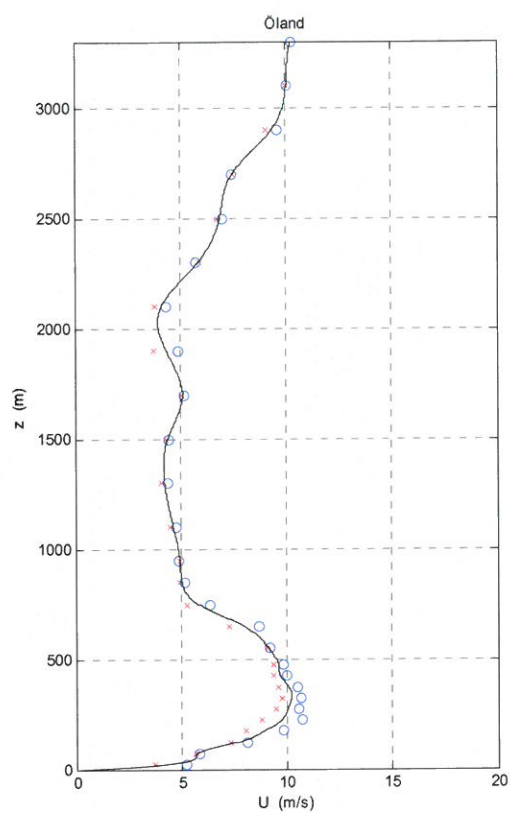


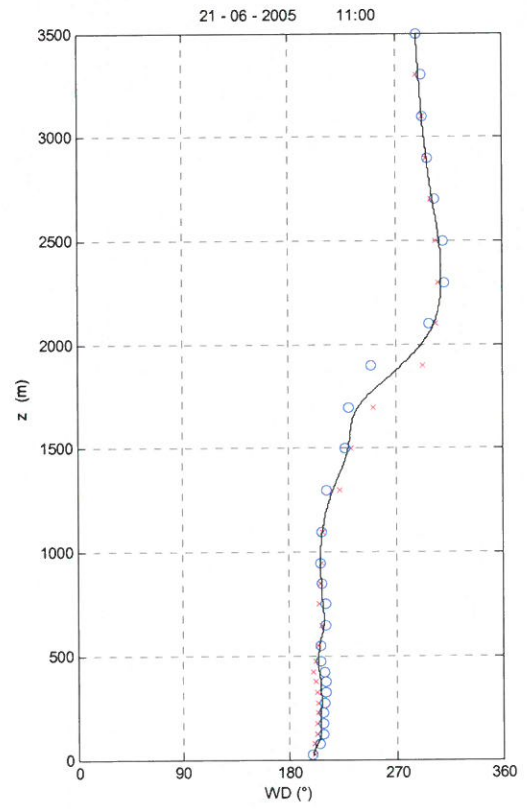
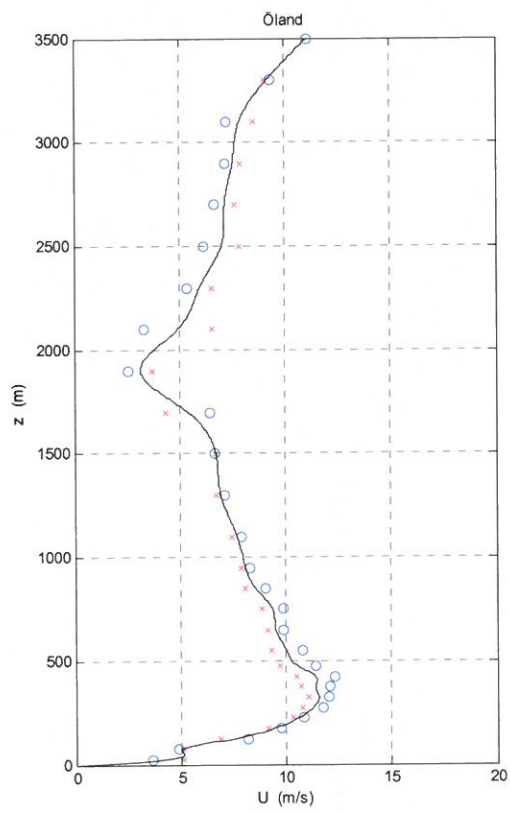
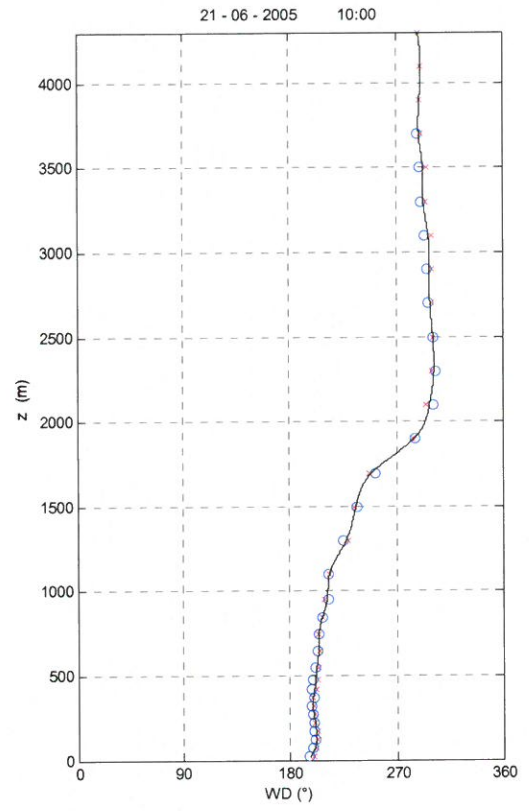
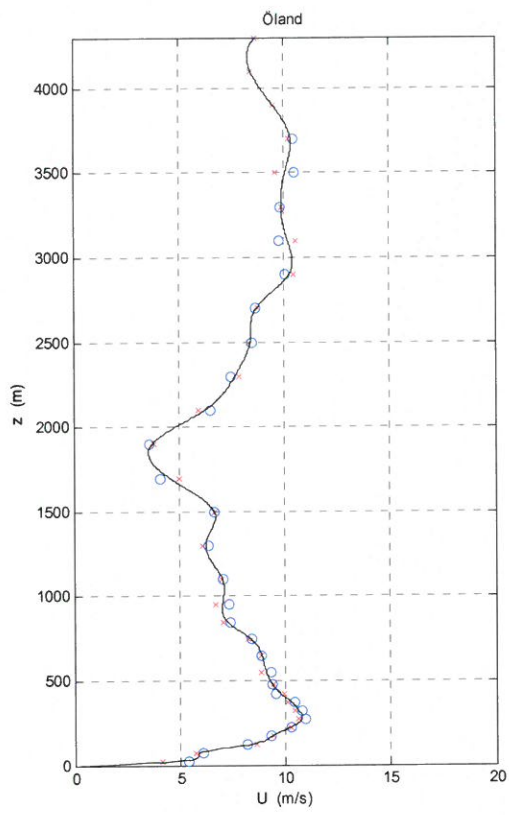


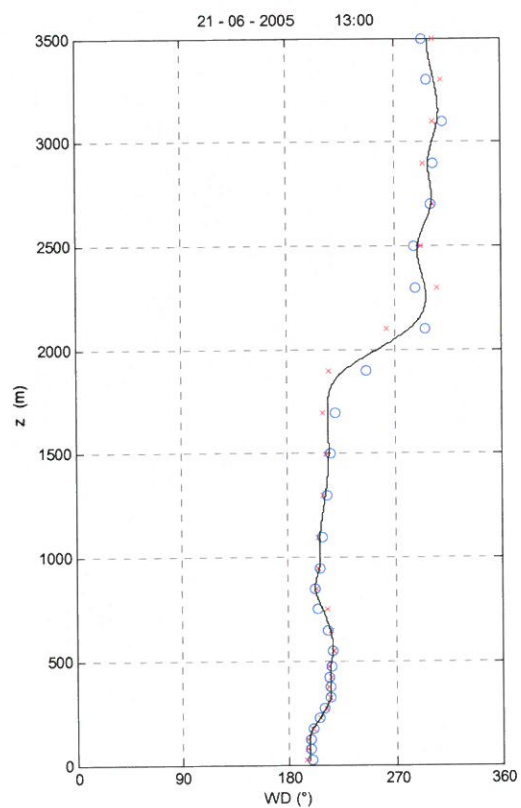
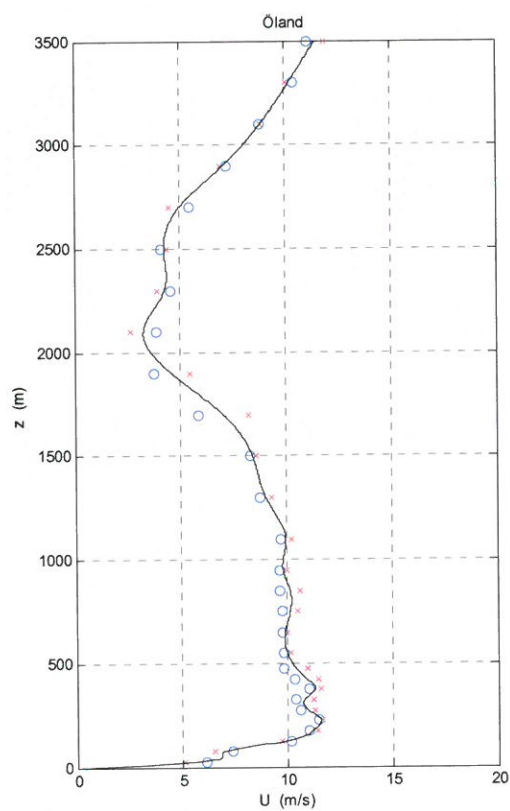
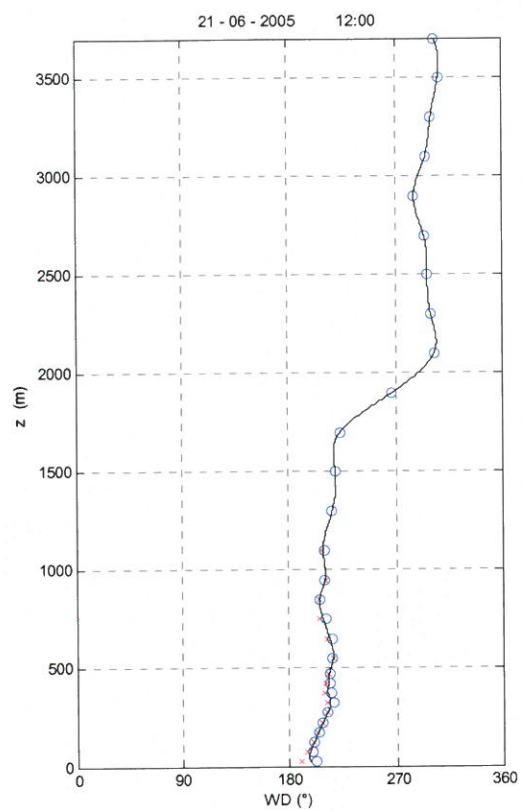
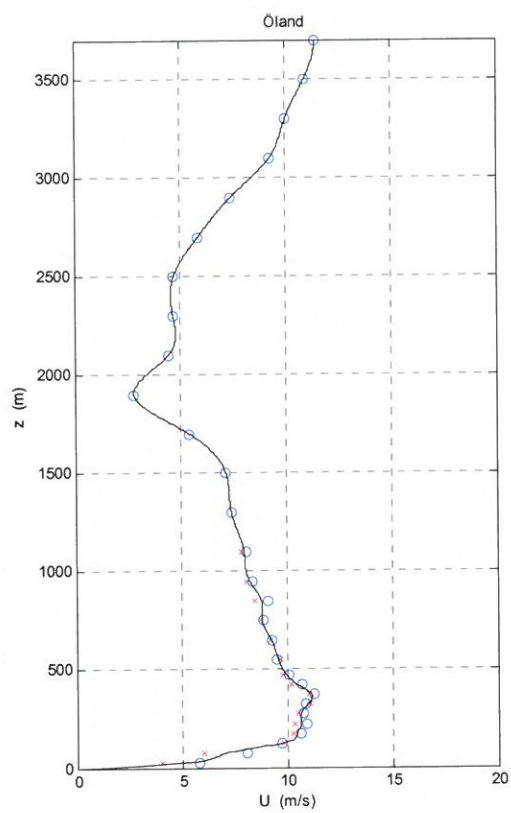


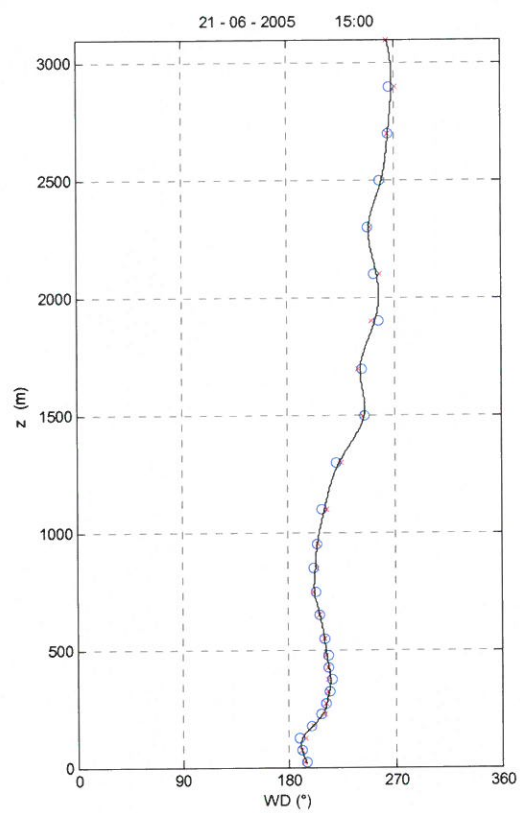
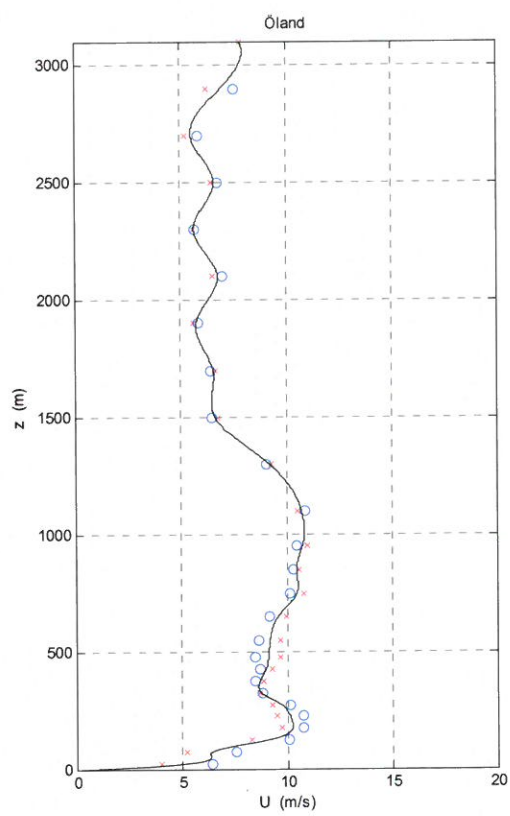












APPENDIX 3: MEASUREMENT DATA (ALL UNITS ARE SI)

Note the last column gives the transmission loss corrected for atmospheric damping only, i.e., $TL = TL_{tot} + 3 - \alpha \cdot \log_{10} r$, see Eq. 11. This value includes the effects of shore and ground damping.

DATE	TIME	Wind direction	Wind Speed	T	H%	alpha 200 Hz	alpha 400 Hz	alpha 80 Hz	atmospheric absorption 200 Hz	atmospheric absorption 400 Hz	atmospheric absorption 80 Hz	DAMPING CORRECTED 200 Hz	DAMPING CORRECTED 400 Hz	DAMPING CORRECTED 80 Hz
20050615	13,05	281	1,90	13,15	74,70	7,95E-04	1,82E-03		7,75	17,76		90,1	70,6	
20050615	13,10	273	1,85	13,25	73,10	8,03E-04	1,83E-03		7,83	17,80		89,3	70,8	
20050615	13,15	273	1,85	13,25	73,10	8,03E-04	1,83E-03		7,83	17,80		96,4	89,1	
20050615	13,20	260	1,82	13,41	71,20	8,13E-04	1,83E-03	1,74E-04	7,92	17,87	1,70	89,9	73,1	94,1
20050615	13,30	251	1,97	13,50	70,70	8,15E-04	1,84E-03		7,95	17,92		96,0	83,1	
20050615	13,35	251	1,97	13,50	70,70	8,15E-04	1,84E-03		7,95	17,92		95,9	84,2	
20050615	13,40	250	2,25	13,64	70,00	8,19E-04	1,85E-03		7,99	17,99		94,9	82,7	
20050615	13,45	250	2,25	13,64	70,00	8,19E-04	1,85E-03		7,99	17,99		97,2	82,8	
20050615	13,55	254	2,66	13,62	70,50	8,16E-04	1,85E-03		7,96	17,99		99,0	84,6	
20050615	14,00	252	2,60	13,72	70,10	8,19E-04	1,85E-03		7,98	18,05		95,1	80,3	
20050615	14,20	260	1,99	13,88	69,30	8,23E-04	1,86E-03		8,02	18,13		108,5	98,6	
20050615	14,25	260	1,99	13,88	69,30	8,23E-04	1,86E-03		8,02	18,13		107,5	98,9	
20050615	14,30	266	2,08	14,07	68,00	8,30E-04	1,87E-03		8,09	18,23		100,8	94,3	
20050615	14,40	277	2,28	13,99	67,30	8,34E-04	1,86E-03		8,13	18,17		104,4	95,3	
20050615	14,50	276	1,76	14,25	64,40	8,50E-04	1,87E-03		8,29	18,27		102,7	95,0	
20050615	14,55	276	1,76	14,25	64,40	8,50E-04	1,87E-03		8,29	18,27		103,6	93,6	
20050615	16,20	225	2,66	14,42	61,80	8,65E-04	1,88E-03		8,43	18,32		107,5	102,6	
20050615	16,45	210	2,85	14,21	61,70	8,65E-04	1,86E-03		8,43	18,18		107,3	114,3	
20050615	17,05	219	2,66	14,35	61,70	8,65E-04	1,87E-03		8,43	18,27		104,4	95,2	
20050615	17,10	218	2,60	14,36	62,20	8,62E-04	1,88E-03		8,41	18,29		108,3	98,9	
20050615	17,15	218	2,60	14,36	62,20	8,62E-04	1,88E-03		8,41	18,29		103,0	84,7	
20050615	17,20	225	2,66	14,42	61,80	8,65E-04	1,88E-03		8,43	18,32		107,6	99,2	
20050615	17,25	225	2,66	14,42	61,80	8,65E-04	1,88E-03		8,43	18,32		109,4	101,6	
20050615	17,30	217	2,98	14,34	62,80	8,59E-04	1,88E-03		8,38	18,29		108,0	96,2	
20050615	17,35	217	2,98	14,34	62,80	8,59E-04	1,88E-03		8,38	18,29		103,3	83,8	
20050615	17,40	210	2,85	14,21	61,70	8,65E-04	1,86E-03		8,43	18,18		106,9	88,1	
20050615	17,45	210	2,85	14,21	61,70	8,65E-04	1,86E-03		8,43	18,18		105,5	99,2	
20050616	10,10	57	5,98	15,69	42,90	9,77E-04	1,88E-03	2,49E-04	9,53	18,35	2,43	88,1	77,1	96,7
20050616	10,20	56	5,82	15,73	42,50	9,80E-04	1,88E-03	2,51E-04	9,55	18,36	2,45	88,8	80,5	101,7
20050616	10,30	58	5,64	15,95	40,50	9,92E-04	1,89E-03	2,59E-04	9,67	18,39	2,53	88,9	82,8	101,1
20050616	10,40	58	5,64	15,95	40,50	9,92E-04	1,89E-03	2,59E-04	9,67	18,39	2,53	94,9	86,8	89,7
20050616	11,00	71	5,37	15,80	52,20	9,28E-04	1,94E-03		9,05	18,93		90,1	80,2	
20050616	12,00	75	6,42	15,80	56,50	9,01E-04	1,96E-03		8,79	19,10		94,5	81,9	
20050616	12,10	74	6,62	15,79	57,20	8,97E-04	1,96E-03		8,74	19,11		93,1	80,3	
20050616	12,30	71	6,11	15,99	57,90	8,93E-04	1,98E-03		8,70	19,27		93,4	83,9	
20050616	12,50	81	6,02	16,08	59,90	8,80E-04	1,99E-03		8,58	19,38		88,8	79,4	
20050616	14,00	88	5,20	16,00	64,20	8,51E-04	1,99E-03		8,30	19,39		77,4	61,6	
20050616	14,10	88	4,89	16,02	64,50	8,49E-04	1,99E-03		8,28	19,40		80,5	58,3	
20050616	14,20	89	4,55	16,02	64,90	8,47E-04	1,99E-03	1,76E-04	8,26	19,41	1,71	78,6	61,4	99,8
20050616	14,30	89	4,38	16,05	65,50		1,99E-03	1,74E-04	0,00	19,43	1,70		47,2	84,5
20050616	14,40	92	4,45	16,07	65,60	8,42E-04	1,99E-03		8,21	19,44		70,4	62,9	
20050616	14,50	90	4,26	16,10	65,60	8,42E-04	2,00E-03	1,74E-04	8,21	19,46	1,69	75,0	61,2	99,0
20050616	15,00	94	3,48	16,20	65,00	8,46E-04	2,00E-03		8,24	19,51		75,3	64,2	
20050616	16,00	157	1,93	15,67	72,00	8,03E-04			7,83	0,00		89,5		
20050616	16,20	123	2,27	15,68	73,20	7,96E-04	1,97E-03		7,76	19,19		101,2	73,5	
20050616	16,30	109	3,11	15,45	73,20	7,97E-04	1,96E-03		7,77	19,07		85,4	77,3	
20050616	16,40	103	3,69	15,52	69,60	8,18E-04	1,96E-03		7,98	19,12		81,2	71,5	
20050616	16,50	103	3,79	15,63	68,10	8,27E-04	1,97E-03	1,70E-04	8,07	19,19	1,66	83,6	67,4	101,5
20050616	17,00	93	3,64	15,73	67,60	8,30E-04	1,97E-03		8,09	19,24		81,9	71,6	
20050616	18,00	85	3,68	15,47	70,20	8,15E-04	1,96E-03		7,95	19,09		99,8	80,0	
20050616	18,10	103	3,60	15,25	73,10	7,98E-04	1,94E-03		7,78	18,96		88,0	74,8	
20050616	18,20	105	4,02	15,23	70,50	8,14E-04	1,94E-03		7,94	18,96		86,5	74,2	
20050616	18,30	107	3,17	15,24	70,20	8,16E-04	1,94E-03	1,68E-04	7,95	18,96	1,64	82,8	66,9	98,9
20050616	19,00	102	3,07	14,95	71,50	8,09E-04	1,93E-03	1,66E-04	7,89	18,80	1,62	91,0	73,3	89,7
20050617	9,00	189	2,74	12,89	90,90	7,18E-04	1,81E-03	1,43E-04	7,00	17,60	1,39	83,0	65,4	83,1
20050617	9,30	172	2,77	12,91	91,10	7,17E-04	1,81E-03	1,42E-04	6,99	17,61	1,39	77,1	61,4	76,2

20050617	9,40	175	2,90	12,86	90,70	7,19E-04	1,80E-03	1,43E-04	7,01	17,59	1,40	88,0	68,4	88,0
20050617	9,50	180	3,43	12,91	90,20	7,21E-04	1,81E-03	1,44E-04	7,03	17,62	1,40	69,0	68,7	82,6
20050617	10,00	187	3,43	12,85	90,50	7,20E-04	1,80E-03	1,44E-04	7,02	17,59	1,40	77,5	58,4	78,0
20050617	11,00	208	5,43	14,31	82,30	7,52E-04	1,89E-03		7,33	18,39		80,1	60,5	
20050617	11,10	207	5,85	13,98	87,10	7,29E-04	1,86E-03	1,44E-04	7,11	18,16	1,40	79,1	62,4	72,0
20050617	11,20	208	6,05	14,00	88,60	7,22E-04	1,86E-03	1,41E-04	7,04	18,14	1,38	73,1	71,4	81,5
20050617	11,30	211	6,64	14,16	87,90	7,24E-04	1,87E-03	1,42E-04	7,06	18,22	1,38	71,2	62,3	75,3
20050617	11,40	206	6,62	14,71	82,60	7,48E-04	1,90E-03	1,47E-04	7,29	18,57	1,44	77,7	58,3	74,9
20050617	11,50	202	7,39	14,40	87,30	7,25E-04	1,88E-03	1,41E-04	7,07	18,34	1,38	78,6	60,3	67,1
20050617	12,00	204	6,54	14,10	90,30	7,13E-04	1,86E-03	1,38E-04	6,95	18,15	1,35	72,0	60,8	65,1
20050617	13,00	225	8,29	15,23	79,30	7,62E-04	1,94E-03	1,51E-04	7,43	18,88	1,47	74,4	55,4	78,9
20050617	13,10	231	9,40	15,39	77,50	7,72E-04	1,95E-03	1,53E-04	7,52	18,99	1,49	72,8	65,6	68,9
20050617	13,20	227	10,13	15,20	79,60	7,61E-04	1,93E-03	1,50E-04	7,42	18,86	1,46	76,9	69,2	76,1
20050617	13,30	230	10,49	15,24	79,10	7,63E-04	1,94E-03	1,51E-04	7,44	18,89	1,47	72,0	70,7	76,5
20050617	13,40	233	10,65	15,64	74,40	7,88E-04	1,96E-03	1,58E-04	7,69	19,16	1,54	73,2	68,8	80,0
20050617	13,50	232	10,10	15,28	77,30	7,74E-04	1,94E-03	1,54E-04	7,54	18,93	1,50	75,5	70,2	81,2
20050617	14,00	237	11,32	15,10	77,70	7,72E-04	1,93E-03	1,54E-04	7,53	18,84	1,50	73,7	71,7	83,4
20050617	15,00	236	10,53	14,58	84,60	7,38E-04	1,89E-03	1,45E-04	7,20	18,48	1,41	85,6	71,0	80,0
20050617	15,10	235	9,63	14,68	84,20	7,39E-04	1,90E-03	1,45E-04	7,21	18,53	1,41	73,4	64,5	85,0
20050617	15,20	233	10,79	14,29	87,10	7,27E-04	1,88E-03	1,42E-04	7,09	18,30	1,39	73,4	67,4	85,0
20050617	15,30	235	11,32	14,17	87,00	7,29E-04	1,87E-03	1,43E-04	7,10	18,25	1,39	75,2	67,5	76,4
20050617	15,40	234	10,82	13,87	89,10	7,20E-04	1,85E-03	1,41E-04	7,02	18,07	1,38	72,0	68,1	76,5
20050617	15,50	235	10,76	13,62	91,10	7,12E-04	1,84E-03	1,39E-04	6,95	17,93	1,36	75,5	65,5	81,6
20050617	16,00	235	11,34	13,60	91,20	7,12E-04	1,84E-03	1,39E-04	6,94	17,92	1,36	73,5	66,9	79,5
20050617	16,10	237	11,53	13,60	91,40	7,11E-04	1,84E-03	1,39E-04	6,93	17,91	1,36	72,7	70,1	79,3
20050617	16,20	242	10,85	13,46	92,60	7,07E-04	1,83E-03	1,38E-04	6,89	17,83	1,35	76,7	72,2	88,1
20050617	16,30	240	10,66	13,37	93,20	7,04E-04	1,82E-03	1,38E-04	6,87	17,78	1,34	78,9	68,1	74,8
20050618	11,40	359	7,29	15,40	76,00	7,80E-04	1,95E-03	1,56E-04	7,61	19,01	1,52	87,7	76,1	103,6
20050618	11,50	351	6,92	15,53	75,90	7,80E-04	1,95E-03	1,55E-04	7,61	19,08	1,51	87,3	66,6	86,8
20050618	12,00	0	5,91	15,74	75,20	7,83E-04	1,97E-03	1,56E-04	7,63	19,20	1,52	74,6	51,2	77,9
20050618	13,00	13	2,59	15,65	77,20	7,72E-04	1,96E-03	1,52E-04	7,52	19,12	1,49	73,3	56,7	78,2
20050618	13,10	10	2,43	15,71	76,40	7,76E-04	1,97E-03	1,53E-04	7,57	19,16	1,50	68,6	61,8	87,4
20050618	13,30	12	2,26	16,23	73,40	7,91E-04	2,00E-03	1,57E-04	7,71	19,47	1,53	65,7	52,4	75,7
20050618	13,40	8	2,38	16,66	70,10	8,09E-04	2,03E-03	1,61E-04	7,89	19,74	1,57	69,4	54,7	79,2
20050618	13,50	3	2,58	17,58	63,90	8,47E-04	2,08E-03	1,71E-04	8,26	20,32	1,66	78,6	64,4	93,7
20050618	15,00	212	0,67	18,64	59,50	8,76E-04	2,15E-03	1,76E-04	8,54	20,97	1,72	73,2	59,5	90,4
20050618	15,10	231	1,26	18,27	60,90	8,66E-04	2,13E-03	1,75E-04	8,45	20,74	1,70	78,7	65,4	88,4
20050618	15,20	224	0,59	18,05	61,50	8,63E-04	2,11E-03	1,74E-04	8,41	20,61	1,70	83,1	64,0	87,6
20050618	15,35	0	5,91	15,74	75,20	7,83E-04	1,97E-03	1,56E-04	7,63	19,20	1,52	81,9	60,3	90,8
20050618	15,40	208	1,10	18,20	60,80	8,68E-04	2,12E-03	1,75E-04	8,46	20,71	1,71	78,8	71,2	98,4
20050618	15,50	205	2,48	18,14	60,20	8,73E-04	2,12E-03		8,51	20,67		75,9	62,5	
20050618	16,00	201	2,96	18,25	59,50	8,78E-04	2,13E-03		8,56	20,74		65,7	55,6	
20050618	17,00	0	5,91	15,74	75,20	7,83E-04	1,97E-03	1,56E-04	7,63	19,20	1,52	79,7	67,3	100,2
20050618	17,10	148	5,58	15,12	81,40	7,51E-04	1,93E-03	1,48E-04	7,33	18,79	1,44	75,1	62,9	93,1
20050618	17,20	143	5,27	15,82	78,40	7,63E-04	1,97E-03	1,49E-04	7,44	19,17	1,46	70,1	59,4	96,8
20050618	17,30	0	5,91	15,74	75,20	7,83E-04	1,97E-03		7,63	19,20		81,4	66,0	
20050618	17,40	129	5,19	15,88	78,10	7,65E-04	1,97E-03	1,50E-04	7,46	19,21	1,46	74,4	55,7	87,2
20050618	17,50	122	5,20	15,82	78,40	7,63E-04	1,97E-03	1,49E-04	7,44	19,17	1,46	82,8	72,3	88,8
20050618	19,00	119	4,23	16,18	76,20	7,74E-04	1,99E-03	1,52E-04	7,54	19,39	1,48	80,0	72,4	84,4
20050618	19,10	94	4,77	16,12	75,70	7,77E-04	1,99E-03	1,53E-04	7,58	19,37	1,49	72,9	73,2	87,3
20050618	19,20	100	3,81	16,24	74,10	7,86E-04	2,00E-03	1,55E-04	7,67	19,46	1,51	83,7	74,8	84,7
20050618	19,30	105	3,60	16,25	75,00	7,81E-04	1,99E-03	1,54E-04	7,61	19,45	1,50	77,6	71,0	87,6
20050618	19,40	111	3,30	16,12	75,80	7,77E-04	1,99E-03	1,53E-04	7,57	19,37	1,49	84,8	76,3	85,6
20050618	19,50	125	2,49	16,23	74,70	7,83E-04	1,99E-03	1,54E-04	7,63	19,45	1,50	83,2	77,7	99,7
20050618	20,00	169	1,75	15,69	80,20	7,54E-04	1,96E-03		7,35	19,07		95,9	89,3	
20050618	21,30	224	4,23	14,23	82,00	7,54E-04	1,88E-03		7,35	18,35		80,2	57,6	
20050618	21,40	228	4,02	14,50	80,60	7,60E-04	1,90E-03		7,41	18,50		79,3	65,9	
20050618	21,50	230	4,35	14,25	81,60	7,56E-04	1,88E-03		7,37	18,37		80,6	52,1	
20050618	22,00	230	4,29	14,32	80,90	7,59E-04	1,89E-03		7,40	18,41		82,9	59,5	
20050619	12,30	152	3,44	17,06	54,60	9,17E-04	2,04E-03		8,94	19,91		85,7	80,0	
20050619	13,30	203	7,40	15,18	69,60	8,20E-04	1,94E-03		7,99	18,92		98,3	94,0	
20050619	13,50	197	7,08	15,07	71,00	8,12E-04	1,93E-03		7,91	18,86		108,2	105,9	
20050619	14,00	203	7,12	15,12	68,60	8,26E-04	1,94E-03		8,05	18,88		109,5	101,2	
20050619	14,10	206	6,85	15,28	67,40	8,33E-04	1,95E-03		8,12	18,97		109,8	107,8	
20050619	14,20	202	6,56	15,33	66,10	8,40E-04	1,95E-03		8,19	18,99		111,7	112,7	
20050619	14,30	199	6,95	15,13	68,50	8,26E-04	1,94E-03		8,06	18,89		109,4	100,7	
20050619	14,40	199	7,51	14,22	74,70	7,93E-04	1,89E-03	1,64E-04	7,73	18,38	1,59	105,8	96,2	97,2
20050619	14,50	193	7,50	14,48	70,60	8,15E-04	1,90E-03		7,95	18,52		94,0	96,8	
20050619	15,00	192	7,41	14,67	69,7	8,20E-04	1,91E-03	1,72E-04	8,00	18,62	1,67	104,0	90,7	99,3
20050620	10,00	344	2,26	15,58	56	9,03E-04	1,94E-03		8,81	18,93		85,6	65,8	
20050620	10,10	344	2,22	15,8	53,7	9,19E-04	1,95E-03	2,08E-04	8,96	19,00	2,03	81,3	58,8	86,3
20050620	10,20	336	2,39	15,8	53,7	9,19E-04	1,95E-03	2,08E-04	8,96	19,00	2,03	79,3	69,6	86,7
20050620	10,30	343	1,87	15,8	53,6	9,19E-04	1,95E-03	2,08E-04	8,96	18,99	2,03	84,5	62,0	83,2
20050620	10,40	338	1,61	15,9	53,2	9,22E-04	1,95E-03		8,99	19,05		117,0	85,8	
20050620	10,50	332	1,29	15,86	53,20	9,22E-04	1,95E-03	2,09E-04	8,99	19,02	2,04	84,8	70,0	78,7
20050620	12,00	201	2,72	15,65	56,50	9,00E-04	1,95E-03	2,00E-04	8,78	18,99	1,95	117,2	83,3	83,4
20050620	12,10	198	3,86	15,40	59,20	8,83E-04	1,94E-03		8,61	18,91		100,4	94,1	
20050620	12,20	197	5,10	14,64	73,90	7,96E-04	1,91E-03	1,63E-04	7,76	18,62	1,59	102,8	89,1	88,9
20050620	12,30	192	5,32	14,30	79,80	7,65E-04	1,89E-03	1,54E-04	7,46	18,41	1,50	100,2	86,5	86,9
20050620	12,40	186	5,31	14,26	77,90	7,76E-04	1,89E-03	1,57E-04	7,56	18,40	1,53	94,0	81,9	97,7

20050620	12,50	186	5,31	14,26	77,90	7,76E-04	1,89E-03		7,56	18,40		105,8	92,6	
20050620	13,00	195	5,20	14,32	78,70	7,71E-04			7,52	0,00		104,3		
20050620	14,00	189	6,59	13,96	82,10	7,55E-04	1,87E-03	1,52E-04	7,36	18,22	1,48	97,8	90,2	95,8
20050620	14,10	185	7,05	14,03	80,70	7,62E-04	1,87E-03	1,54E-04	7,43	18,26	1,50	107,4	98,1	98,8
20050620	14,20	185	7,07	14,15	79,00	7,70E-04	1,88E-03		7,51	18,34		103,3	96,2	
20050620	14,30	192	6,99	14,03	81,90	7,56E-04	1,87E-03		7,37	18,25		105,7	99,8	
20050620	14,40	193	6,92	13,92	83,50	7,48E-04	1,86E-03		7,29	18,18		104,1	98,8	
20050620	14,50	194	6,82	13,91	83,30	7,49E-04	1,86E-03		7,30	18,18		106,4	97,9	
20050620	15,00	199	6,77	13,90	84,10	7,45E-04	1,86E-03	1,49E-04	7,26	18,16	1,45	103,8	95,0	94,3
20050620	16,00	205	6,26	13,81	89,60	7,18E-04	1,85E-03		7,00	18,04		102,4	87,9	
20050620	16,10	205	6,59	13,78	89,30	7,20E-04	1,85E-03		7,02	18,03		119,0	91,0	
20050620	16,30	197	6,59	13,79	86,50	7,34E-04	1,85E-03	1,45E-04	7,15	18,08	1,42	96,1	74,2	92,7
20050620	16,40	200	6,52	13,74	88,30	7,25E-04	1,85E-03	1,43E-04	7,07	18,03	1,39	95,1	79,4	91,4
20050620	16,50	206	6,40	13,72	90,00	7,17E-04	1,85E-03		6,99	17,99		90,0	73,9	
20050620	17,00	202	6,51	13,77	89,50	7,19E-04	1,85E-03		7,01	18,02		88,2	75,7	
20050620	18,00	200	7,09	14,11	82,90	7,50E-04	1,88E-03	1,50E-04	7,31	18,28	1,46	73,7	67,3	82,9
20050620	18,10	200	7,48	14,14	82,50	7,52E-04	1,88E-03	1,50E-04	7,33	18,30	1,46	79,9	70,7	83,0
20050620	18,30	203	7,41	14,22	81,30	7,58E-04	1,88E-03	1,52E-04	7,39	18,35	1,48	79,3	69,8	87,7
20050621	9,10	209	7,04	14,05	78,70	7,72E-04	1,88E-03	1,57E-04	7,53	18,28	1,53	75,0	64,7	82,9
20050621	9,20	205	7,12	14,04	79,00	7,71E-04	1,87E-03	1,56E-04	7,52	18,28	1,53	77,1	66,1	92,0
20050621	9,30	203	7,01	13,99	80,40	7,64E-04	1,87E-03	1,54E-04	7,45	18,24	1,50	73,7	63,0	88,0
20050621	9,40	204	7,14	14,02	80,40	7,64E-04	1,87E-03	1,54E-04	7,44	18,26	1,50	74,1	63,8	93,2
20050621	9,50	200	7,16	14,05	79,90	7,66E-04	1,87E-03	1,55E-04	7,47	18,28	1,51	72,1	61,3	88,6
20050621	10,00	199	7,45	14,11	78,70	7,72E-04	1,88E-03	1,57E-04	7,53	18,32	1,53	73,5	61,5	93,1
20050621	10,10	198	7,94	14,20	77,10	7,80E-04	1,88E-03	1,59E-04	7,61	18,37	1,55	73,6	60,8	79,7
20050621	11,00	197	8,28	14,30	77,60	7,77E-04	1,89E-03	1,58E-04	7,58	18,42	1,54	77,1	62,9	87,0
20050621	11,10	196	8,17	14,23	79,60	7,67E-04	1,88E-03	1,55E-04	7,48	18,37	1,51	70,9	57,2	85,1
20050621	11,20	196	8,11	14,16	81,00	7,60E-04	1,88E-03	1,52E-04	7,41	18,33	1,49	73,5	53,3	83,7
20050621	11,30	197	8,07	14,07	82,90	7,50E-04	1,87E-03	1,50E-04	7,31	18,26	1,46	69,8	58,6	86,3
20050621	11,40	198	8,13	14,02	84,00	7,45E-04	1,87E-03	1,48E-04	7,26	18,22	1,44	75,4	60,8	80,6
20050621	11,50	201	8,29	13,99	84,80	7,41E-04	1,87E-03	1,47E-04	7,22	18,20	1,43	72,9	57,5	80,6
20050621	13,10	197	9,08	14,02	84,30	7,43E-04	1,87E-03		7,25	18,22		69,0	57,0	
20050621	13,30	196	8,48	14,02	84,70	7,41E-04	1,87E-03		7,23	18,21		72,2	57,4	
20050621	13,40	198	8,12	13,98	85,00	7,40E-04	1,87E-03		7,22	18,19		70,1	56,6	
20050621	13,50	197	7,86	13,97	85,10	7,40E-04	1,87E-03		7,21	18,19		69,3	54,7	
20050621	14,00	197	7,94	14,01	84,70	7,41E-04	1,87E-03	1,47E-04	7,23	18,21	1,43	73,4	59,0	83,5
20050621	14,10	196	7,78	14,01	84,40	7,43E-04	1,87E-03	1,48E-04	7,24	18,21	1,44	67,1	59,1	87,9
20050621	14,20	198	7,88	14,00	84,20	7,44E-04	1,87E-03	1,48E-04	7,25	18,21	1,44	74,1	56,8	88,1
20050621	14,30	199	7,81	13,99	84,00	7,45E-04	1,87E-03	1,48E-04	7,26	18,21	1,45	67,6	60,1	89,9
20060601	11,10	28	6,38	8,24	78,40	7,42E-04	1,50E-03		7,24	14,60		104,7	102,1	
20060601	11,20	23	7,64	8,19	78,50	7,43E-04	1,50E-03		7,24	14,60		105,3	103,1	
20060601	11,30	24	8,10	8,13	80,00	7,34E-04	1,50E-03		7,16	14,59		99,3	94,2	
20060601	11,40	23	8,88	8,05	81,70	7,31E-04	1,49E-03		7,13	14,57		100,9	99,6	
20060601	11,50	27	9,06	8,01	82,60	7,24E-04	1,50E-03		7,06	14,62		93,9	100,0	
20060601	12,00	27	8,81	7,99	82,60	7,26E-04	1,50E-03		7,08	14,58		102,1	99,9	
20060601	12,10	28	8,28	8,05	83,30	7,26E-04	1,50E-03		7,08	14,64		101,9	98,8	
20060601	12,40	37	7,46	8,34	76,10	7,50E-04	1,50E-03		7,31	14,61		103,8	101,4	
20060601	14,00	27	6,58	9,19	75,20	7,60E-04	1,55E-03		7,41	15,15		99,5	78,0	
20060601	14,30	25	6,93	9,19	74,40	7,58E-04	1,55E-03		7,39	15,14		106,4	88,5	
20060601	14,40	23	6,62	9,23	76,60	7,54E-04	1,55E-03		7,35	15,15		102,8	86,7	
20060601	14,50	23	6,96	9,34	75,30	7,62E-04	1,56E-03		7,43	15,21		99,6	79,7	
20060601	15,00	29	6,56	9,52	75,30	7,67E-04	1,57E-03		7,48	15,34		101,8	84,3	
20060601	15,10	26	6,20	9,43	79,40	7,50E-04	1,57E-03		7,31	15,34		100,2	81,9	
20060601	15,20	19	7,04	9,47	75,30	7,78E-04	1,57E-03		7,58	15,33		79,6	58,8	
20060601	15,30	19	5,83	9,52	74,30	7,66E-04	1,57E-03		7,46	15,33		99,9	81,9	
20060601	15,40	11	6,05	9,61	76,90	7,61E-04	1,58E-03		7,42	15,40		99,2	80,9	
20060601	15,50	18	6,83	9,74	77,00	7,58E-04	1,59E-03		7,39	15,55		99,8	83,2	
20060601	16,00	49	5,81	9,85	74,20	7,69E-04	1,59E-03		7,50	15,50		101,7	85,7	
20060601	16,05	49	5,81	9,85	74,20	7,68E-04	1,59E-03		7,49	15,48		99,2	82,8	
20060601	16,10	41	3,76	9,92	74,40	7,68E-04	1,59E-03		7,49	15,52		98,9	79,1	
20060601	16,15	41	3,76	9,92	74,40	7,70E-04	1,59E-03		7,51	15,54		100,8	83,3	
20060601	16,20	21	4,01	9,84	74,90	7,63E-04	1,59E-03		7,44	15,48		103,1	83,4	
20060601	16,25	21	4,01	9,84	74,90	7,62E-04	1,58E-03		7,43	15,45		103,1	81,9	
20060601	16,30	17	3,46	9,89	75,40	7,64E-04	1,59E-03		7,45	15,52		101,2	80,7	
20060601	16,35	17	3,46	9,89	75,40	7,65E-04	1,59E-03		7,46	15,51		96,3	75,1	
20060602	9,00	214	4,70	8,97	92,70	7,04E-04	1,57E-03	1,50E-04	6,86	15,31	1,46	83,2	69,9	68,7
20060602	9,05	214	4,70	8,97	92,70	7,02E-04	1,57E-03	1,50E-04	6,85	15,30	1,46	84,8	72,9	58,4
20060602	9,10	216	5,52	9,16	91,40	7,09E-04	1,58E-03	1,51E-04	6,91	15,38	1,47	90,6	75,0	72,3
20060602	9,15	216	5,52	9,16	91,40	7,08E-04	1,58E-03	1,51E-04	6,90	15,38	1,47	82,7	68,0	71,3
20060602	9,20	220	5,60	9,54	88,30	7,20E-04	1,60E-03	1,36E-04	7,02	15,59	1,33	89,6	74,1	55,3
20060602	9,25	220	5,60	9,54	88,30	7,18E-04	1,60E-03	1,54E-04	7,00	15,57	1,50	83,1	68,3	65,7
20060602	9,30	212	6,10	9,42	89,00	7,16E-04	1,59E-03	1,53E-04	6,98	15,50	1,50	85,8	70,7	64,9
20060602	9,35	212	6,10	9,42	89,00	7,16E-04	1,59E-03	1,54E-04	6,98	15,51	1,50	78,8	64,3	71,8
20060602	9,40	210	6,44	9,26	90,90	7,09E-04	1,58E-03	1,51E-04	6,91	15,44	1,48	76,4	65,0	71,4
20060602	9,45	210	6,44	9,26	90,90	7,09E-04	1,58E-03	1,51E-04	6,92	15,43	1,48	85,0	68,6	69,4
20060602	10,00	210	7,24	9,28	90,40	7,13E-04	1,58E-03	1,52E-04	6,95	15,45	1,48	77,9	65,1	63,6
20060602	10,05	210	7,24	9,28	90,40	7,11E-04	1,58E-03	1,52E-04	6,93	15,43	1,48	83,0	68,5	62,4
20060602	10,10	212	7,56	9,83	86,40	7,26E-04	1,61E-03	1,67E-04	7,08	15,72	1,63	87,8	74,4	71,5
20060602	10,15	212	7,56	9,83	86,40	7,27E-04	1,61E-03		7,09	15,73		84,1	68,4	
20060602	10,20	210	7,98	9,64	87,60	7,21E-04	1,60E-03	1,66E-04	7,03	15,62	1,62	79,9	67,0	69,5

20060602	10,25	210	7,98	9,64	87,60	7,21E-04	1,60E-03	1,66E-04	7,03	15,61	1,62	80,3	65,9	70,1
20060602	10,30	207	8,47	9,41	89,20	7,14E-04	1,59E-03	1,64E-04	6,96	15,51	1,60	82,5	67,7	71,9
20060602	10,35	207	8,47	9,41	89,20	7,16E-04	1,59E-03	1,67E-04	6,98	15,50	1,62	88,0	73,6	53,0
20060602	10,40	208	8,97	9,35	89,00	7,16E-04	1,59E-03	1,65E-04	6,98	15,47	1,61	88,0	74,2	70,4
20060602	10,45	208	8,97	9,35	89,00	7,17E-04	1,59E-03	1,65E-04	6,99	15,47	1,61	84,7	70,8	69,6
20060602	11,00	205	9,42	9,22	89,10	7,16E-04	1,58E-03	1,65E-04	6,98	15,40	1,61	91,2	76,6	72,8
20060602	11,05	205	9,42	9,22	89,10	7,14E-04	1,58E-03	1,65E-04	6,96	15,40	1,61	89,0	74,3	70,8
20060602	11,10	204	9,60	9,10	90,10	7,11E-04	1,57E-03	1,64E-04	6,93	15,33	1,60	84,8	67,8	70,3
20060602	11,15	204	9,60	9,10	90,10	7,13E-04	1,57E-03	1,86E-04	6,95	15,33	1,81	86,4	71,5	60,1
20060602	11,20	208	9,65	9,21	90,50	7,11E-04	1,58E-03	1,52E-04	6,93	15,38	1,48	84,4	70,1	70,3
20060602	11,25	208	9,65	9,21	90,50	7,12E-04	1,58E-03	1,52E-04	6,94	15,38	1,48	87,6	72,7	69,8
20060602	11,30	210	10,25	9,56	88,30	7,19E-04	1,60E-03	1,54E-04	7,01	15,58	1,50	81,9	67,6	69,3
20060602	11,35	210	10,25	9,56	88,30	7,16E-04	1,59E-03	1,54E-04	6,98	15,55	1,50	82,5	68,2	68,2
20060602	11,40	211	10,75	9,81	86,00	7,25E-04	1,61E-03	1,56E-04	7,07	15,70	1,52	79,2	64,7	65,4
20060602	11,45	211	10,75	9,81	86,00	7,26E-04	1,61E-03	1,56E-04	7,08	15,69	1,52	81,2	67,5	66,0
20060602	12,00	209	11,10	9,73	85,60	7,31E-04	1,61E-03	1,57E-04	7,13	15,67	1,53	80,6	67,4	70,2
20060602	12,10	209	11,11	9,71	86,20	7,26E-04	1,60E-03	1,56E-04	7,08	15,64	1,53	79,5	64,7	71,2
20060602	12,15	209	11,11	9,71	86,20	7,25E-04	1,60E-03	1,56E-04	7,07	15,65	1,53	85,1	70,5	68,4
20060602	12,20	209	10,81	9,68	86,80	7,23E-04	1,60E-03	1,56E-04	7,05	15,64	1,52	81,8	68,5	67,2
20060602	12,25	209	10,81	9,68	86,80	7,23E-04	1,60E-03	1,56E-04	7,05	15,62	1,52	79,9	63,5	63,7
20060602	12,30	210	10,74	9,63	87,90	7,19E-04	1,60E-03	1,54E-04	7,01	15,61	1,50	79,1	64,8	70,2
20060602	12,35	210	10,74	9,63	87,90	7,19E-04	1,60E-03	1,54E-04	7,01	15,58	1,50	80,7	65,1	69,6
20060602	12,40	211	11,06	9,57	88,50	7,21E-04	1,59E-03	1,54E-04	7,03	15,54	1,50	81,9	67,7	68,6
20060602	12,45	211	11,06	9,57	88,50	7,18E-04	1,60E-03	1,54E-04	7,00	15,60	1,50	81,7	67,3	69,4

REFERENCES:

- ¹ J.F.Manwell, J.G. Mc Gowan, A.L. Rogers “ Wind Energy Explained”, Wiley 2002
- ² S. Ljunggren “Ljudutbredning kring havsbaserade vindkraftverk. Resultat från en litteraturstudie”, Arbetsrapport 1999:6, KTH, Augusti 1999
- ³ H.H. Hubbard and K.P. Shepherd, “Aeroacoustics of large wind turbines”, JASA Vol 89 No 6, June 1991
- ⁴ C. Larsson, “Ljudutbredning från vindkraftverk”, Uppsala University, 1999
- ⁵ Reference 6 from [2]
- ⁶ L. Johansson “Sound Propagation around off-shore Wind Turbines -Long-Range Parabolic Equation Calculations for Baltic Sea Conditions”, Licentiate Thesis, KTH, Stockholm 2003
- ⁷ Ljud från Vindkraftverk Naturvårdsverket Rapport 6241 , Dec 2001
- ⁸ K. Konishi, Y Tanioku, Z Maekawa, “Long time measurement of a long range sound propagation over an ocean surface”, Applied Acoustics 61 , 2000
- ⁹ K. Konishi, Z. Maekawa, “Interpretation of long term data measured continuously on long range propagation over sea surfaces”, Applied Acoustics 62, 2001
- ¹⁰ F.W.Embleton, G A. Daigle “Chapter 12: Atmospheric Propagation in Aeroacoustics of Flight Vehicles”, Theory and Practice Volume 2: Noise Control, Harvey H. Hubbard Editor, 1991
- ¹¹ Acoustics – “Attenuation of sound during propagation outdoors. Part I: Calculation of the absorption of sound by the atmosphere”. ISO 9613-1-1993(E)
- ¹² K. Törnblom, “Thermally driven wind modification in coastal areas and its influence on sound propagation with application to wind power, Licentiate thesis, Department of Earth Sciences, Uppsala University, 2006.
- ¹³ R. G. Brown, P.Y.C. Hwang, “Introduction to random Signals and Applied Kalman filtering”, John Wiley and Sons, 1997
- ¹⁴ R.E. Kalman, “A New Approach to Linear Filtering and Prediction Problems”, ASME – Journal of basic Engineering, 1960
- ¹⁵ S. Ljunggren, Mätning av bullerimmission från vindkraftverk. Elforsk rapport 98:24, 1998.
- ¹⁶ R. Raspet, W. Wu, “Calculation of average turbulence effects on sound propagation based on the fast field program formulation”, JASA 97(1) 147-153, 1995
- ¹⁷ T.L. Richard, K. Attenborough “Accurate FFT-based Hankel Transform for predictions of outdoor sound propagation”, JSV 109 (1) 157-167, 1986.
- ¹⁸ S.W. Lee, N. Bong “Impedance formulation of the fast field program for acoustic wave propagation in the atmosphere”, JASA 79 (3) 628-634, 1986
- ¹⁹ R. Raspet, S.W. Lee “A fast field program for sound propagation in a layered atmosphere above an impedance ground”, JASA 77 (2) 345-352, 1985
- ²⁰ S.J. Franke, G.W. Swenson Jr. “A brief tutorial on the fast field program (FFP) as applied to sound propagation in the air”, Applied Acoustics 27, 203-215, 1989
- ²¹ M. West, R.A. Sack, F. Walkden The FFP: “A second tutorial Application to long range sound propagation in the atmosphere”, Applied Acoustics 33, 199-228, 1991

²² M. Boué, “Outdoor sound propagation under the influence of atmospheric turbulence”, Lic Thesis, KTH, Stockholm, 2003

²³ C.I. Chessel, “Three-dimensional acoustic-ray tracing in an inhomogeneous anisotropic atmosphere using Hamilton's equations”, JASA 53(1) 83-87, 1973

²⁴ Personal communication with Prof. Ilkka Karasalo, FOI (www.foi.se); Stockholm, Sweden.

²⁵ F.D. Tappert, “The parabolic approximation method”, In “Wave Propagation Underwater Acoustics” ed Keller Papadakis. Springer-Verlag, 1977Tappert [33]

²⁶ M. West, K. Gilbert, R.A. Sack “A tutorial on the PE model used for long range propagation in the atmosphere”, Applied Acoustics 37 31-49, 1992

²⁷ E.M.Salomons “ Improved Green’s function parabolic equation method for atmospheric sound propagation”, JASA 104(1) 100-111, 1998

²⁸ K.E. Gilbert, X. Di, “ A fast Green’s function method for one way propagation in the atmosphere” JASA 94(4) 2343-2352, 1993

SOUND PROPAGATION FROM OFF-SHORE WIND TURBINE ARRAYS

John Harrison

January 2012

INTRODUCTION

There is, presently, intensive lobbying by a few wind energy developers and their potential sub-contractors to remove the present moratorium on off-shore wind energy generation in the Great Lakes. It has even reached the point of pushing to build a project and use it as a study. The proposal is not for a pilot project but for a full 300 MW, 100+ wind turbine development just 5 to 7 km off-shore. This is a transparent attempt to get a permit to build, by political means, a development that will never pass an environmental review. The effort ignores the fact that the residents of Wolfe Island, Amherst Island and along the waterfronts of Kingston and Prince Edward County will be treated as guinea pigs. The following report presents what is known about sound propagation across water and applies it to off-shore wind energy generating systems.

SUMMARY

Sound propagates readily across water. This common knowledge and experience is supported by European work on sound propagation modelling backed up by measurements of propagation over water. In the case of an exclusion zone of 5 km, it is demonstrated that for a typical wind-energy generating system, which may include 60 or more large turbines, the sound pressure on-shore level will be 46 dBA on average for the time that the sound power level is 107 dBA per turbine. This is significantly in excess of typical rural night-time background noise levels of 25 to 30 dBA, of the present Ontario 40 dBA noise limit for on-shore wind-energy generating systems and the German night-time limit of 35 dBA. For 10% of the time that the sound power level is 107 dBA per turbine the sound pressure level on-shore will be 51 dBA, well in excess of the Ontario noise limit. This 10% criterion can be used as the worst case scenario, the basis for the Ontario turbine noise regulations. These estimates do not include the effect of turbulence in the atmosphere and its impact on the generation of excess low frequency noise. They do not include any allowance for uncertainty in the estimate, uncertainty in the sound power of the individual turbines or of increase in sound power level of the turbines as they age. The proposed 5 km exclusion zone is far from adequate. The exclusion zone needs to depend upon the number of turbines in the development. Even with the present inadequate Ministry of the Environment turbine noise regulations the exclusion zone needs to vary from a minimum 5 km for a 5 turbine project to beyond 20 km for a 60 plus project.

SOUND PROPAGATION OVER WATER – GENERAL COMMENTS

First and foremost it is our common experience that sound propagates readily over water, particularly at night when background sounds die down and when the atmosphere becomes

stable. I well remember a comment by Mr. Phil Brennan, Manager of Environmental Assessment and Approvals Branch at the Ontario Ministry of the Environment (MOE), at the first focus group meeting that I attended: *A neighbour's generator, 2 km across the lake from my cottage, drives me crazy in a way that no noise does at home in Toronto.* (This is not an exact quotation but does represent the point that he was making.) Two things are important here: the ease of sound propagation over water and the low background noise in rural Ontario, particularly at night. The propagation of sound over water is discussed in the next section.

The low background noise at night is what allows the intrusion of turbine noise. Let us be clear here: there is no difference in the average wind speed at hub height (80 to 100 metres) between day-time and night-time and hence no difference in the turbine noise between day-time and night-time. This is demonstrated by the wind energy output of the Ontario wind generating systems. The following table summarizes data from the Ontario Independent Energy System Operator (IESO). The months chosen represent the four seasons. The capacity factor is the monthly average power output (MW) divided by the nameplate power output (1085 MW for the period July 2009 to April 2010). The averages were taken for day-time (6:00 am to 6:00 pm) and night-time (6:00 pm to 6:00 am). The ratios demonstrate that there is no significant difference in power output and hence noise output between day and night.

Month	July 2009	Oct. 2009	Jan. 2010	April 2010
Day-Time Capacity Factor	15.4%	31.4%	32.8%	31.9%
Night-Time Capacity Factor	14.1%	30.9%	33.1%	34.8%
Ratio: Day/Night	1.09	1.02	0.99	0.92

By contrast, there is a significant difference in wind speed at ground level between day and night. To those of us who have any experience of rural areas and particularly of Ontario lakes large and small, this is demonstrated by the calming of the wind and the consequent calming of the lakes at night. For those without that experience, data from meteorological towers offer the proof. A summary of data from 28 sites, world-wide, was that the average (day and night) ratio of wind speed at a height of 10 metres to that at 80 metres was 0.7 ± 0.1 whereas the night-time average was 0.5 ± 0.1 . During the summer months the difference is magnified.

SOUND PROPAGATION OVER WATER – LITERATURE REVIEW

The science of noise from off-shore wind turbines has been reviewed by Sondergaard and Plovsing (SP) in a report to the Danish Ministry of the Environment:

<http://www2.mst.dk/udgiv/publications/2005/87-7614-687-1/pdf/87-7614-689-8.pdf>

The report consists of two parts: (a) measurement of emission of offshore turbine noise and (b) calculation of sound propagation from offshore turbines. Part (a) is not relevant here. The difficulty of measuring sound emission is that the measurement must be made at sea and

hence with a sound meter on a boat. The background noise from the boat was 55 to 58 dBA. Nevertheless at the required range of 85 to 125 metres from the turbine the methodology was shown to work. Part (b) was a combination of literature review and calculation using Swedish and Danish propagation models.

SP summarized the earlier work of Hubbard and Shepherd who measured turbine noise propagation over desert sand, like water an acoustically hard surface. Hubbard and Shepherd showed good correlation with spherical spreading and air absorption of sound for “high” frequency sound (630 Hz). However, in the infrasound region the results were better described by cylindrical spreading. Note that at low and infrasound frequencies absorption by the air is negligible. Where the crossover occurs is not known. However, the cylindrical spreading over an acoustically hard surface is very important because it means that the sound pressure level decreases by only 3 dB for each doubling of distance from the turbine rather than 6 dB for spherical spreading.

SP go on to discuss propagation models formulated in Europe. The so-called Danish method is very simplistic with spherical spreading, a single parameter for air absorption (0.005 dB/metre) and a +3 dB correction for incoherent reflection from acoustically hard ground. In 1998, further work under the auspices of the European Union was presented for propagation over ground and water. This new model took account of the frequency dependence of the air absorption coefficient and so was viable for larger propagation distances. However, the model for propagation over water was tested for distance only up to 350 metres.

In 2001, a Swedish report specifically addressed larger distances both over ground and over water. The model assumed a transition from spherical spreading to cylindrical spreading at a distance of 200 metres. This 200 metre break point is a function of the sound speed gradient in the atmosphere. In turn, the sound speed gradient depends upon the wind speed gradient and the temperature gradient. Both of these gradients, and therefore the sound speed gradient, vary with time. This Swedish propagation model, for distances larger than 200 metres, is written as:

$$L = L_s - 20 \log(r) - 11 + 3 - \Delta L_a + 10 \log\left(\frac{r}{200}\right)$$

L is the sound pressure level at the observer, L_s is the turbine sound power (e.g. 105 dBA), 11 is $10 \log(4\pi)$, 3 is 3 dBA of ground reflection, ΔL_a is the integrated frequency dependent absorption coefficient, a function of r , and r is the distance from turbine hub to the observer. The second term on the right gives the spherical spreading and the final term corrects for cylindrical spreading beyond 200 metres. SP have calculated the integrated absorption coefficient and show the result in figure 17 of their report. For instance, at a distance of 5 km, it is 8 dBA. Given that the break point distance for the onset of cylindrical spreading was

uncertain, the authors of the model specify that the model gives an upper limit to the sound pressure level at the observer.

In a report for the Swedish Energy Agency - *"Long-Range Sound Propagation over the Sea with Application to Wind Turbine Noise"*,

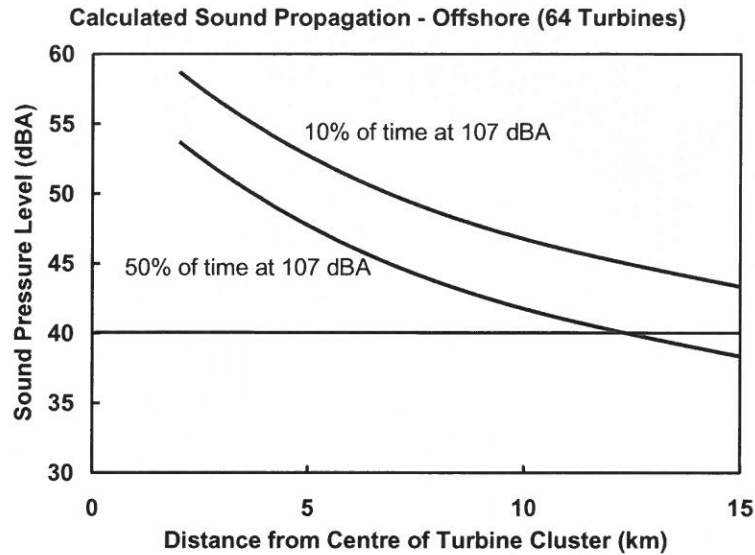
http://www.vindenergi.org/Vindforskrappporter/V-201_TRANS_webb.pdf

Boué investigated the Swedish propagation model by making sound propagation measurements over sea in the Kalmar Strait between Sweden and the island Öland in the Baltic Sea. The separation between source and receiver was 9.7 km. Measurements of average sound transmission loss showed agreement with the Swedish propagation model with a break between spherical and cylindrical spreading at 700 metres rather than the token 200 metres in the model. Furthermore, the measured TL(90), the transmission loss exceeded 90% of the time, was in agreement with the Swedish propagation model with the 200 metre break point. Therefore, Boué's measurements allow a reliable estimate of the sound pressure level as a function of distance over water from a turbine. Interestingly, Dr. Phillip Dickinson, Emeritus Professor of Acoustics at Massey University, has found the break point of 750 metres for turbine noise propagation over land. (See Sound, Noise Flicker, B. Rapley and H. Bakker, eds.; Atkinson and Rapley (2010), p. 175)

I would like to add to this discussion and enlarge on an aspect of the Swedish model. At large distances, such as 5 km, the path difference between the direct and reflected pathways from turbine to receptor become small. For instance, at a distance of 5 km, the path difference is equal to or less than a quarter-wavelength for frequencies at and below 1700 Hz. That is, for the spectrum of sound that reaches a receptor the direct and reflected sound waves add coherently. This adds 3 dB to the sound pressure level.

NUMERICAL EXAMPLES

It is instructive to consider numerical examples based upon the Swedish propagation model with both the 200 and 700 metre break points. These correspond to the sound pressure levels exceeded 10% and 50% of the time respectively. Consider 64 large turbines (say 3MW) each generating 107 dBA of sound power. The total sound power is then $L_s = 125$ dBA ($107 + 10 \log 64$). The result of the model is shown in the figure below as the sound pressure level, exceeded 10% and 50% of the time that the turbines are emitting a sound power of 107dBA, as a function of distance. For multiple turbines this distance is from the mean position of the turbines cluster. The turbines will not emit at 107 dBA all of the time. However, for fixed speed turbines such as the Siemens 2.3MW machines, the sound power level reaches its maximum value at an electrical power output of about 25% of its nameplate electrical power output.



As an appendix, similar graphs are given for clusters of 32, 16 and 8 off-shore turbines. Consider also, for interest, the specific case of the proposed Wolfe Island Shoals wind generating system with 24 turbines located 5 to 7 km from the nearest shoreline and a further 100 located 12 to 15km from the shoreline. Although not specified, these will probably be 2.3 MW turbines with a sound power of 105 dBA. The sound pressure level at the nearest shoreline will be greater than 50 dBA and 45 dBA for 10% and 50% respectively of the time that the turbines are operating with a sound power of 105 dBA. Again note that the sound power will be 105 dBA for all times that the electrical power generation is at and above about 25% of the nameplate power.

This review of the work of SP and the measurements made by Boué and the above analysis makes clear that a 5 km setback of wind turbines from rural shorelines is far from adequate from an acoustic perspective. For the cases considered, the predicted sound pressure levels are collected into a table for an exclusion zone of 5 km. A setback for the centre of the cluster is 6 km in each case; apart from the Wolfe Island Shoals project (WIS) for which the proposed turbine locations are used.

Number of Turbines (3MW)	8	16	32	64	WIS
Sound Pressure Level (10%) (dBA)	42	45	48	51	50
Sound Pressure Level (50%) (dBA)	37	40	43	48	45

In all cases, treating the 10% results as representative of the worst case scenario, the on-shore sound pressure level is far in excess of the typical night-time rural background sound pressure level, the present Ontario wind turbine noise limit of 40 dBA and the more realistic 35 dBA

German night-time limit. There are other concerns that to date have been ignored by the Ministry of the Environment.

DISCUSSION

All measurements and calculations are subject to uncertainty. Specifications for turbine noise quote uncertainty of 1 or 2 dBA. ISO 9613, the standard model for calculating noise at a receptor from an on-shore wind turbine, includes an uncertainty of 3 dBA. SP made a measurement of turbine sound power level for an off-shore turbine and found a difference from the sound power level of a same type on-shore turbine of between 1 and 3 dBA, depending upon the wind speed. They write: *"The difference is within what could be expected when comparing two different turbines of the same type on land"*.

There is turbulence in the atmosphere over water just as there is over land. In a published paper Barthelmie has measured a turbulent intensity at a Danish off-shore turbine site to be 7%. The author was more interested in the turbulence of the downwind wake from the turbines and so was not looking for the range of turbulence out at sea. Turbulence adds significantly to turbine noise, particularly to the low frequency component of the turbine noise. It is the low frequency noise which propagates with little absorption by the atmosphere, which is most subject to cylindrical spreading and coherent reflection and which causes the most annoyance. Part of any renewable energy approval process should be the measurement of the turbulent intensity over the range of height traversed by the blades.

It is now clear that the MOE noise regulations for on-shore wind turbines were and are woefully inadequate. They allow noise intrusion of more than 15 dBA in rural areas at night; neglect MOE's own general penalty of 5 dBA for noise of a periodic or cyclic character (amplitude modulation); included an allowance for masking noise for several years beyond the time that research in Europe had shown that masking noise is generally just not present at night; ignore the contribution of turbulent air to low frequency turbine noise; ignore the uncertainty in the sound power of turbines and in the propagation models; and finally, ignore the recommendations of medical and other authorities that setbacks from modern large up-wind turbines should be 1.5 to 2 km. The failure of MOE to correct these inadequacies (masking noise apart) could be the embarrassment of admitting its initial lack of judgement, knowledge or spine.

Now that we are seeing the advent of off-shore turbines in Ontario it is vital to get things right at the beginning. The proposals coming forward involve hundreds of turbines in the Great Lakes. A 5 km exclusion zone is far from adequate. The exclusion zone needs to vary from a minimum 5 km for a 5 turbine project to beyond 20 km for a 60 plus project. I would like to support a point made by Bill Palmer in his EBR commentary. In Europe, as they have gained

experience with off-shore wind turbines, regulators have been increasing the setbacks from shore, to far beyond the meagre 5 km proposal for the Great Lakes. Rather than go through the same learning curve, Ontario needs to make use of the European experience.

harrisjp@physics.queensu.ca

APPENDIX - Calculated Sound Pressure Levels at Shore for Clusters of 32, 16 and 8 Turbines.

The sound pressure levels are calculated with the Swedish model supported by Boué's measurements of sound propagation over water. In addition, 3 dBA has been added for coherent reflection at the ground.

